7/25/83

NESTOR —

FYI —

THIS IS THE DRAFT FINAL
REPORT FOR PHASE I OF
OUR ELECTROSLAG WELDING
PROJ —

WE HOPE AISC WILL

PROVIDE SUPPORT FOR

PHASE II THRU APR 30, 1984 —

AL KUENTZ

The Pennsylvania State University

The Graduate School

Department of Architectural Engineering

Examination of Resistance Factor for
Load and Resistance Factor Design Criteria

A Thesis in

Architectural Engineering

by

Hasun Jeong

Submitted in Partial Fulfillment
of the Requirements
for the Degree of

Master of Science

May 1981

I grant The Pennsylvania State University the nonexclusive right
to use this work for the University's own purposes and to make single
copies of the work available to the public on a not-for-profit basis if
copies are not otherwise available.

Hasun Jeong

# THE PENNSYLVANIA STATE UNIVERSITY

104 ENGINEERING "A" BUILDING
UNIVERSITY PARK, PENNSYLVANIA 16802

College of Engineering
Department of Architectural Engineering

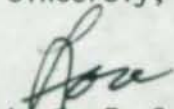Area Code 814
865-6394

November 8, 1983

Mr. John Edinger
AISC
400 North Michigan Avenue
Chicago, Illinois  60611

Dear John:

It was good to meet you in Minneapolis and then again in Houston.  I hope you found my paper interesting.  Enclosed is the thesis we were talking about at the Minneapolis meeting.  I think the student has presented some interesting thoughts.

I recently received "Modern Steel Construction" which included the awards won by some of my students.  I would like to obtain 20 more copies of these issues if that is possible.  Can you help?  Thanks, too, for sending the LRFD specifications.  I look forward to the feedback we get.

Sincerely,

Louis F. Geschwindner, Ph.D.
Assistant Professor of
Architectural Engineering

LFG/sew

Enc.

We approve the thesis of Hasun Jeong.

Date of Signautre:

April 22, 1981

Louis F. Geschwindner, Assistant
Professor of Architectural Engineering,
Thesis Advisor

22 April 1981

Gifford H. Albright, Professor and
Head of the Department of
Architectural Engineering

Luis H. Summers, Professor of
Architectural Engineering

April 23, 1981

April 24, 1981

Richard M. McClure, Associate Professor
of Civil Engineering

# ABSTRACT

The study presented here deals with a probability-based safety factor of structures known as resistance factor. Resistance factors are determined for plate girders in bending, shear, and combined shear and bending, and are compared with those obtained by T. V. Galambos at Washington University in St. Louis, Missouri.

Five major steps are followed in this study: 1) Selection of a probabilistic design format. 2) Selection of load and plate-girder strength prediction models. 3) Collection of data of parameters which affect the strength of plate girders. 4) Determination of characteristic values of the parameters. 5) Calibration with an existing design specification.

Cornell's first-order, second-moment format is used as a probabilistic design format, and predictions of plate-girder strengths employ formulas which include the Basler-Thürlimann models. Experimental data from related studies is analyzed by statistical methods to determine their characteristic values. Calibrations are performed with Part 1 of the AISC Specification.

Results of the study yield more conservative values for resistance factors than those recommended by T. V. Galambos. This can be attributed to differing characteristic values for parameters selected in each study.

Key words:  Buildings, Coefficients, Load factors, Plate girders, Statistical analysis, Structural design

# TABLE OF CONTENTS

# LIST OF TABLES

## LIST OF FIGURES

# LIST OF SYMBOLS

| | |
|---|---|
| $A_I$ | Influence area |
| $A_T$ | Tributary area |
| $C_b$ | Bending coefficient depending upon moment gradient |
| $C_D$ | Deterministic dead load influence factor |
| $C_L$ | Deterministic live load influence factor |
| C.O.V. | Coefficient of variation |
| D | Dead load |
| $D_c$ | Code specified dead load |
| $D_m$ | Mean dead load |
| E | Modulus of elasticity |
| E[X] | Expectation or the mean of a random variable X |
| $F_b$ | Allowable bending stress |
| $F_{bu}$ | Nominal ultimate bending stress |
| $F_{bum}$ | Mean ultimate bending stress |
| $F_{cr}$ | Nominal critical bending stress |
| $F_v$ | Allowable shear stress |
| $F_{vcr}$ | Nominal critical shear stress |
| $F_{vcri}$ | Inelastic critical shear stress |
| $F_{vu}$ | Ultimate shear stress |
| $F_{vy}$ | Nominal shear yield stress |
| $F_y$ | Nominal or specified yield stress |
| $F_{ys}$ | Static yield stress |
| $F_{ysf}$ | Static yield stress of the flange |
| $F_{ysw}$ | Static yield stress of the web |
| $F_{ysm}$ | Mean static yield stress |
| G | Shear modulus of elasticity |

| | |
|---|---|
| $I$ | Moment of inertia |
| $K$ | Effective-length coefficient |
| $L$ | Live load |
| $L_c$ | Code specified live load |
| $L_m$ | Mean live load predicted by a live load prediction model |
| $M$ | Applied moment |
| $M_{cr}$ | Critical moment |
| $M_{ex}$ | Experimental bending strength |
| $Mim$ | Mean bending strength in the interaction range |
| $Min$ | Nominal bending strength in the interaction range |
| $M_m$ | Mean measured bending strength |
| $M_{th}$ | Theoretical bending strength |
| $M_u$ | Ultimate bending strength |
| $M_y$ | Yield moment |
| $M_{yf}$ | Flange yield moment |
| $P$ | Applied load (in experiment) |
| $P_{ex}$ | Experimental ultimate applied (in experiment) |
| $P_{th}$ | Theoretical ultimate applied (in experiment) |
| $Q$ | Applied load |
| $Q_{mm}$ | Mean applied moment |
| $Q_{vm}$ | Mean applied shear force |
| $R$ | Resistance capacity |
| $R_{LL}$ | Live load reduction factor |
| $R_m$ | Mean measured resistance capacity |
| $R_n$ | Nominal resistance capacity |
| $R_{PG}$ | Stress reduction factor |
| $V$ | Applied shear force |

| | |
|---|---|
| $V_{cr}$ | Critical shear strength to beam action |
| $V_{ex}$ | Experimental shear strength |
| $V_{im}$ | Mean shear strength in the interaction range |
| $V_{in}$ | Nominal shear strength in the interaction range |
| $V_t$ | Shear strength due to tension field action |
| $V_{th}$ | Theoretical shear strength |
| $V_u$ | Ultimate shear stress |
| $V_{um}$ | Mean ultimate shear strength |
| a | Width of the web panel |
| b | Width of the flange |
| $f_b$ | Nominal bending stress in the interaction range |
| $f_v$ | Nominal shear stress in the interaction range |
| h | Depth of the web |
| k | Plate buckling coefficient |
| $\ell$ | Length of span of the girder |
| m | (Subscript) Mean value |
| n | (Subscript) Nominal value |
| p | Ratio of the web yield stress to the flange yield stress |
| s | Ratio of the web area to the flange area |
| t | Thickness of the web |
| u | (Subscript) Ultimate value |
| v | (Subscript) Shear value |
| w | Thickness of the flange |
| $\alpha$ | Linearization factor |
| $\alpha_m$ | Linearization factor for bending in the interaction range |
| $\alpha_v$ | Linearization factor for shear in the interaction range |
| $\beta$ | Safety factor |

$\beta_m$      Safety index for bending in the interaction range

$\beta_v$      Safety index for shear in the interaction range

$\nu$      Poisson's ratio

$\sigma$      Standard deviation

$\phi$      Resistance factor

$\phi_i$      Resistance factor for interaction range

$\phi_m$      Resistance factor for bending

$\phi_v$      Resistance factor for shear

$\Omega$      Coefficient of variation (C.O.V.)

$\Omega_F$      C.O.V. of cross-sectional properties

$\Omega_M$      C.O.V. of material properties

$\Omega_P$      C.O.V. of the ratio of the experimental strength to the theoretical strength

## ACKNOWLEDGEMENT

## Chapter 1

## INTRODUCTION

### 1.1 Evolvement of the Safety Concept of Structural Systems

It has been well known since analysis techniques for structural systems were developed that the strength of a structural system and the loads acting on the system do not have any deterministic values but are affected by many chance factors, and that absolute safety or reliability of structural systems is not feasible. From past experiences of success and failure recorded for similar types of structures, "factors of safety" have been determined. The safety or reliability of a structure is presumably assured by those factors of safety. This factors of safety concept based on past experience has been widely adopted in many current codes and specifications.

Since the 1950's, there have been significant efforts to reevaluate the traditional safety concept for structural systems. The concept and methods of probability theory have been introduced in evaluating the reliability of structural systems. Theoretical bases for this approach were formulated by Freudental (21). However, the complexity and overly idealistic aspect of the completely probablitistic approach limited its application to design practices.

Researchers then turned their efforts toward achieving a compromise solution by retaining some of the simplicity of the traditional approach while incorporating some probabilistic concepts. The first results of this effort appeared as load factors, which may be determined by the ratio of the characteristic strength of a structure to the characteristic applied loads. This approach has been applied in the American Concrete Institute (ACI) Code and the American Association of State Highway and

Transportation Officials (AASHTO) Specification. In this approach, the characteristic values are taken to be equal to the respective mean values minus or plus a certain number times the corresponding standard deviations. However, this semi-probabilistic format cannot reflect in a consistent manner the uncertainties in various parameters which affect the safety of structural systems (47).

In the middle of the 1960's, a significant improvement in the probabilistic safety concept was made by C. A. Cornell (15). By employing the first-order approximation and the second-moment theorem in probability theory, he derived a relatively simple and practically feasible design format. In this approach, no assumption on probabilitistic distribution of the design variables is made, and only their mean and the variance are required.

Since the Cornell format was introduced, the second-moment format has become important for evaluating structural safety. This approach has been well summarized in the articles (3,44) prepared by the Task Committee on Structural Safety of the American Society of Civil Engineers (ASCE). No codes nor specificiations have adopted this approach in their practices. However, a proposal by T. V. Galambos (24) is now under review by the Committee on Specification for Buildings of the American Institute of Steel Construction (AISC).

## 1.2 Scope of Study

The first explicit application of the probability-based design format to design practices may be due to T. V. Galambos. Through the studies (24,25,26) presented in the Journal of Structural Division of ASCE, Galambos proposed new design criteria for steel structures in-

cluding design criteria for plate girders. These design criteria are called the Load and Resistance Factor Design (LRFD).

For assuring the safety of structures, the following general formula should be satisfied:

$$\phi R_n \geq \sum_{k=1}^{n} \gamma_k Q_k \tag{1.1}$$

in which $\phi$ is the "resistance factor" reflecting uncertainties in the resistance of a structure, $R_n$ is the nominal resistance determined by a theoretical structural analysis model, $\gamma$ is the "load factor" reflecting uncertainties in the loads acting on the structure, and Q is the applied load effect estimated by a load predicting model. The summation in Eq. (1.1) represents linear combination of applied loads from various sources.

Galambos' load and resistance factors for plate girders were developed by carrying out the following studies: 1) Cornell's format (15) was selected as a design format. 2) Data obtained at Lehigh University in the late 1950's and early 1960's was used for determining characteristic values of parameters affecting girder strengths. 3) Theories developed by Basler and Thürlimann (8,9,10), and McGuire and Cornell (37) were employed to determined $R_n$ and Q in Eq. (1.1). 4) Calibrations with Part 2 (plastic design) of the AISC Specification were carried out.

The main concern of the research presented here is a reexamination of the Galambos resistance factors for plate girders in pure bending, shear, and combined shear and bending. For this, strength prediction models, load prediction models, and probabilistic design formats are reviewed. However, the main effort is given to the evaluation of the characteristic values of parameters which affect the strength of plate girders. Since the 1960's, numerous additional tests of plate girders

have been conducted around the world. By adding new data from those recently carried-out tests to the data used in the Galambos study, and by investigating the collected data with statistical methods, more representative characteristic values of parameters may be expected.

This research is limited in scope to the same girders as used in the Galambos study (welded, transversely stiffened, single web plate girders). Within these limits, reevaluated resistance factors of plate girders in bending, shear, and combined shear and bending are developed, and new design criteria are recommended through calibration with Part 1 (elastic design) of the AISC Specification. Details of plate-girder design such as end panel requirements and intermediate-stiffner requirements are assumed to be satisfied by following the provisions of the AISC Specification.

## Chapter 2

### RELIABILITY ANALYSIS MODEL

#### 2.1 Probability-Based Design Format

It is well recognized that absolute safety and reliability of engineering systems are not feasible because the information used in the development of a design invariably contains some kinds of uncertainties. The reliability or safety of a design can be assured only in terms of probability -- specifically, in terms of probability of survival or in terms of probability of failure.

Traditionally, safety or reliability is presumably assured by prescribing conservative conditions in design through the use of "factors of safety". However, the factor of safety is never analyzed nor evaluated quantitatively but is determined through accumulated experience.

Since the lack of absolute reliability is due to the uncertainties involved in a design, the evaluation of reliability naturally requires a consideration of uncertainties, which is a subject of probability.

In development of Load and Resistance Factor Design (LRFD) criteria, the methods and concepts of probability have a major role. The probability-based design model is a scheme to evaluate structural safety or reliability quantitatively in explicit manner by probabilistic treatment of uncertainties in the applied forces and in the structural resistance.

Among the proposed probabilistic design models, the CEB-ISO format (36) proposed by the European Concrete Committee to the International Standard Organization is perhaps the most general format. Although it may give relatively accurate results in evaluating reliability of a design, complexity of the procedure in CEB-ISO format may limit its use in practice.

A major contribution in this field is due to C. A. Cornell (15). He suggested a simplified probabilistic design format by utilizing a first-order approximation method. The strength of this format is its simplicity without a significant sacrifice of accuracy. In this format, only the first two moments, the mean and the variance, are used. Thus, Cornell's format is sometimes referred to as the first-order, second-moment theory. With the linearization factor proposed by Lind (36), Cornell's format may be further simplified.

Since Cornell's format was proposed, considerable efforts have been made in this field, and some criticism about the second moment theory has evolved. Ove Ditlevsen (17) showed that a measure of reliability in the domain of very small probability of failure was very sensitive to the terms which were truncated in the first-order approximation and that the second-moment theory was valid only in the case where superposition held.

In spite of such criticism, the first-order, second-moment design format such as Cornell's format provides the conceptual base for recent studies, for instance, the studies (3,19,44) done by the American Society of Civil Engineers, Task Committee on Structural Safety.

Use of only two characteristic values of sampling data, the mean and the standard deviation which is a square root of the variance, may be the most important advantage of Cornell's format because the mean and the standard deviation are the only values, in most cases, available in practice. Because of this advantage, Cornell's format is used in this work for developing LRFD resistance factor. Galambos also used Cornell's format in his study (54).

## 2.2 First-Order, Second-Moment Theory

Since the reliability of an engineering structure or its component is defined as the probability that the system or its component will successfully perform its intended function, a reliability measure would be a function of design variables (2). If a performance function or resistance of a structure is defined as

$$R = g_R(X_1, X_2, \ldots, X_n) \tag{2.1}$$

where $X_1$, $X_2$, $\ldots$, and $X_n$ are random variables representing design variables and design parameters and $g_R$ is a special functional relation, then it is clear that R is also a random variable, whose values, r, represent levels of performance dependent on the design variables.

The minimum performance of a structure or its component should not be less than the loads acting on it. The loads coming from various sources can be expressed as

$$Q = g_Q(Y_1, Y_2, \ldots, Y_n) \tag{2.2}$$

in which $Y_1$, $Y_2$, $\ldots$, $Y_n$ are random variables representing loading variables and $g_Q$ is a specified functional relation. Therefore, Q is also a random variable.

The measure of reliability or the probability of survival, $P_s$, can be defined as

$$P_s = P(R > Q) \tag{2.3}$$

where P denotes a probabilistic function of the random variable $(R > Q)$. Conversely, the probability of failure, $P_f$, is

$$P_f = P(R < Q) \quad . \tag{2.4}$$

If probabilistic information on R is known, in other words, if the shape of the distribution and values of its parameters are known, the

probability of survival expressed by Eq. (2.3) can be written as (2)

$$P_s = \int_{-\infty}^{\infty} f_R(r) dr = 1 - F_R(Q) \tag{2.5}$$

where $f_R(r)$ and $F_R(Q)$ are the probability density function and cumulative distribution function of R, respectively.

In practice, data may be available only for the basic variables $X_i$. Therefore, any probabilistic information on R must be derived from those $X_i$. Furthermore, the shapes of probability distributions of $X_i$ are usually not known. Information on $X_i$ is invariably limited and may be sufficient only to evaluate the mean values of $X_i$ and the standard deviation, from which the coefficient of variation (C.O.V.) can be determined. Thus, any practical formulation of reliability must be based on information for the first and second moments, that is, the mean and variance, of $X_i$ only.

If the relationship $Y = g(X)$ for a function is sufficiently well behaved, and if the coefficient of variation of X is not large, the following approximations are valid (4)

$$E[Y] = g(E[X]) \tag{2.6}$$

and

$$Var[Y] = Var \ [X][\frac{dg(X)}{dX}\big|_{m_x}]^2 \tag{2.7}$$

in which $E[\cdot]$ and $Var[\cdot]$ denote the mean value and the variance, respectively. Since Eqs. (2.6) and (2.7) are derived from exact solutions by keeping only first-order terms, they are called first-order approximations of the first and second moments.

## 2.3 Derivation of Probabilistic Design Format

As defined by Eq. (2.3), when the resistance of a structural element, R, is greater than the load, Q, acting on it, the element per-

forms successfully its intended purpose. Since R and Q are random variables, (R-Q) defines a probability distribution function as shown in Figure 1a. Then, the probability of survival, $P_s$, is defined as

$$P_s = P[(R - Q) > 0] \qquad (2.8)$$

An equivalent representation of structural safety is shown in Figure 1b where the probability distribution of the random variable (R-Q) is given on a lognormal scale. In this case, the probability of survival, $P_s$, is defined by

$$P_s = P[\ln(\frac{R}{Q}) > 0] \quad . \qquad (2.9)$$

If the "standardized variable", U, of the random variable $\ln(R/Q)$ is introduced, Eq. (2.9) can be rewritten as (2)

$$P_s = P[\ln(R/Q) > 0] = P[\frac{\ln(R/Q) - \ln(R/Q)_m}{\sqrt{Var\ [\ln(R/Q)]}} > - \frac{\ln(R/Q)_m}{\sqrt{Var[\ln(R/Q)]}}]$$

$$= P[U > - \frac{\ln(R/Q)_m}{\sqrt{Var[\ln(R/Q)]}}] = 1 - F_u(-\beta) \qquad (2.10)$$

in which m denotes the mean, $F_u$ is the cumulative probability distribution function of the standardized variable U, and $\beta$ is defined as

$$\beta = \frac{\ln(R/Q)_m}{\sqrt{Var[\ln(R/Q)]}} \quad or \quad \beta = \frac{\ln(R/Q)_m}{\sigma_{\ln(R/Q)}} \qquad (2.11)$$

in which $\sigma_{\ln(R/Q)}$ is the standard deviation of the random variable $\ln(R/Q)$. From Eq. (2.10), it is clear that the probability of failure, $P_f$, is defined by

$$P_f = F_u(-\beta) = F_u[- \frac{\ln(R/Q)_m}{\sqrt{Var[\ln(R/Q)]}}] \quad . \qquad (2.12)$$

As seen in Eq. (2.12) and Figure 1b, since the probability of failure corresponding to a larger $\beta$ is smaller than that corresponding to a smaller $\beta$, $\beta$ can be used as a parameter of structural safety or
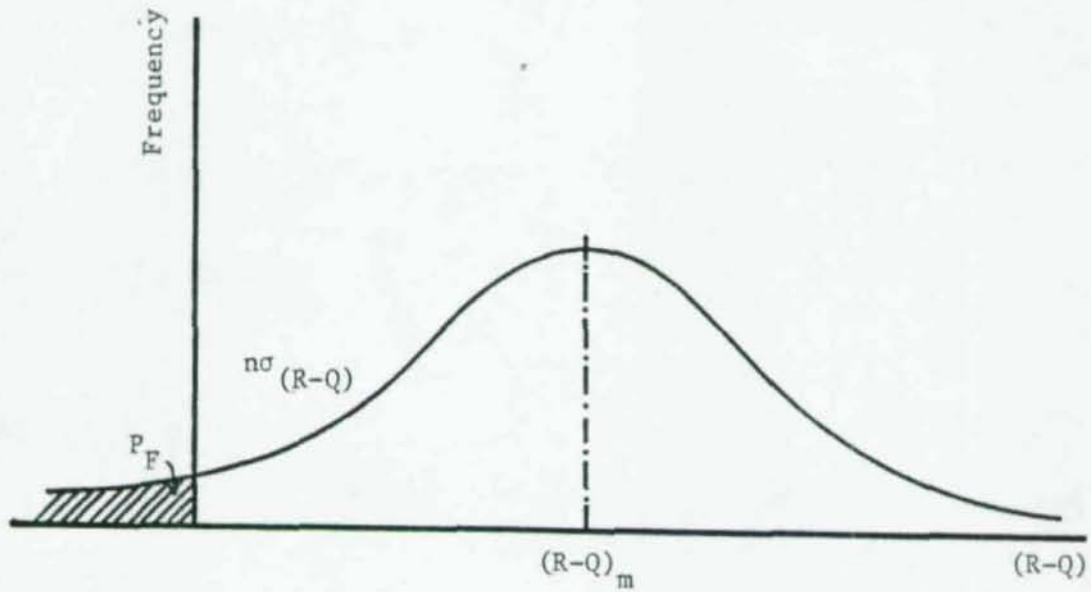
(a)  Probabilistic model
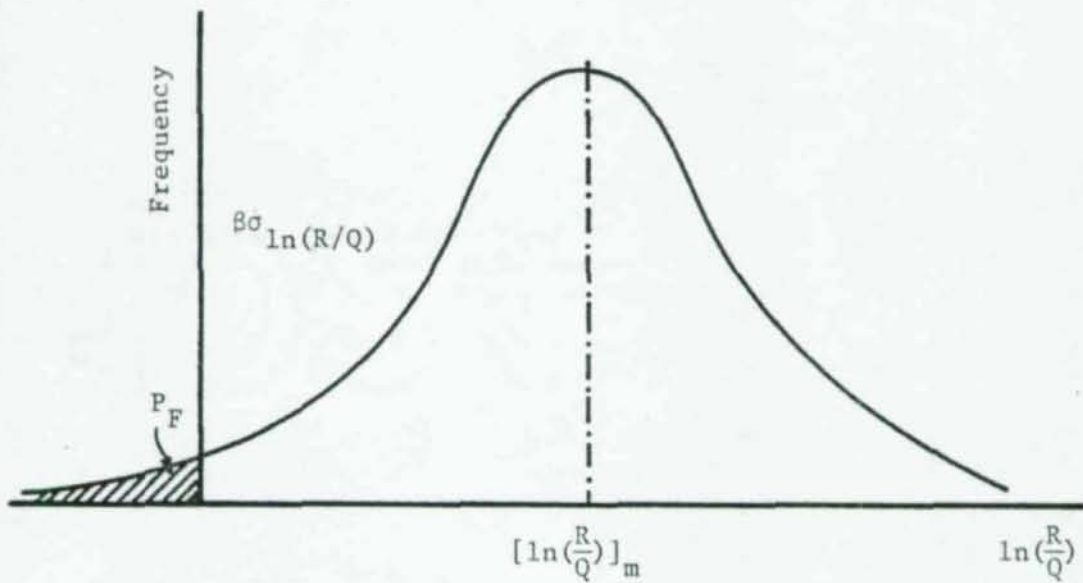
(b)  Definition of safety index

Figure 1.  Definition of structural safety

structural reliability. Thus, $\beta$ is called a "safety index". Specified values of $\beta$ corresponding to different levels of reliability are shown in Table 1 (2).

## Table 1

### Safety Level Corresponding to $\beta$

| $P_f$ | $\beta$ | $P_f$ | $\beta$ |
|-------|---------|-------|---------|
| $10^{-1}$ | 1.28 | $10^{-5}$ | 4.25 |
| $10^{-2}$ | 2.33 | $10^{-6}$ | 4.75 |
| $10^{-3}$ | 3.09 | $10^{-7}$ | 5.20 |
| $10^{-4}$ | 3.72 | $10^{-8}$ | 5.60 |

The safety index $\beta$ in Eq. (2.11) can be simplified, by use of Eqs. (2.6) and (2.7), as

$$\beta = \frac{\ln(\frac{R_m}{Q_m})}{\sqrt{\Omega_R^2 + \Omega_Q^2}} \tag{2.13}$$

in which $\Omega_R$ and $\Omega_Q$ represent the Coefficient of Variance (C.O.V) of resistance and applied loads, respectively. The C.O.V. of any random variable X is defined as $\sigma_x/X_m$.

Eq. (2.13) can be rearranged in the traditional "central factor of safety" format. For insuring the safety of a structural element, the central safety factor format takes the form

$$R_m \geq \theta Q_m \tag{2.14}$$

in which $\theta$ is a central factor of safety. Comparing Eq. (2.13) and Eq. (2.14) gives

$$\theta = \exp(\beta\sqrt{\Omega_R^2 + \Omega_Q^2}) \ . \tag{2.15}$$

The central factor of safety, however, combines the uncertainties inherent in the resistance and the applied load effects, which are independent from each other. Thus, it would be advantageous if the central factor of safety $\theta$ could be split into two parameters which could represent the uncertainties in the resistance and in the applied loads. This can be accomplished by using the linear expansion technique developed by Lin (36), that is

$$\sqrt{\Omega_R^2 + \Omega_Q^2} = \alpha(\Omega_R + \Omega_Q) \qquad (2.16)$$

in which $\alpha$, the linearization factor, is given by

$$\alpha = \frac{\sqrt{1 + (\Omega_Q/\Omega_R)^2}}{1 + \Omega_Q/\Omega_R} \qquad (2.17)$$

Substitution of Eqs. (2.15) and (2.16) into Eq. (2.14) gives

$$\exp(-\alpha\beta\Omega_R)R_m \geq \exp(\alpha\beta\Omega_Q)Q_m \quad . \qquad (2.18)$$

The right-hand side of Eq. (2.18) can be further separated to allow an independent treatment of the effects of the different types of load.

## 2.4 Resistance Factor and the C.O.V. of Applied Load

If the nominal resistance of a structural element, $R_n$, determined by any theoretical analysis model of a structure is used with split safety factors, the design criterion can be expressed as (24)

$$\phi R_n \geq \sum_{k=1}^{n} \gamma_k Q_{k_m} \qquad (2.19)$$

where $\phi$ denotes the resistance factor, $\gamma$ represents the load factors, and summation means the linear combination of load effects from different sources.

### 2.4.1 Resistance factor

By comparing Eq. (2.18) with Eq. (2.19), the resistance factor $\phi$ can be defined by

$$\phi = \exp(-\alpha\beta\Omega_R)\frac{R_m}{R_n} \tag{2.20}$$

in which $\alpha$ and $\beta$ are determined by Eq. (2.17) and Eq. (2.13), respectively, $R_m$ is the mean resistance capacity which would be determined from experimental data, $R_n$ is the nominal resistance capacity determined by a theoretical structural analysis model, and $\Omega_R$ represents the C.O.V. of resistance capacity calculated from experimental data.

The strength of a structural element is a random variable reflecting many chance factors. These may be separated into three terms; uncertainties inherent in mechanical properties, uncertainties of cross-sectional properties, and uncertainties associated with the professional assumptions adopted in the structural analysis. Thus, for defining $\Omega_R$, it is assumed that the resistance capacity of a structural element could be expressed by multiplication of these three factors such that

$$R = M \cdot F \cdot P \tag{2.21}$$

in which M, F, and P represent material properties which are usually expressed in terms of stress, cross-sectional properties such as section modulus, moment of inertia, and cross-sectional area, and a professional factor associated with assumptions or simplification in structural analysis, respectively. Then, by utilizing Eq. (2.7), $\Omega_R$ can be expressed as

$$\Omega_R = \sqrt{\Omega_M^2 + \Omega_F^2 + \Omega_P^2} \tag{2.22}$$

where $\Omega_M$, $\Omega_F$, and $\Omega_P$ are the C.O.V.'s of the stress due to variation of material properties, of cross-sectional properties due to fabrication

error, and of errors in assumptions or simplifications in the structural analysis.

Thus, by substituting Eq. (2.22) into Eq. (2.20), the resistance factor is redefined as

$$\phi = \frac{R_m}{R_n} \exp(-\alpha\beta\sqrt{\Omega_M^2 + \Omega_F^2 + \Omega_P^2}) \quad . \tag{2.23}$$

### 2.4.2 C.O.V. of applied loads

As implied in Eq. (2.19), it is assumed that loads on a structural member are the linear summation of separate load effects of random magnitude. It is also assumed that each load effect is the product of four factors (36); a random variable representing the ratio of the real to calculated load effect, i.e., error in idealization or simplification in structural analysis, a deterministic calculated influence factor, a random variable representing the uncertainties in assumptions about the spatial and temporal variation of each type of load, and independent load intensity. Therefore, by denoting these four factors as S, C, K, and q, respectively, the total applied load on a structural element, Q, can be expressed as

$$Q = \sum_{i=1}^{n} S_i C_i K_i q_i \quad . \tag{2.24}$$

For simplification, dead and live loads are assumed to be present, and S is assumed the same for all types of loads. The, Eq. (2.24) can be simplified to

$$Q = S(C_D AD + C_L BL) \tag{2.25}$$

in which S is a random variable representing uncertainties in load effect prediction, $C_D$ and $C_L$ are deterministic calculated dead and live load influence factors, A and B are random variables representing un-

certainties in the assumptions of the spatial and temporal variation in dead and live loads, and D and L denote dead and live load intensities. With an assumption that the mean of S is unity, and by applying Eq. (2.7), the mean of the random variable Q and the C.O.V. are given by the following equations (25)

$$Q_m = C_D A_m D_m + C_L B_m L_m \tag{2.26}$$

and

$$\Omega_Q = [\Omega_s^2 + \frac{C_D^2 A_m^2 D_m^2 (\Omega_A^2 + \Omega_p^2) + C_L^2 B_m^2 L_m^2 (\Omega_B^2 + \Omega_L^2)}{(C_D A_m D_m + C_L B_m L_m)^2}] \tag{2.27}$$

in which the subscript m denotes the mean value.

Since it is not easy to obtain information about A and B, Ravindra (44) has simplified the above equations with assumptions that $A_m$ and $B_m$ are unity, that is

$$Q_m = C_D D_m + C_L L_m \tag{2.28}$$

and

$$\Omega_Q = [\Omega_s^2 + \frac{\Omega_D^2 + (L_m/D_m)^2 \Omega_L^2}{(1 + L_m/D_m)^2}] \qquad . \tag{2.29}$$

Eq. (2.29) implies $C_D = C_L$ which is valid for uniformly distributed dead and live loads. The simplified equations given by Eqs. (2.28) and (2.29) are used in this study to determine the safety index $\beta$ represented by Eq. (2.13).

## Chapter 3

### UNCERTAINTIES OF APPLIED LOADS AND THE RESISTANCE

### 3.1 Introduction

As shown in Eq. (2.20), it is necessary, in order to estimate the resistance factors, that the safety index $\beta$ and the C.O.V. of the resistance, $\Omega_R$, be defined.

The safety index $\beta$ given by Eq. (2.13) involves variables associated with applied loads as well as variables associated with the resistance capacity of a structural element; that is, the mean applied loads, the mean resistance, and their C.O.V., $\Omega_Q$ and $\Omega_R$, respectively.

The C.O.V. of the resistance, $\Omega_R$ given by Eq. (2.22) is determined from three independent variables: the material factor (M), the cross-sectional factor (F), and the professional factor (P). The professional factor which reflects the differences between actual resistance and predicted resistance cannot be estimated unless the types of forces (e.g., bending and shear) resisted by a structural member are defined. Therefore, only the material factor and the cross-sectional or the dimensional factor are discussed in this chapter. The professional factor is discussed in the following chapters.

The C.O.V. of applied loads, $\Omega_Q$, which is independent of the resistance, is also discussed in this chapter.

### 3.2 Variation in Loading

Applied load on a structural member is a random variable which is influenced by the variation of each load from different sources. As shown in Eq. (2.13), data relating to the applied load, specifically its mean and the C.O.V., are necessary to determine the safety index. This

safety index is finally used to evaluate the resistance factor, $\phi$, defined by Eq. (2.20).

Eqs. (2.28) and (2.29) give the mean applied load and its C.O.V. for presenting dead and live loads. For convenience, the equations are rewritten below:

$$Q_m = C_D D_m + C_L L_m \qquad (2.28)$$

and

$$\Omega_Q = [\Omega_s^2 + \frac{\Omega_D^2 + (L_m/D_m)^2 \Omega_L^2}{(1 + L_m/D_m)^2}] \qquad (2.29)$$

To define $Q_m$ and $\Omega_Q$, data for each type of load, dead and live load in this case, are necessary.

### 3.2.1 Dead load

The dead load is relatively constant in the service life of a structure. Although major deviation in dead loads are reported in the literature, these may be attributed to significant alterations in the structures (44). Therefore, it is assumed that the mean dead load, $D_m$, is equal to a code specified value, $D_c$, which is usually given by the unit weight of materials used in the structure. The C.O.V. of the dead load intensity, $\Omega_D$, has been estimated by Ravindra (44) to be 0.04.

### 3.2.2 Live load

Live loads arise from moveable fixtures, types of occupancy, and other non-permanent loads. Design of a structure under dead and live loads should consider the extreme value statistics of the live load over the life time of the structure.

In this study, office type occupancy is assumed as a standard case because office-type buildings provide a common type of live load with

the possibility of significant variation over its service life. Several
prediction models (18,34,37,49,54) for extreme live load effects in
office buildings have been proposed. Out of these models, McGuire and
Cornell's simplified formula (37) and Ellingwood and Culver's model (18)
may be suitable for development of LRFD criteria because of their sim-
plicity and their agreement with surveyed data. The McGuire-Cornell
formula were used in Galambos' research (24). Although the Ellingwood-
Culver formula takes the same form as the McGuire-Cornell formula, the
former was developed based on a large amount of data recently surveyed
in the United States, while the latter was induced from surveyed data
in the United Kingdom. These equations are given below:

$$\text{McGuire-Cornell;} \quad L_m = 14.9 + \frac{763}{\sqrt{A_I}} \text{ (psf)} \tag{3.1}$$

$$\sigma_L = \sqrt{11.3 + \frac{15,000}{A_I}} \tag{3.2}$$

$$\text{Ellingwood-Culver;} \quad L_m = 18.7 + \frac{520}{\sqrt{A_I}} \text{ (psf)}$$

$$\sigma_L = \sqrt{14.2 + \frac{13,900}{A_I}} . \tag{3.4}$$

In the above equations, $L_m$ denotes the maximum mean lifetime total live
loads, $\sigma_L$ is the standard deviation of live load, and $A_I$ is the influence
area equal to twice the tributary area of the floor beam-type member.

While no reduction factor has been suggested in the McGuire-Cornell
model, Ellingwood and Culver have recommended a reduction factor for an
influence area exceeding 200 sq. ft. as given by

$$R.F = 0.34 + \frac{9.45}{\sqrt{A_I}} . \tag{3.5}$$

A comparison of the unit live load between the McGuire-Cornell formula, Ellingwood-Culver formula, American National Standard Institute (ANSI) A58.1-1972 (5), and ANSI A58.1-1980 Draft (6) is given in Figure 2.

The figure shows that the ANSI A.58-1980 Draft takes a more conservative view than that of the ANSI A.58-1972, and also shows that the Ellingwood-Culver formula, without using the reduction factor, matches very well with the load given by the ANSI A.58-1980 Draft.

Therefore, it is concluded that the Ellingwood-Culver formula given by Eqs. (3.3) and (3.4) provides a proper measurement of the maximum mean live load and its standard deviation, from which the C.O.V. of live load can be determined.

### 3.2.3 Other factors

The only remaining factor required in order to determine $\Omega_Q$ in Equation (2.29) is the C.O.V. associated with simplification or idealization of load effect, $\Omega_S$. But, few reports are available from which to obtain this information. Thus, $\Omega_S = 0.10$ is selected by adopting the value used in Galambos' work and in a study (44) done by the Task Committee on Structural Safety of the American Society of Civil Engineering (ASCE).

A comparison of the load-related factors selected in this research with those used in Galambos' work is summarized in Table 2.

Figure 3 shows the variation of the C.O.V. of applied load with respect to tributary area or influence area for four different code specified dead loads. Since the average dead load of an office type building is rarely less than 50 psf (6), it is concluded that $\Omega_Q = 0.13$ is a proper value for the C.O.V. of applied load. This value may be
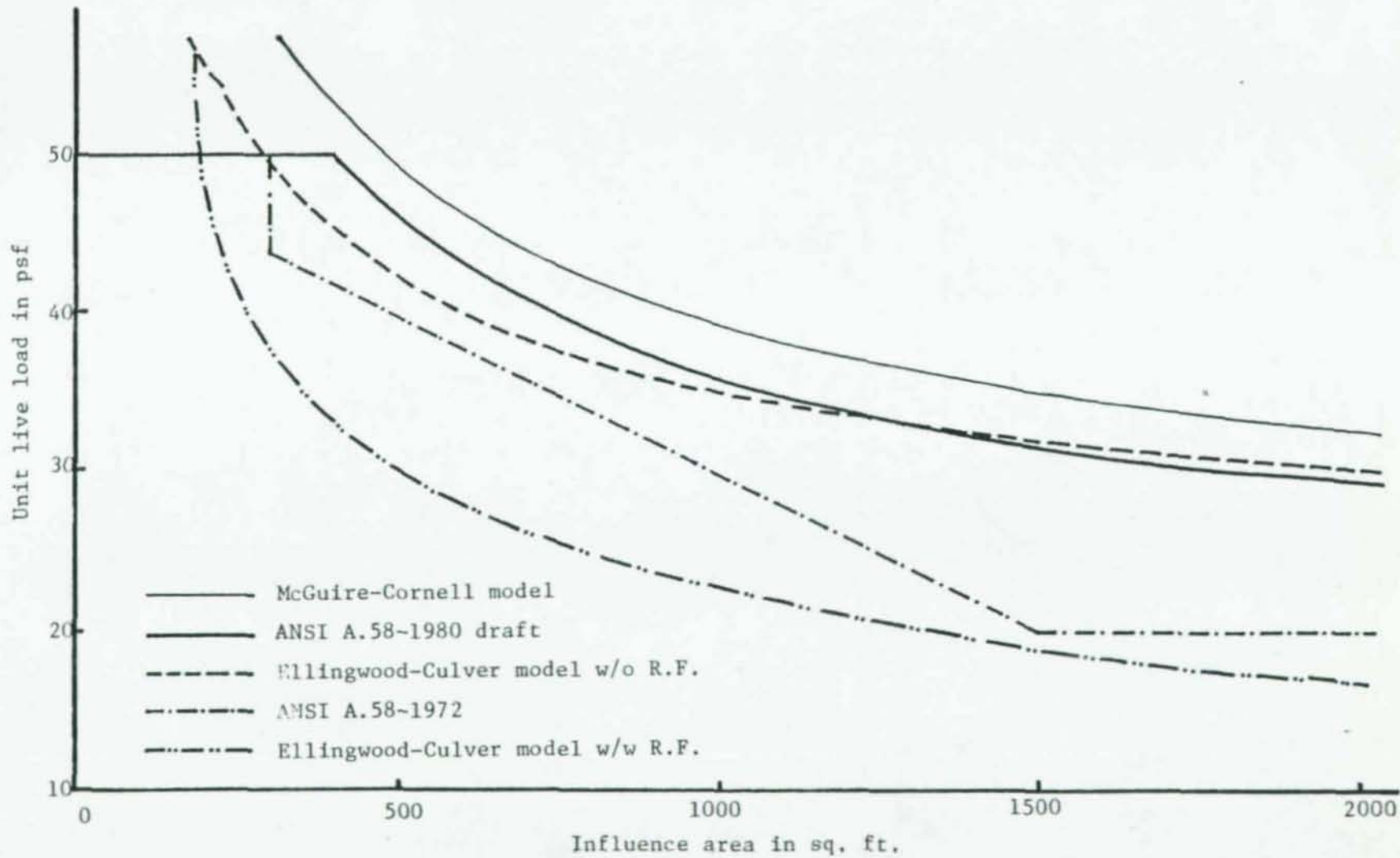
Figure 2. Comparison of design live load from several prediction models

## Table 2

## Load-Related Parameters

| Factor | Selected value | Galambos value |
|---|---|---|
| Mean dead load, $D_m$ | Code specified load, $D_c$ | Code specified load, $D_c$ |
| C.O.V. of $D_m$ | 0.04 | 0.04 |
| Mean live load, $L_m$ | $18.7 + \dfrac{520}{\sqrt{A_I}}$ (a) | $14.9 + \dfrac{763}{\sqrt{A_I}}$ (b) |
| Standard deviation | $14.2 + \dfrac{18900}{\sqrt{A_I}}$ (a) | $11.3 + \dfrac{15000}{\sqrt{A_I}}$ (b) |
| C.O.V. of live load effect | 0.10 | 0.10 |

Note:  (a) the Ellingwood-Culver formula
       (b) the McGuire-Cornell formula
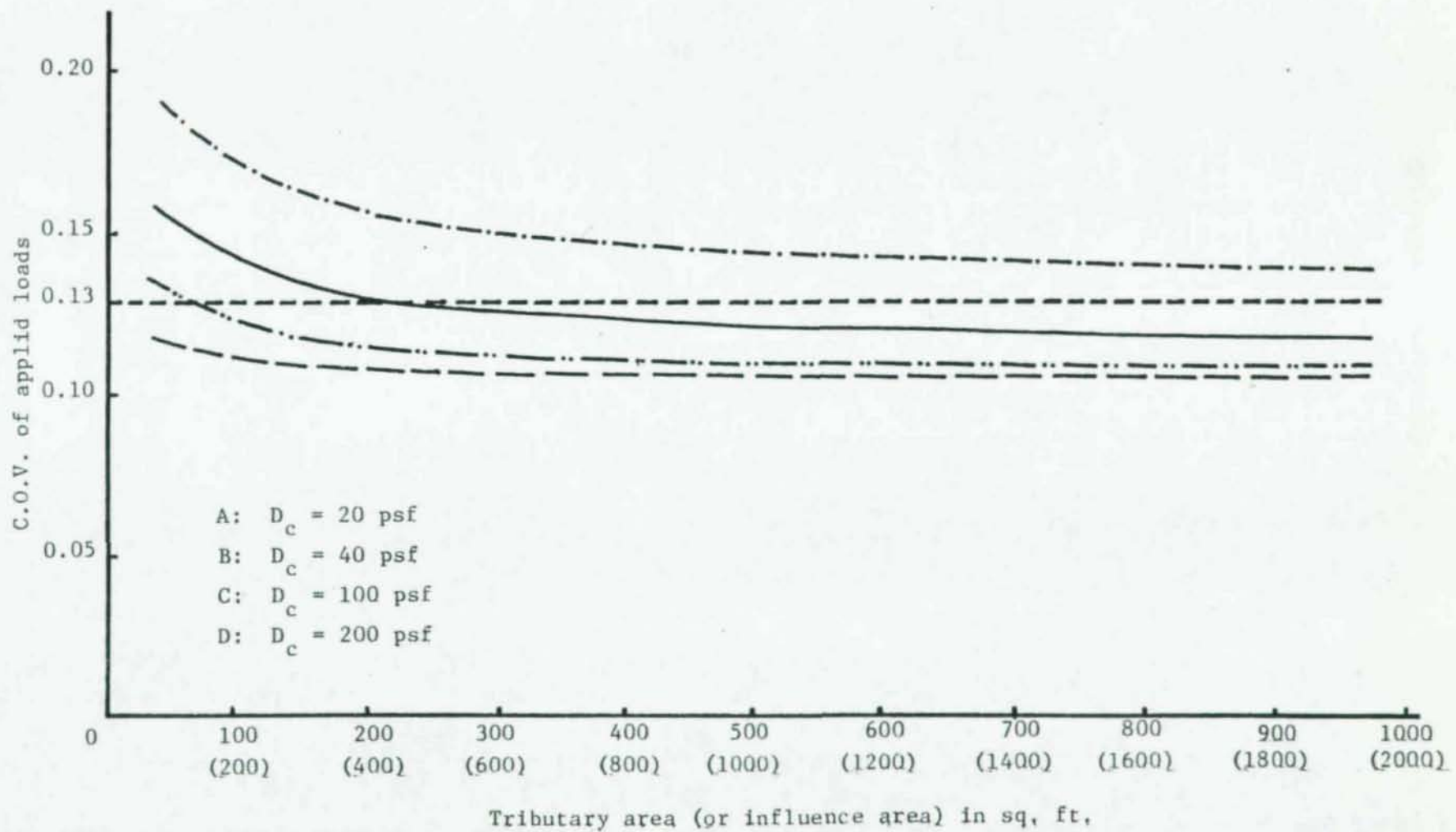
Figure 3. Variation of the C.O.V. of applied loads with respect to tributary (or influence) area

22

conservative for most reinforced concrete buildings, for which $\Omega_Q = 0.11$ may be proper. However, $\Omega_Q = 0.13$ is used in this study.

## 3.3 Variation of Mechanical Properties of Steel

Mechanical properties of steel are commonly described by the elastic moduli in tension, compression and shear; the yield strength in tension, compression and shear; and strain hardening properties. The strain hardening properties, however, are rarely used in design practice for plate girders. In a fabricated structural member such as plate girders, the residual stress may have an effect on the member strength. For the plate girder, the residual stress has a role in the limitation of the web slenderness ratio, but several tests have shown that this limit is too conservative and could be neglected in design practice (33).

Therefore, only the variations of the elastic moduli and the yield strength or yield stress in tension, compression and shear are examined here.

### 3.3.1 Elastic properties

The specified elastic properties in standards, codes and specifications are the modulus of elasticity, $E = 29,000$ ksi, Poisson's ratio, $\nu = 0.3$ and the shear modulus of elasticity, $G = E/2(1 + \nu)$. Measured elastic moduli may have different distributions due to different testing methods and equipments, testing materials from different mills, direction and position of the specimen in the steel plates, and thickness of specimens (1,32).

Since no data could be added to the data used in Galambos' research, his samples shown in Table 3 are used to estimate characteristic values of the elastic properties of steel. This data could be considered

Table 3

Elastic Moduli of Structural Steel From Galambos (26)

| Property | Investigator | Mean(ksi) | C.O.V. | No. of tests | Type of test |
|----------|--------------|-----------|--------|--------------|--------------|
| E | Lyse, Keyser | 29,360 | 0.010 | 7 | Tension coupon |
| E | Rao, et al. | 29.437 | 0.042 | 56 | Tension coupon |
| E | Julian | 29,500 | 0.010 | 67 | Tension coupon |
| E | Julian | 29,550 | 0.010 | 67 | Compression coupon |
| E | Johnston, Opila | 291774 | 0.038 | 50 | Tension and compression coupon |
| E | Tall, Alpsten | 31,200 | 0.060 | 94 | Tension coupon and stub column |
| G | Lyse, Keyser | 12,000 | 0.042 | 5 | Torsion coupon |
| $\nu$ | Julian | 0.296 | 0.026 | 57 | Tension coupon |
| $\nu$ | Julian | 0.298 | 0.021 | 48 | Compression coupon |

representative because they represented the work of different investigators over a time period of more than 20 years, using materials from two major mills in the United States.

From the sampled data in Table 3 with his professional judgement, rather than statistical values of the sampled data, Galambos was selected $E = 29,000$ ksi and its C.O.V. $= 0.06$, $G = 11,200$ ksi and its C.O.V. $= 0.06$, and $\nu = 0.3$ and its C.O.V. $= 0.03$. However, if the same degree of significance of test results in Table 3 is assumed (and, in fact, it is not easy to say that any one result is superior to any other), the use of the mean values and its C.O.V.s obtained by statistical method is desirable according to the concept of the probabilistic design format. Therefore, as shown in Appendix I, $E = 30,000$ ksi and its C.O.V. $= 0.05$ which are the statistical values of E from Table 3 can be said to represent the true mean and the C.O.V. of E with significance level of 1%. Table 4 shows other test results by Huber and Beedle (32).

Table 4

Modulus of Elasticity of Structural
Steel From Huber and Beeble (32)

| Property | Mean (ksi) | C.O.V. | No. of Tests | Type of Test |
|----------|-----------|--------|--------------|--------------|
| E | 29,436 | 0.010 | 22 | Tension coupon |
| E | 29,860 | 0.022 | 20 | Compression coupon |

There are no significant changes in the characteristic values of E if the sampled data in Tables 3 and 4 are pooled. Therefore, $E = 30,000$ ksi and C.O.V. $= 0.05$ are taken as the proper mean and C.O.V. of E in this study.

Galambos' values for Poisson's ratio, $\nu = 0.3$, and its C.O.V. $= 0.03$, are adopted in this work with no argument because they are based on the sample data in Table 3.

Table 3 gives the shear modulus of elasticity from only one source with a sample size of 5. It may not be significant to evaluate its characteristic values from this data. Theoretically, the shear modulus of elasticity is given by $G = E/2(1 + \nu)$. Thus, the characteristic values of G are affected by the characteristic values of E and $\nu$. Therefore, the mean value of $G = 11,550$ and its C.O.V. $= 0.06$ is determined from Eqs. (2.7) and (2.8).

### 3.3.2 Yield stress

The principal material property affecting the strength of steel structures is the yield stress. Test results (1,7,40) show that the yield stress is greatly affected by the strain rate, test method and equipment, chemical composition of steel, thickness of the specimens, and location and direction of the specimens in steel plates. Moreover, there are several methods to define the yield stress (51). In this study, the static yield stress which is defined by the yield stress under zero strain is used as the yield stress to predict the strength of plate girders because the static yield stress is an appropriate yield parameter for building structures with predominantly static load (1). Figure 4 gives the definition of the static yield, which is obtained by stopping the straining after the stress-strain curve has reached the plastic plateau.

Nagarja Rao, et al. (40), have developed an equation to estimate the static yield stress from the dynamic yield stress. Their equation is $F_{yd} - F_{ys} = 3.2 + 0.001 \dot{\varepsilon}$ where $\dot{\varepsilon}$ is the strain rate in micro-inches
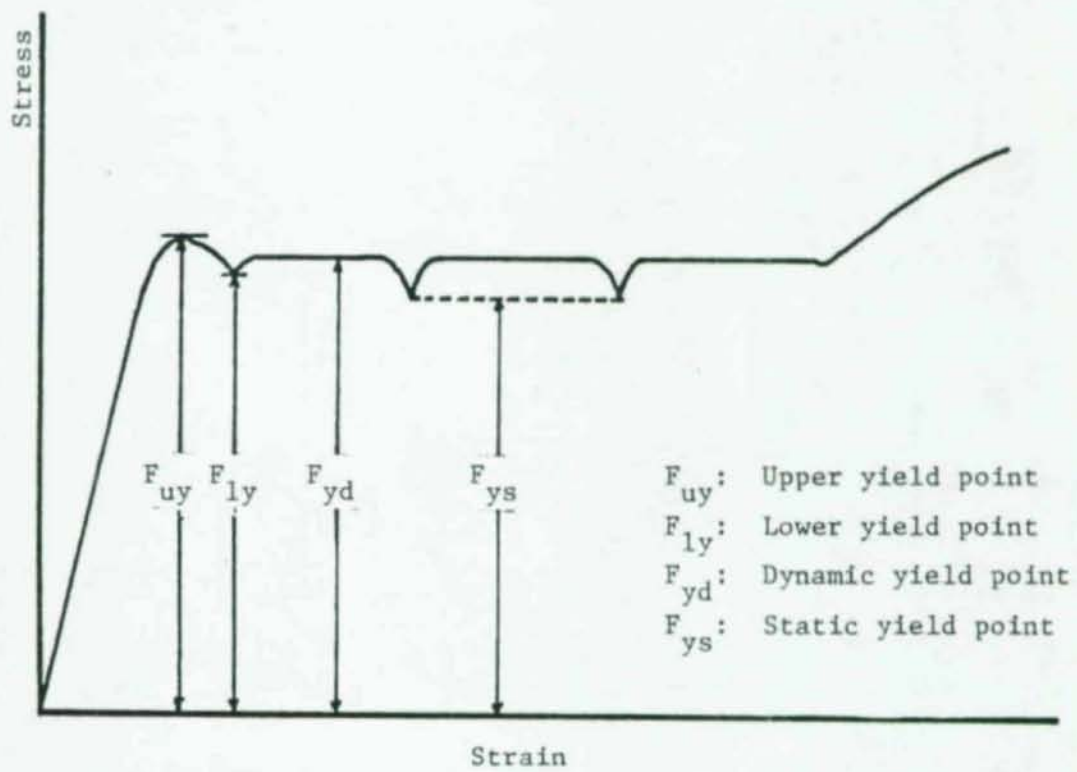
Figure 4. Typical stress-strain curve (40)

per inch per second. Unfortunately, most reported test results do not provide the strain rates.

Values of the measure static yield stress from various sources are summarized in Table 5.

In general, the thinner plate of the same grade steel has greater yield point than the thicker plate (1,7). Since most plate-girder webs are thinner than the flanges, a coupon from the web has greater yield stress than a coupon from the flange if the plate girder has been made of the same grade of steel. Since the flanges of plate girders have an important role in the bending strength and the webs mainly contribute to the shear strength, separation of characteristic values of the web yield stress from those of the flange yield stress may be significant. However, it is not practical to use different characteristic values of the yield stress for different thickness of the flange or the web within the range specified by the ASTM Standards (28).

Compared with $F_{ysm} = 1.05F_y$ and C.O.V. = 0.10, which were used in Galambos' work, Table 5 yields $F_{ysm} = 0.98F_y$ and C.O.V. = 0.12 for the flange. From this result, it is concluded, for the convenience of practical use that $F_{ysm} = F_y$ and the C.O.V. = 0.12 represent true characteristic values of $F_{ys}$ of the flange with the significance level of 1.0%.

For the web of plate girders, the mean static yield stress is obtained from the table to be $1.09F_y$ and the C.O.V. = 0.21 rather than $F_{ysm} = 1.1F_y$ and the C.O.V. = 0.11 used in Galambos' work (24). Again, for the convenience of practical use, $F_{ysm} = 1.1F_y$ and the C.O.V. = 0.21 are used in this study as characteristic values of the web static yield stress.

## Table 5

### Values of Measured Static Yield Stress

| Reference Source | Location on Section | Specified $F_y$ (ksi) | Measured Mean $F_{ys}$ (ksi) | Mean $F_{ys}$/Spec. $F_y$ | C.O.V. | No. of Samples |
|---|---|---|---|---|---|---|
| 11 | Flange | 40.0 | 35.2 | 0.88 | 0.130 | 22 |
|  | Web | 40.0 | 37.1 | 0.93 | 0.073 | 14 |
| 40,47 | Flange | 36.0 | 34.6 | 0.96 | 0.037 | 13 |
|  | Web | 36.0 | 49.8 | 1.38 | 0.229 | 15 |
| 34 | Flange | 100.0 | 104.9 | 1.05 | 0.001 | 14 |
|  | Web | 36.0 | 37.6 | 1.04 | 0.098 | 14 |
| 42 | Flange** | 36.0 | 28.5 | 0.79 |  | 4 |
|  | Web** | 36.0 | 36.5 | 1.01 |  | 2 |
| 14 | Flange** | 100.0 | 106.6 | 1.07 |  | 4 |
|  | Web** | 100.0 | 109.1 | 1.09 |  | 2 |
| 24* | Flange** and Web | 55.0 | 54.9 | 1.00 |  | 24 |
| 24* | Flange** | 36.50,65 |  | 1.08 | 0.090 | 16 |
| 24* | Box** | 36.0 | 38.1 | 1.06 | 0.070 | 80 |
|  | Flange | 50.0 | 54.2 | 1.08 | 0.080 | 13 |
| 24* | Flange | 33.0 | 33.0 | 1.00 | 0.120 | 34 |
|  | Web | 33.0 | 34.5 | 1.05 | 0.130 | 36 |

Note:  * are the data used in Galambos' work
      ** are the data not used in determining characteristic values of the static yield stress

The differences between these characteristic values and those in Galambos' work (24) arise mainly from the differences of dispersion of collected data; that is, the data used in Galambos' work have smaller dispersion than those used in this research.

In Table 6 the selected characteristic values of mechanical properties of structural steel for this study are summarized along with the values used in the Galambos research. While Galambos' values were adjusted from statistical values by professional judgement, the values selected in this research have been obtained by utilizing statistical methods with some modification for the convenience of practical use. Although it is recognizied that professional judgement can not be entirely eliminated in determining characteristic values of any random variable, particularly in the case of limited data available, it is desireable to use statistical values since that is consistent with the concept of the probabilistic design format.

## 3.4  Variations in Cross-Sectional Properties

Very little statistical data for the cross-sectional properties of welded shapes are available in the literature, while some information regarding rolled shapes has been reported. Tomonaga (53) reported that the C.O.V.s of height and width of Japanese heavy rolled H-shapes were 0.002. It could be expected that the welded shape has much larger dimensional variation than the rolled shaped. Variations of cross-sectional properties of welded shapes may come from dimensional variations of component plates and inaccuracy of welding. Dimensional variations of steel plates are summarized in Table 7 from three sources.

The most important cross-sectional properties affecting the strength of plate girders are moment of inertia, section modulus and cross-

## Table 6

### Summary of Characteristic Material Properties

| Property | Galambos' Value Mean | C.O.V | Selected Value Mean | C.O.V. |
|---|---|---|---|---|
| Modulus of elasticity (E) | 29,000 ksi | 0.06 | 30.000 ksi | 0.05 |
| Shear elastic modulus (G) | 11,200 ksi | 0.06 | 11,550 ksi | 0.06 |
| Poisson's ratio ($\nu$) | 0.30 | 0.03 | 0.30 | 0.03 |
| Flange yield stress ($F_{ysf}$) | $1.05F_y$ | 0.10 | $1.0F_y$ | 0.12 |
| Web yield stress ($F_{ysw}$) | $1.10F_y$ | 0.11 | $1.1F_y$ | 0.21 |

## Table 7

### Dimensional Variations of Steel Plates

| Reference Source | Dimension | Mean Measured/Nominal | C.O.V. | No. of Samples |
|---|---|---|---|---|
| 29 | Thickness | 0.998 | 0.019 | 33 |
| 42 | Width | 1.006 | 0.005 | 4 |
|    | Thickness | 1.016 | 0.019 | 6 |
| 34 | Width | 1.002 | 0.004 | 14 |
|    | Thickness | 1.050 | 0.007 | 14 |

sectional area. These properties have the units of $L^4$, $L^3$ and $L^2$, respectively. If inaccuracy of welding were neglected for a while, the largest C.O.V. of cross-sectional properties, which correspond to moment of inertia, would be estimated at 0.022 from the above data. However, there are many other dimensional factors causing variation of the strength of plate girders, such as the squareness of the section and the flatness of component plates. These factors may be greatly affected by inaccuracy of welding.

The other comparative measurement would be dimensional variations of concrete beams. Investigations (20,39) on dimensional variations of concrete beams show that the C.O.V.s of concrete cover over the reinforcing steel has a value between 0.07 and 0.45. The C.O.V. of the ratio of furnished to calculated area of reinforcing steel in concrete beams was between 0.03 and 0.07. Ravindra (44) used the C.O.V. = 0.08 for the cross-sectional variation of concrete beams.

The C.O.V. of cross-sectional properties of welded shapes will likely have a value between 0.022, which represents the dimensional variations of the component plates of welded shapes, and 0.08, which represents cross-sectional variations of concrete beams.

From this comparative information, it is concluded that the C.O.V. = 0.05 which was adopted by Galambos under the assumption of well-controlled fabrication, is a reasonable value reflecting the cross-sectional variation of plate girders. Differences between furnished mean cross-sectional properties and nominal specified cross-sectional properties are assumed to be negligible.

Strength of plate girders, of course, is a function of various cross-sectional properties such as flange area, slenderness ratio,

section modulus and moment of inertia, all of which may have different C.O.V.s. However, due to the lack of information on cross-sectional variations, separate values of the C.O.V. corresponding to each cross-sectional property are not obtained. A C.O.V. = 0.05 will be used as the representative value for all cross-sectional properties which may affect the strength of plate girders.

Chapter 4

## PLATE GIRDERS IN BENDING

### 4.1  Flexural Capacity of Plate Girders

The design of steel plate girders was first based on the theoretical
web buckling strength which is analogous to column buckling theory.  How-
ever, it has been shown through research that there is no direct rela-
tionship between the elastic web buckling strength and the ultimate
strength of plate girders.  This is due to the so-called "postbuckling
strength".  Significant work in this field was carried out by Basler and
his associates at Lehigh University.  The current American Institute of
Steel Construction (AISC) Specifications (50) for transversely stiffened
plate girders are based on the works of Basler and Thürlimann (8,9,10).
Following the work of Basler and Thürlimann, more exact models (29,42,
45) have been proposed.  Although other models would be more exact,
particularly for analysis of hybrid girders and unsymmetrical girders,
the Basler-Thürlimann model, with a little support from other models
when it is necessary, is used in this study to predict the ultimate
bending strength of plate girders.  The choice of the Basler-Thürlimann
model has been made because designers in the United States are most
familiar with the model.  Whether or not one is more exact than the other,
the selection of a model does not make any significant difference in the
probabilistic design format because the different predicted values are
adjusted by the resistance factor.

In general, plate girders are categorized into regular girders and
hybrid girders, where the former has the same grade of steel in the web
as in the flange and the latter has different grades of steel in the two

components. These girders sometimes have unequal top and bottom flange and are called unsymmetrical plate girders.

Although the Basler-Thürlimann model does not distinguish hybrid girders and unsymmetrical girders from regular girders, the model explains in a clear manner the general behavior of plate girders. Therefore, the Basler-Thürlimann model based on regular girders is first introduced, with discussion on unsymmetrical girders and hybrid girders following as special cases of regular girders.

### 4.1.1 General equation for predicting ultimate bending strength (10, 27,33,38)

When a plate girder is subject to bending, the critical stress, $F_{cr}$, of the web is, from the elastic buckling theory,

$$F_{cr} = \frac{k\pi^2 E}{12(1 - \nu^2)(h/t)} \tag{4.1}$$

in which k is the plate buckling coefficient, E is the modulus of elasticity, $\nu$ is Poisson's ratio, h is depth of the web, and t is the web thickness. The ratio $(h/t)$ is commonly called the slenderness ratio of the web. For preventing the web from buckling before yielding, the web slenderness ratio should not exceed $(h/t)_o$ given by

$$(h/t)_o = \sqrt{\frac{k\pi^2 E}{12(1 - \nu^2)F_y}} \tag{4.2}$$

where $F_y$ is the yield stress of the plate girder.

When the slenderness ratio exceeds $(h/t)_o$ of Eq. (4.2), the web starts to buckle and postbuckling behavior occurs. Provided no lateral buckling of the flange occurs, the top and bottom edges of the girder remain straight and extreme-fiber stress continues to increase. If the web were to remain flat, proportionate increases in stress would develop

in the remainder of the web. Because the web has buckled, however, the variation in stress will be nonlinear in the compression zone as shown in Figure 5a. During the increase in moment beyond that corresponding to the critical stress of the web, the neutral axis moves down to balance the moment. The maximum moment is reached at an extreme-fiber stress of $F_y$. Since the variation in stress in the postbuckling state is not known, Basler and Thürlimann assumed a linear distribution in stress as shown in Figure 5b over an effective depth of the web, $h_e$, as shown in Figure 5c. The effective depth of the web, $h_e$, was assumed to be 30 times the web thickness for girders with the web slenderness ratio $(h/t)_{max}$ given by

$$(h/t)_{max} = \sqrt{\frac{\pi^2 E^2}{24(1 - \nu^2)(F_{rt} + F_y)F_y} \cdot \frac{A_w}{A_f}} \qquad (4.3)$$

in which $F_{rt}$ is the residual stress in the tension flange, $A_w$ is the web area, and $A_f$ is the flange area. The term $(h/t)_{max}$ defines the maximum web slenderness ratio which assures no vertical buckling of the compression flange and flange stress of $F_y$. Linear variation of the effective depth of the web, $h_e$, was assumed between $(h/t)_o$ and $(h/t)_{max}$. Thus, with known $h_e$ and $A_w/A_f$, the ultimate bending strength, $M_u$, of plate girders can be expressed in terms of $A_f$, $F_y$, and h, by calculating a reduced section modulus. The variation of $M_u/M_y$ with various values of $(h/t)$ and $A_w/A_f$ is shown in Figure 6 where $(h/t)_p$ is the slenderness ratio for development of the plastic stress distribution. Since a curve passing through points A, 0, and B in Figure 6 is a straight line, the following equation of the ultimate bending moment was obtained (10):

$$M_u/M_y = 1 - 0.0005\frac{A_w}{A_f}[h/t - (h/t)_o] \qquad (4.4)$$
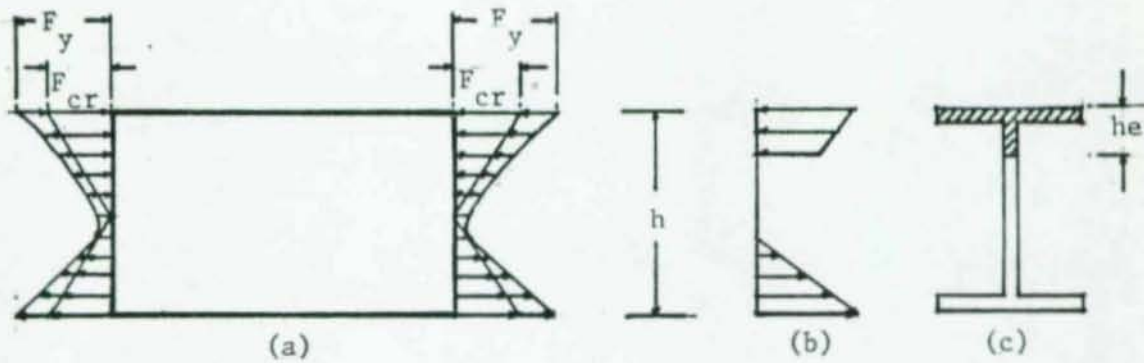
Figure 5. Stress redistribution after web buckling
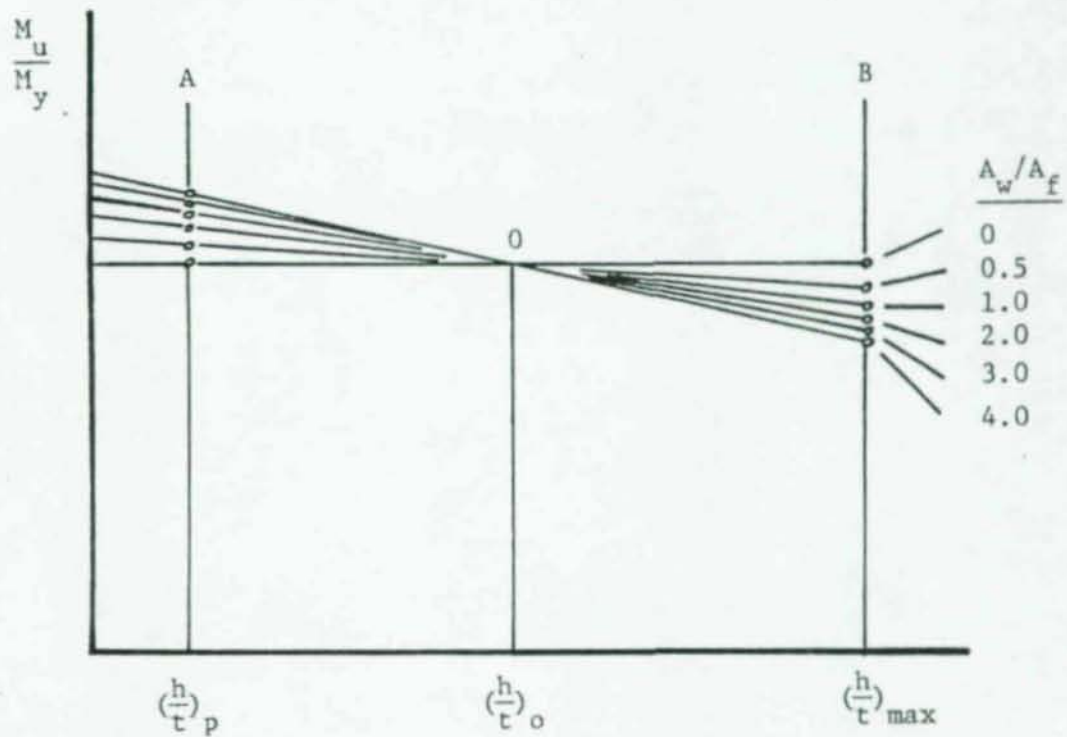


Figure 6. Variation of $M_u/M_y$ with $(\frac{h}{t})$ and $(A_w/A_f)$ (9)

Since a rapid increase of the ultimate strength is doubtful for $(h/t) <$

$(h/t)_o$, Eq. (4.4) was recommended to apply to plate girders with the web

slenderness ratio between $(h/t)_o$ and $(h/t)_{max}$.

Eq. (4.4) was derived with the assumption of a stable compression

flange. However, the yield moment, $M_y$, in Eq. (4.4) may not be reached

due to instability of the compression flange. Such instability may come

from lateral buckling, local buckling, or vertical buckling of the com-

pression flange. Thus, Basler and Thürlimann suggested substitution of

$M_{cr} = F_{cr} \cdot S_x$ for $M_y$ in Eq. (4.4), where $F_{cr}$ is the smallest critical

stress being determined by lateral, local or vertical buckling of the

compression flange.

After the Basler-Thürlimann formula was proposed, Cooper (14) modi-

fied Eq. (4.4) from several test results; that is, the Basler-Thürlimann

formula could be used for plate girders with $(h/t) > (h/t)_{max}$ by replac-

ing $(h/t)_o$ in Eq. (4.4) by $(h/t)_r$ given by

$$(h/t)_r = \sqrt{\frac{k\pi^2 E}{12(1 - \nu^2)F_{cr}}} \qquad (4.5)$$

in which $F_{cr}$ is the lower critical stress due to either lateral buckling

or local buckling of the compression flange. Eq. (4.5) means that ver-

tical buckling of the compression flange due to failure of the web can

be ignored. Therefore, by incorporating the influence of local or lat-

eral buckling of the compression flange in Eq. (4.4), the ultimate bend-

ing strength of plate girders can be expressed by

$$M_u = F_{cr} \cdot S_x [1 - 0.0005 \frac{A_w}{A_f}(\frac{h}{t} - \sqrt{\frac{k\pi^2 E}{12(1 - \nu^2)F_{cr}}})] . \qquad (4.6)$$

The bending buckling coefficient k in Eq. (4.6) is determined by

the degree of flange restraint provided by the web. If no flange

restraint is assumed, the theoretical value of k is 23.9, and if full flange restraint is assumed, k is equal to 41.8. In this study, k = 35.9 for the bending buckling coefficient is used as implied in the AISC Specification. The remaining factor, $F_{cr}$, which is related to instability of the compression flange, is discussed in the following.

### 4.1.1.1 Lateral buckling of the compression flange

Figure 7 shows a plate girder in pure bending, simply supported, held against tipping at both ends, and laterally unbraced between the ends. The top flange of the girder is under uniform compression and would buckle in its weak direction, downward, if the web would not prevent this. However, if the force in the compression flange is large enough, it will tend to buckle in the only direction in which it is free to move, horizontally. The bottom flange, being in tension, tends to remain straight. Since the two flanges and the web actually form a rigid unit, buckling can take place only in the manner shown in Figure 7b. This phenomenon is termed "lateral buckling of the compression flange". In this case, the critical moment, $M_{cr}$, at the mid-span is expressed by (27)

$$M_{cr}^2 = \frac{\pi^2}{\ell^2} EI_y GJ + \frac{\pi^4}{\ell^4} EI_y EC_w \tag{4.7a}$$

in which $\ell$ is the length of the span, $I_y$ is the moment of inertia about y-axis, J is the torsional constant, and $C_w$ is the warping constant. A more general formulation, including restraints at the ends corresponding to bending about y-axis, is given by (27)

$$M_{cr}^2 = C_b^2 \left[ \frac{\pi^2}{(K\ell)^2} EI_y GJ + \frac{\pi^4}{(K\ell)^4} EI_y EC_w \right] \tag{4.7b}$$
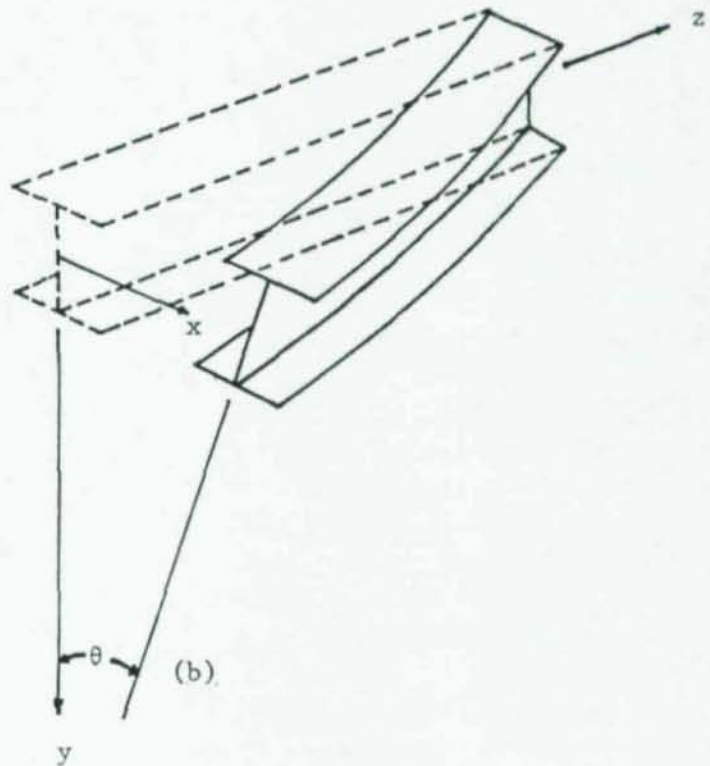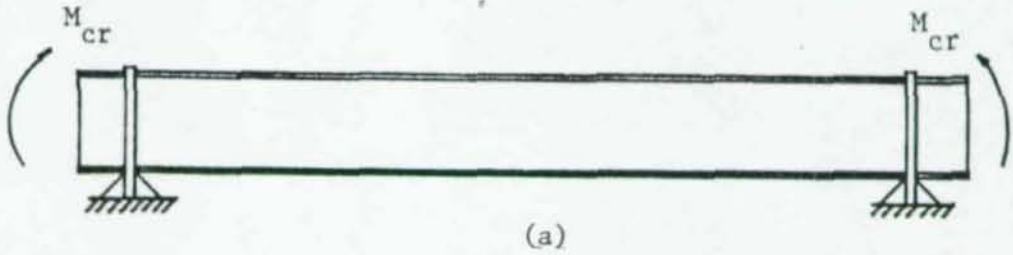
Figure 7. Lateral buckling of compression flange

in which $C_b$ is a coefficient which depends on the variation in moment along the span, and K is an effective-length coefficient which depends on the condition of restraints at the supports. In the bracket of the right-hand side of Eq. (4.7b), the first term represents the St. Venant stiffness and the second term represents the warping stiffness. However, the St. Venant stiffness is negligible for plate girders, which usually have wide flanges, because the torsional constant is much smaller than the warping constant. Thus, the critical stress, $F_{cr}$, due to lateral buckling can be approximated as (27)

$$F_{cr} = C_b \frac{\pi^2 E}{(\frac{K\ell}{r_T})^2}$$ (4.8)

in which

$$r_T^2 = \frac{I_y/2}{A_f + A_w/6} \ .$$ (4.9)

Eq. (4.9) applies to the compression flange in the elastic range. Basler and Thürlimann (10) recommended a transition curve from $F_{cr}$ at $L = 0$ to $F_{cr} = F_y/2$ at $\ell = r_T\sqrt{(2EC_b)/F_y}$, thus,

$$F_{cr} = F_y[1 - \frac{(\frac{K\ell}{r_T})^2 F_y}{4\pi^2 EC_b}] \ .$$ (4.10)

Although there have been several different suggestions (13,52) for K and $C_b$ in Eqs. (4.8) and (4.10), the provisions in the AISC Specification will be used in this research to determine these values because the provisions give a good approximation (38) and have been widely used in the United States.

According to the AISC Specification (50), $C_b$ is determined by

$$C_b = 1.75 + 1.05(M_1/M_2) + 0.3(M_1/M_2)^2 \le 2.3$$ (4.11)

in which $M_1$ is the smaller and $M_2$ the larger bending moment at the ends of the unbraced length, and $M_1/M_2$ is positive for reversed-curvature bending and negative for single-curvature bending. If the bending moment at any point within the span is larger than that at both ends, $C_b$ is taken as unity. The value of K is taken as 1.0 when both ends are hinged and 0.5 when both ends are fixed.

### 4.1.1.2  Local buckling of the compression flange

A slender plate under uniform compression may develop a wave form as shown in Figure 4.4a. The critical stress for this rectangular plate is given by (27)

$$F_{cr} = \frac{k\pi^2 E}{12(1 - \nu^2)(\frac{b}{w})^2} \tag{4.12}$$

in which k is the plate buckling coefficient, and b and w are the width and thickness of the plate, respectively.

This same phenomenon can occur in the compression flange of plate girders. This is called "local buckling of the compression flange". For plate girders, b and w in Eq. (4.12) denote half of the flange width and the flange thickness, respectively.

The value of k is approximately determined by edge conditions of the plate as shown in Figure 8b (13). Basler and Thürlimann (10) assumed no restraint on the flange from the web and recommended the use of k = 0.425.

Eq. (4.12) is applicable as long as the flange is in the elastic range. In the inelastic range, Basler and Thürlimann (10) suggested the transition curve such that for

$$b/w < 0.45 \sqrt{\frac{k\pi^2 E}{12(1 - \nu^2)F_y}} \quad ,$$

(a)



k = 4.0



k = 5.42



k = 6.97



k = 1.277



k = 0.425

Fixed end

Pinned end

(b)
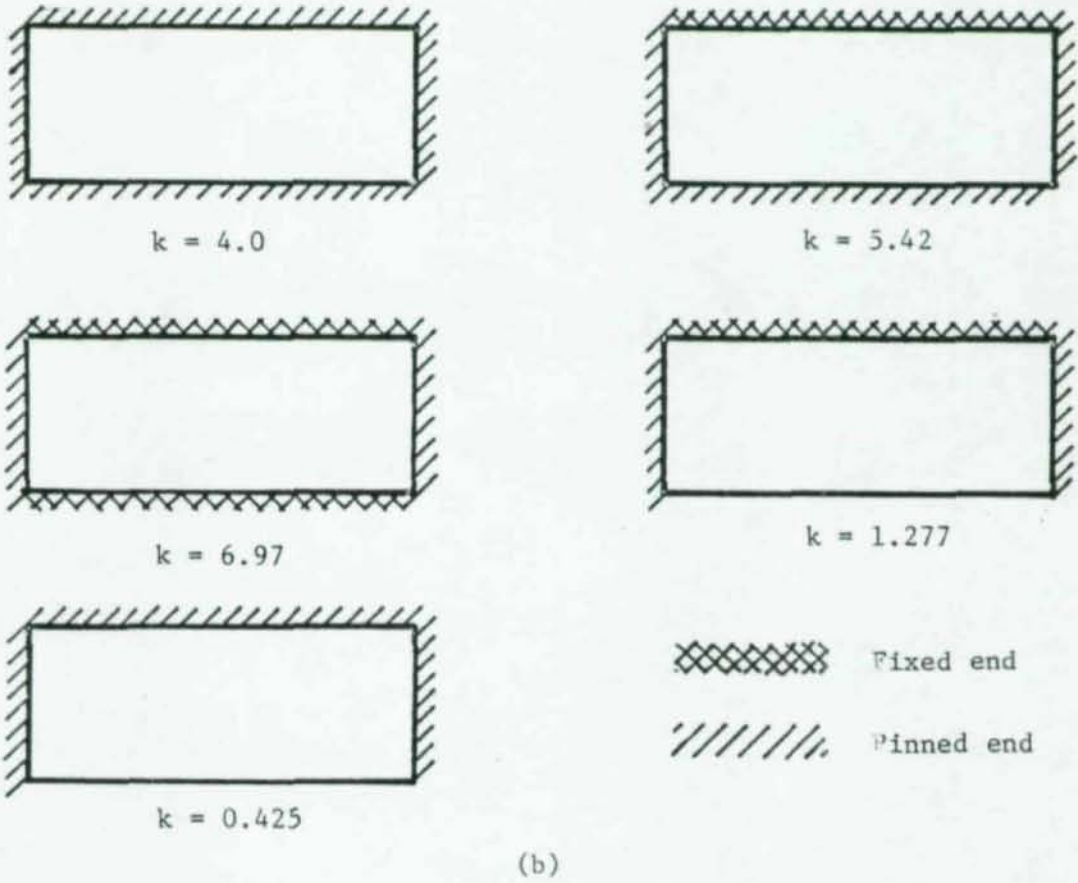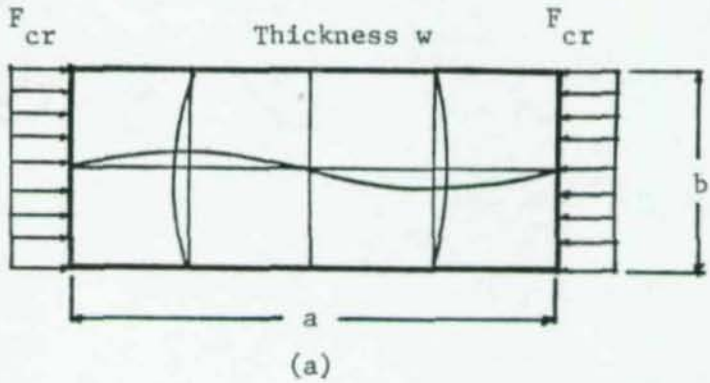
Figure 8.  Values of plate buckling coefficient k

$$F_{cr} = F_y \ , \tag{4.13}$$

and for

$$0.45 \sqrt{\frac{k\pi^2 E}{12(1 - v^2)F_y}} < b/w < \sqrt{\frac{k\pi^2 E}{6(1 - v^2)F_y}} \ ,$$

$$F_{cr} = F_y[1 - 0.53(\frac{b}{w}\sqrt{\frac{12(1 - v^2)F_y}{k\pi^2 E}} - 0.45)^{1.36}] \ . \tag{4.14}$$

### 4.1.2 Hybrid girders

The equations discussed in the previous section are for regular girders. Since the web of a plate girder contributes only a small part of the bending resistance, and its shear resistance depends on the web area and its slenderness ratio, a plate girder may be designed such that the web is of a lower-grade steel than the flange. This kind of plate girders is called the hybrid girder.

The general bending behavior (16) of hybrid girders is shown in Figure 9 with the corresponding variation of stress distribution. In the figure, linearity between load and deflection holds only up to the point where the web immediately adjacent to the flange begins to yield (point A). However, the curvature of the segment AB is so small that OAB is practically straight. After yielding of the flange (point B), the increasing rate of moment falls off rapidly. Thus, the bending behavior of the hybrid girders is virtually the same as that of homo-geneous or regular girders, though the ultimate bending strength of regular girders is higher than that of hybrid girders. Therefore, the ultimate bending strength of hybrid girders can be determined by either the flange-yield moment or the moment determined by Eq. (4.6), whichever
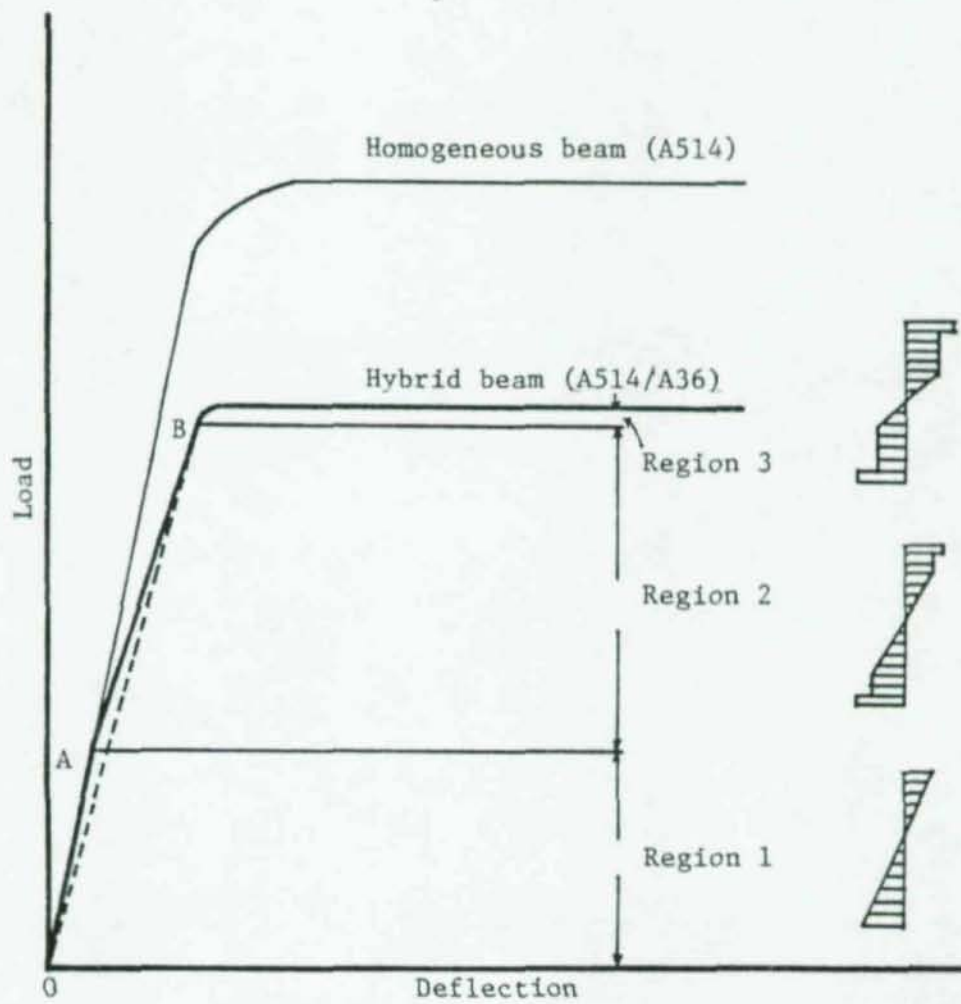
Figure 9. Theoretical load deflection curve for hybrid girder (16)

is smaller. A Joint ASCE-AASHO Committee (16) suggested the following equation for the flange-yield moment, Myf.

$$Myf = My[\frac{12 + p(3s - s^2)}{12 + 2p}]$$

(4.15)

in which s is the ratio of the web yield stress to the flange yield stress, and p is the ratio of the web cross-sectional area to the flange cross-sectional area. If instability of the flange is incorporated into Eq. (4.15), the ultimate bending strength of hybrid girders can be determined by either

$$M_u = F_{cr} \cdot S_x [1 - 0.0005 \frac{A_w}{A_f}(\frac{h}{t} - \sqrt{\frac{k\pi^2 E}{12(1 - v^2)Fcr}})]$$

(4.16)

or

$$M_u = F_{cr} \cdot S_x [\frac{12 + p(3s - s^2)}{12 + 2p}]$$

(4.16)

whichever is smaller. Lew, et al. (35), showed that this approach agreed well with test results, and the AISC Specification (50) has adopted this model. In Eqs. (4.6) and (4.16), $F_{cr}$ is determined by either Eqs. (4.8) or (4.13) in the elastic range, whichever is smaller. In the inelastic range, Eqs. (4.10), (4.13) or (4.14) are used for $F_{cr}$ in the above equations.

### 4.1.3 Unsymmetrical girders

Unsymmetrical plate girders have cross-sections whose centroidal axes do not coincide with the horizontal centerline of the web plate. Although more exact solutions (29,42,45) for the ultimate bending strength of unsymmetrical girders exist, present design specifications do not take into consideration the behavior of unsymmetrical girders. Test results by Ostapenko, et al (41,48) showed that the ultimate

bending strength of unsymmetrical girders was 6%-9% above that predicted by the equations for symmetrical girders, with modification of the neutral axis. Since this variation from the predicted values is even smaller than the variation of ultimate bending strength of regular girders, no particular consideration is given for unsymmetrical girders in this study, except the adjustment of the neutral axis according to geometric shapes of the cross-section.

## 4.2 Variation of the Ultimate Bending Strength

The theoretical ultimate bending strength of plate girders can be simply expressed by

$$M_u = F_{cr} \cdot S_x \cdot R_{PG} \tag{4.17}$$

in which $F_{cr}$ is the smallest critical stress corresponding to instability of the compression flange, $S_x$ is the section modulus, and $R_{PG}$ is a reduction factor. Variations of measured ultimate bending strength may come from variations of the three factors in Eq. (4.17) and idealization or simplification of bending behavior of the plate girder in the theoretical model.

To determine the resistance factor in Eq. (2.23), data on variations associated with these factors are necessary. This is discussed in the following sections.

### 4.2.1 Variation in stress due to variation of material properties

If instability of the compression flange exists, the critical stress, $F_{cr}$, is, as shown in Eqs. (4.9) and (4.13), a function of the modulus of elasticity, E, Poisson's ratio, $\nu$, and a cross-sectional property, (h/t) or (b/w). Otherwise, it is a function of the flange yield stress only. Variation of critical stress due to variations of material properties E

and $\nu$ can be determined from Eqs. (2.6) and (2.7) by substituting E = 30,000 ksi, the C.O.V. of E = 0.05, $\nu$ = 0.3, and the C.O.V. of $\nu$ = 0.03 into Eqs. (4.9) and (4.12). The result, the C.O.V. of $F_{cr}$ for bending due to instablity of the compression flange, is equal to 0.06. In the case that the critical stress is the same as the flange yield stress, the C.O.V. of $F_{cr}$ is equal to 0.12. Since most plate girders in practice are designed to prevent instability of the compression flange, the C.O.V. = 0.12 is selected as a characteristic value representing stress variation of bending due to variation of material properties.

### 4.2.2 Variation of cross-sectional properties

Cross-sectional properties affecting the ultimate bending strength of plate girders are the section modulus, $S_x$, and the reduction factor, $R_{PG}$, which is a function of the web slenderness ratio. However, as discussed in Section 3.3, it is difficult to estimate the C.O.V. of every cross-sectional property due to a lack of information. Thus, as previously shown, a C.O.V. = 0.05 will be used for variation of cross-sectional properties.

### 4.2.3 Uncertainty in the theoretical model

By virtue of simplification or idealization of structural behavior, theoretical models invariably have some amount of error in the prediction of strengh of structural members. The error can be measured by comparison of experiment ultimate bending strength with theoretical values. A comparison of experimental bending strength with theoretical ultimate bending strength is given in Table 8. For the theoretical values, E = 30,000 ksi and $\nu$ = 0.3 have been used with the measured static yield stress.

## Table 8

## Comparison of Experimental and Theoretical Ultimate Bending Strength

| Reference Source | Test No. | h/t (1) | b/w (2) | $S_x$ (3) | $F_{ys}$ (4) | $\frac{(F_{cr}) \text{lat}/}{F_{ys}}$ (5) | $\frac{(F_{cr}) \text{loc}/}{F_{ys}}$ (6) | $R_{PG}$ (7) | $M_{ex}/M_{th}$ (8) |
|---|---|---|---|---|---|---|---|---|---|
| | G1-T1 (a) | 185 | 24 | 555 in$^3$ | 35.4 ksi | 1.00 | 0.56 | 1.000 | 1.11 |
| | G2-T1 (a) | 185 | 8 | 577 | 38.6 | 0.98 | 1.00 | 0.983 | 0.96 |
| | G2-T2 (a) | 185 | 8 | 577 | 38.6 | 1.00 | 1.00 | 0.982 | 0.99 |
| | G3-T1 (a) | 185 | – | 561 | 35.5 | 0.96 | 1.00 | 0.983 | 1.03 |
| (11) | G3-T2 (a) | 185 | – | 561 | 35.5 | 0.99 | 1.00 | 0.985 | 1.05 |
| | G4-T1 (a) | 388 | 8 | 522 | 37.6 | 0.98 | 1.00 | 0.911 | 1.00 |
| | G4-T2 (a) | 388 | 8 | 522 | 37.6 | 1.00 | 1.00 | 0.921 | 1.03 |
| | G5-T1 (a) | 388 | – | 509 | 35.5 | 0.97 | 1.00 | 0.912 | 1.04 |
| | G5-T2 (a) | 388 | – | 509 | 35.5 | 0.99 | 1.00 | 0.913 | 1.14 |
| | G-A | 166.7 | 6.5 | 2300 cm$^3$ | 3240 kg/cm$^2$ | 0.79 | 1.00 | 0.989 | 0.81 |
| | G-B | 166.7 | 7.5 | 1960 | 3810 | 0.72 | 1.00 | 1.000 | 0.81 |
| | G-C | 133.3 | 5.5 | 1520 | 7850 | 0.59 | 1.00 | 0.985 | 0.99 |
| (23) | G-D | 133.3 | 5.5 | 1520 | 7850 | 0.71 | 1.00 | 0.962 | 1.03 |
| | G-E | 133.3 | 5.5 | 1680 | 7850 | 0.73 | 1.00 | 0.964 | 1.04 |
| | G-F | 133.3 | 5.5 | 1680 | 7850 | 0.80 | 1.00 | 0.954 | 1.11 |
| | G-G* | 133.3 | 5.5 | 1520 | 7850 | 0.59 | 1.00 | 0.953 | 1.01 |
| | B-1* | 288 | 8 | 171 in$^3$ | 116.4 ksi | 1.00 | 1.00 | 0.89 | 0.948 |
| | B-2* | 144 | 8 | 198 | 116.4 | 1.00 | 1.00 | 0.81 | 0.988 |
| | B-4* | 288 | 8 | 171 | 110.4 | 1.00 | 1.00 | 0.89 | 0.951 |
| (35) | B-5* | 288 | 8 | 171 | 110.4 | 1.00 | 1.00 | 0.89 | 0.861 |
| | B-6* | 192 | 8 | 185 | 110.4 | 1.00 | 1.00 | 0.81 | 0.870 |
| | B-7* | 144 | 8 | 198 | 110.4 | 1.00 | 1.00 | 0.81 | 0.924 |
| | B-8* | 144 | 8 | 198 | 110.4 | 1.00 | 1.00 | 0.81 | 0.933 |
| (41) | UG1.2** | 295 | 6.4 | 224 | 34.2 | 0.91 | 1.00 | 0.95 | 1.158 |
| | UG2.3** | 295 | 6.4 | 224 | 36.7 | 0.91 | 1.00 | 0.95 | 0.912 |

Notes:  
    *:   Hybrid girder  
    **:  Unsymmetrical girder  
  (a):  Data used in Galambos' study  
  (1):  Web slenderness ratio  
  (2):  Flange slenderness ratio  
  (3):  Section modulus  
  (4):  Mean measured static yield stress of the flange  
  (5):  Critical stress due to lateral buckling/(4)  
  (6):  Critical stress due to local buckling/(4)  
  (7):  Reduction factor  
  (8):  Experimental/theoretical ultimate bending strength

From Table 8, the mean value of $M_{ex}/M_{th}$ is estimated to be 1.0 and the C.O.V. of $M_{ex}/M_{th}$, $\Omega_p$, to be 0.10.

Therefore, by substituting the values of $\Omega_M = 0.12$, $\Omega_F = 0.05$ and $\Omega_p = 0.10$ into Eq. (2.22), the C.O.V. associated with the bending resistance, $\Omega_R$, is equal to 0.16.

### 4.3 Bending Resistance Factor

### 4.3.1 Safety index β

The safety index β which is given by Eq. (2.13) can be obtained through calibration with currently used specifications such that the same degree of reliability is obtained in the new criterion as in the existing design method for a member in a standard situation. In this work, calibration is performed with the AISC Specification for a simply supported, compact, adequately braced regular girder. A plate girder is assumed to be designed according to Part 1 (elastic design) of the AISC Specification (50).

If a plate girder is the standard situation described above is loaded with uniformly distributed dead and live loads, the maximum moment on the girder is expressed by

$$M_{max} = C_D \cdot D_c + C_L \cdot L_c \cdot R_{LL} \tag{4.18}$$

in which $C_D$ and $C_L$ are influence coefficients of dead and live loads, respectively, $D_c$ and $L_c$ are, respectively, dead and live load intensities defined by the code (6), and $R_{LL}$ is a live load reduction factor which is, according to ANSI A.58.1-1980 Draft, given by

$$R_{LL} = (0.25 + \frac{15}{\sqrt{A_I}}) \text{ for } L_c \leq 100 \text{ psf and } A_I \geq 400 \text{ sq. ft.} \tag{4.19}$$

in which $A_I$ is the influence area which is twice the tributary area for a beam-type member.

According to Part 1 of the AISC Specification, the elastic section modulus $S_x$ is determined by

$$S_x = \frac{M_{max}}{F_b \cdot R_{PG}} = \frac{C_D D_c + C_L L_c R_{LL}}{F_b \cdot R_{PG}} \qquad (4.20)$$

in which $F_b$ is the allowable bending stress defined by the specification and $R_{PG}$ is a stress reduction factor. For the standard case, $F_b$ is given by

$$F_b = 0.66 F_y \quad . \qquad (4.21)$$

Since the critical stress is the same as the yield stress for the given standard situation, the mean experimental ultimate bending strength, $M_m$, of plate girders may be expressed by

$$M_m = F_{ysm} \cdot S_x \cdot R_{PG} \cdot (M_{ex}/M_{th})_m \qquad (4.22)$$

in which $F_{ysm}$ is the mean static yield stress and $(M_{ex}/M_{th})_m$ is the mean ratio of experimental to theoretical ultimate bending strength. $F_{ysm} = 1.0 F_y$ and $(M_{ex}/M_{th})_m = 1.0$ have been estimated in Section 3.3 and Section 4.2, respectively.

Substitution of Eqs. (4.20) and (4.21) into Eq. (4.22), and simplification yields

$$M_m = 1.515 (C_D \cdot D_c + C_L \cdot L_c \cdot R_{LL}) \quad . \qquad (4.23)$$

The mean applied load, moment in this case, $Q_m$, is given by

$$Q_m = C_D \cdot D_m + C_L \cdot L_m \qquad (4.24)$$

in which $D_m$ and $L_m$ are the mean applied dead and live load intensities, respectively. The mean applied dead load intensity, $D_m$, is assumed to be the same as the code specified load $D_c$. The applied live load intensity, $L_m$, is, according to the Ellingwood-Culver equation,

$$L_m = 18.7 + \frac{520}{\sqrt{A_I}} \quad . \qquad (3.3)$$

The C.O.V. of applied loads, $\Omega_Q$, which is independent from resistance capacity, and the C.O.V. of bending resistance, $\Omega_R$, have been estimated in previous sections to be 0.13 and 0.16, respectively. $C_D$ and $C_L$ are the same for the uniformly distributed dead and live loads.

The determination of $\beta$ is accomplished by knowing $M_m$, $Q_m$, $\Omega_R$, and $\Omega_Q$. By taking $L_c = 50$ psf for office buildings, variation of $\beta$ with respect to tributary area, $A_T$, and code specified dead load, $D_c$, is shown in Figure 10. The figure shows that the value of $\beta$ approaches 2.0 with an increase of the code specified dead load and the tributary area. Therefore, $\beta = 2.0$ is selected as a safety index for bending resistance.

### 4.3.2  Resistance factor $\phi_m$

The resistance factor for bending is determined by

$$\phi_m = \frac{R_m}{R_n} \exp(-\alpha\beta\Omega_R) \tag{2.20}$$

in which $R_m$ is the mean experimental ultimate bending strength, $M_m$; $R_n$ is the theoretical ultimate bending strength, $M_n$; and $\alpha$ is a linearization factor which is determined by Eq. (2.17). Thus, from $\Omega_R = 0.16$ and $\Omega_Q = 0.13$, $\alpha = 0.70$ is obtained.

The nominal ultimate bending strength for plate girders in the standard situation is given by

$$M_n = F_y \cdot S_x \cdot R_{PG} \tag{4.26}$$

and the mean measured ultimate bending strength can be expressed as

$$M_m = F_{ysm} \cdot S_x \cdot R_{PG} \cdot (M_{ex}/M_{th})_m . \tag{4.22}$$

Since $F_{ysm}/F_y = 1.0$ and $(M_{ex}/M_{th})_m = 1.0$ from Section 3.3 and Section 4.2, $M_m/M_n$ becomes unity.

Therefore, by substituting $M_m/M_n = 1.0$, $\alpha = 0.70$, $\beta = 2.0$ and $\Omega_R = 0.16$ into Eq. (2.20), the resistance factor $\phi_m = 0.80$ is obtained for bending.
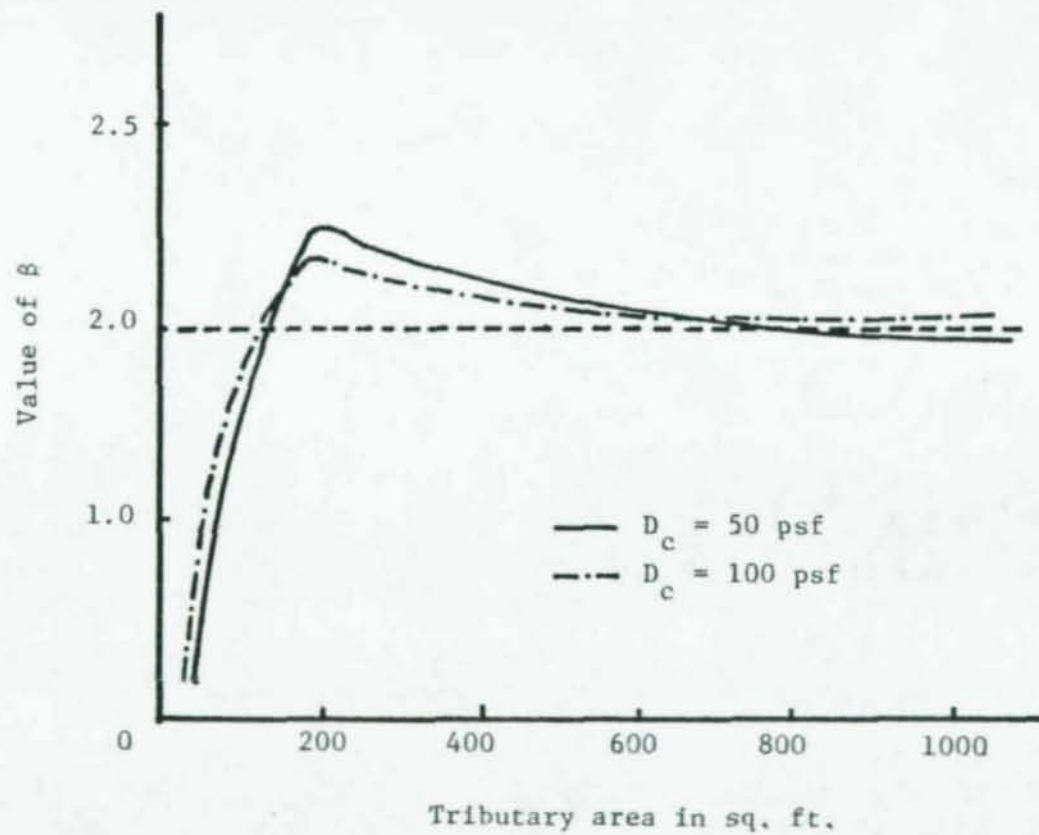
Figure 10. Variation of safety index β for bending with tributary area

Compared with a value of $\phi_m = 0.86$ presented in Galambos' work (24), $\phi_m = 0.80$ is relatively small, which means this study has selected a more conservative value for the bending resistance. This difference is, as shown in Table 9, due to differences of most factors used in the determination of $\phi_m$, though almost the same equations have been used in Galambos' work and in this work.

In general, the sampled data in the works of Galambos (24,25,26) have smaller variations than those used in this research, which resulted in the difference in the resistance factors. Furthermore, $\alpha = 0.55$ used in Galambos' work is unreasonably small. In the range of $1/3 < \Omega_Q/\Omega_R < 3$, $\alpha = 0.75$ gives a good approximation with less than 6% error (36). The value of $\alpha$ used in his study could not be far beyond this range because he used the McGuire-Cornell live load model which gives almost the same distribution of live load as that used in this study.

## Table 9

### Summary of Results -- Bending Resistance Factor

| Parameter | Galambos' Value (24) | Selected Value |
|---|---|---|
| $\Omega_R$ | 0.14 | 0.16 |
| $\Omega_M$ | 0.10 | 0.12 |
| $\Omega_F$ | 0.05 | 0.05 |
| $\Omega_P$ | 0.08 | 0.10 |
| $\Omega_Q$ | Not shown | 0.13 |
| $\alpha$ | 0.55 | 0.70 |
| $\beta$ | 3.0 | 2.0 |
| $M_m/M_n$ | 1.03 | 1.0 |
| $\phi_m$ | 0.86 | 0.80 |

## Chapter 5

### PLATE GIRDER IN SHEAR

## 5.1 Ultimate Shear Strength

In evaluating the behavior of plate girders subject to shear, it is assumed that the web is a plane and the material is elastic-plastic. Such a web buckles at a stress that can be predicted by (38)

$$F_{vcr} = \frac{k\pi^2 E}{12(1 - \nu^2)(\frac{h}{t})^2} \tag{5.1}$$

in which $F_{vcr}$ denotes the critical shear stress, k is the shear buckling coefficient, and h and t are the depth and thickness of the web, respectively. The behavior explained by Eq. (5.1) is called "beam action" of plate girders. Subsequent to the web buckling, the stress distribution in the web changes and considerable postbuckling strength may be developed due to diagonal tension. This is called "tension field action" of plate girders and is shown in Figure 11. However, the exact distribution of the diagonal tension has been unknown (33).

Basler (9) was the first to successfully formulate a model for the tension field action of plate girders. Since the Basler formula was proposed, many variations of the postbuckling tension field have been developed (22,42,46). The main differences among them are in their explanation of the tension field distribution. Johnston (33) showed a comparison of experimental to theoretical shear strength predicted by seven different models, in which the Basler formula gave good agreement with test results, even though it had a slightly larger variation than the other models.

Since it is a good predictor, and since it is familiar to designers in the United States mainly due to adoption in the AISC Specification,
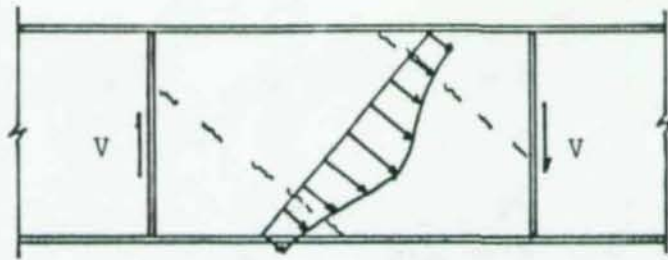
Figure 11.   General distribution of tension field
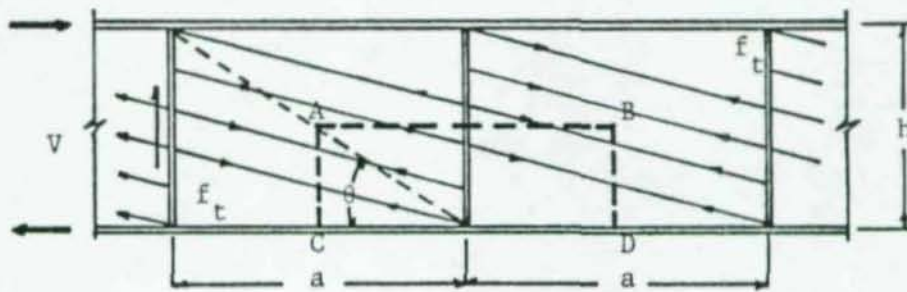


Figure 12.   Basler's tension field
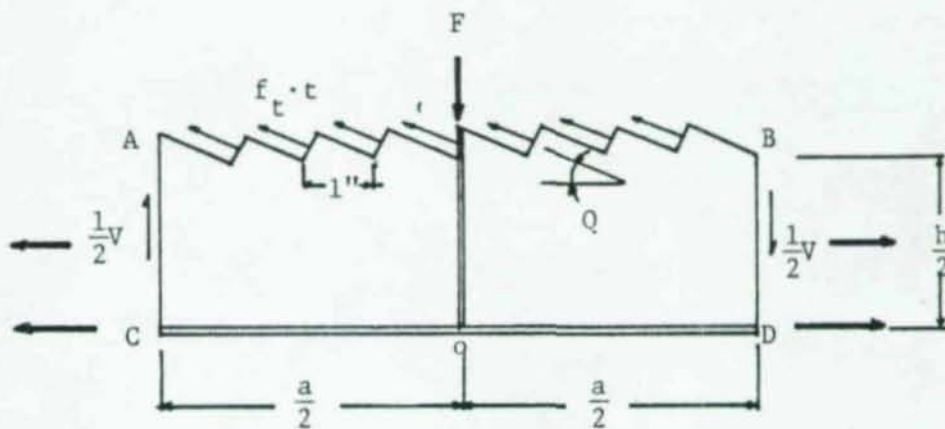


Figure 13.   Equilibrium conditions applied to a free body

the Basler formula is used in this research for prediction of the ulti-
mate shear strength of plate girders.

### 5.1.1 General equation for predicting ultimate shear strength

The tension field in a girder with transverse stiffeners is anchored
by the flanges and stiffeners, and the resulting lateral load on the flange
from the tension field causes the flange to bend inward. Therefore, the
nature of the tension field is influenced by the bending stiffness of the
flange.

Basler assumed that the flange was too flexible to support a lateral
loading from the tension field, so that the band shown in Figure 12
determines the shear strength.

A free body taken from Figure 12 is given in Figure 13. By taking
moments about point 0 in Figure 13, the shear strength, $V_t$, due to the
tension field action is predicted by

$$V_t = \frac{1}{2}f_t \cdot h \cdot t \cdot \sin 2\phi . \tag{5.2}$$

It is postulated that at ultimate shear, the angle $\phi$ in the figure will
be such as to maximize $V_t$. Thus,

$$\frac{dV_t}{d\phi} = f_t \cdot t(h\cos 2\phi - a\sin 2\phi) = 0 \tag{5.3}$$

from which

$$\tan 2\phi = \frac{h}{a} . \tag{5.4}$$

Since $\tan\theta = \frac{h}{a}$ is obtained from Figure 12, $2\phi$ is equal to $\theta$. Thus,
Equation (5.2) becomes

$$V_t = \frac{1}{2}f_t \cdot h \cdot t \cdot \sin\theta . \tag{5.5}$$

In the plate girders with slender webs, neither the pure beam action
nor the pure tension field action occurs alone, but rather the sum of

both. Therefore, the ultimate shear strength, $V_u$, is

$$V_u = V_{cr} + V_t \tag{5.6}$$

in which $V_{cr}$ is the shear strength through beam action. $V_{cr}$ is approximately given by

$$V_{cr} = F_{vcr} \cdot h \cdot t \quad . \tag{5.7}$$

Substitution of Eqs. (5.5) and (5.7) into Eq. (5.6) gives the ultimate shear strength as

$$V_u = F_{vcr} \cdot h \cdot t + \frac{1}{2} f_t \cdot h \cdot t \cdot \sin\theta \tag{5.8}$$

It has been found that the following equation approximates the von Mises yield criterion with less than 10% error (9)

$$\frac{f_t}{F_y} = 1 - \frac{F_{vcr}}{F_{vy}} \quad . \tag{5.9}$$

According to the von Mises yield criterion, the shear yield stress, $F_{vy}$ (27), is

$$F_{vy} = \frac{F_y}{\sqrt{3}} \quad . \tag{5.10}$$

Thus, by substituting Eqs. (5.9) and (5.10) into Eq. (5.8), the ultimate shear strength of plate girders is finally expressed as

$$V_u = A_w \left[ F_{vcr} + \frac{\sqrt{3}}{2} F_{vy} \left(1 - \frac{F_{vcr}}{F_{vy}}\right) \frac{1}{\sqrt{1 + u^2}} \right] \tag{5.11}$$

in which $u = \frac{a}{h}$ and $1/\sqrt{1 + u^2} = \sin\theta$. The ultimate shear stress $F_{vu}$ is obtained from Eq. (5.11) by dividing both sides by $A_w$; that is,

$$F_{vu} = F_{vcr} + \frac{\sqrt{3}}{2} F_{vy} \left(1 - \frac{F_{vcr}}{F_{vy}}\right) \frac{1}{\sqrt{1 + u^2}} \quad . \tag{5.12}$$

The critical shear stress, $F_{cr}$, given in Eq. (5.1) is valid only in the elastic range. The actual failure stress of compression elements

with a low slenderness ratio may exceed $F_{cr}$. Considering this effect, Basler (9) assumed that inelastic buckling would occur if $F_{vcr}$ exceeded $0.8F_{vy}$, and took the inelastic shear stress, $F_{vcri}$, as

$$F_{vcri} = \sqrt{0.8F_{vcr} \cdot F_{vy}} \ . \tag{5.13}$$

He also assumed that if $F_{vcri}$ exceeded $F_{vy}$, the tension field action could be neglected. Thus, the ultimate shear strength in this range is

$$V_u = F_{vcri} \cdot A_w \ . \tag{5.14}$$

### 5.1.2 Shear buckling coefficient k

For the shear buckling of plate girders, the web panel is considered as a plate. The shear buckling coefficient, k, of a plate is a function of not only the boundary conditions along the edges but the aspect ratio of the plate, $\frac{a}{h}$ in Figure 12. By the nature of the flexible flange in his model, Basler (9) assumed four pinned edges of the web panel. For this case, the following equation (13) gives a good approximation to the value of k as long as the aspect ratio, $u = \frac{a}{h}$, is greater than 1:

$$k = 5.34 + \frac{4.0}{u^2} \ . \tag{5.15}$$

If the aspect ratio is less than 1, the roles of two sides of the web panel in preventing buckling are reversed, and the value of k is given by

$$k = 4.0 + \frac{5.34}{u^2} \ . \tag{5.16}$$

### 5.2 Variation of Ultimate Shear Strength

The ultimate shear strength can be simply expressed by

$$V_u = F_{vu} \cdot A_w \tag{5.17}$$

in which $F_{vu}$ is determined by either Eq. (5.12) or Eq. (5.13). Thus, the ultimate shear stress is expressed in terms of stress and a dimensional property. Since these two terms vary due to variations of material properties and of dimensional properties, the ultimate shear strength also shows variation. Uncertainty associated with the theoretical model is another factor causing variation in the ultimate shear strength.

To determine the shear resistance factor, $\phi_v$, in Eq. (2.23), data on variations in these factors should be known. They are discussed in the following sections.

### 5.2.1 Variation of the ultimate shear stress

The ultimate shear stress of plate girders with slender webs is, as shown in Eqs. (5.12) and (5.1), determined not only by material properties, E, $\nu$, and $F_{yw}$, but also by dimensional properties, $\frac{h}{t}$ and $\frac{a}{h}$. Since variation of dimensional properties is separately reflected in the C.O.V. of cross-sectional properties, $\Omega_F$, only the material properties are considered as random variables here. Thus, by utilizing Eqs. (2.6) and (2.7), the mean ultimate shear stress and the variance are expressed by

$$F_{vum} = (1 - \frac{1}{2\sqrt{1 + u^2}})\frac{k\pi^2 E_m}{12(1 - \nu_m^2)(\frac{h}{t})^2} + \frac{1}{2}F_{yswm}\frac{1}{\sqrt{1 + u^2}} \qquad (5.18)$$

and

$$Var[F_{vu}] = [1 - \frac{3}{4(1 + u^2)}]Var[F_{vcr}] + \frac{1}{4(1 + u^2)}Var[F_{ysw}] \qquad (5.19)$$

in which the subscript m denotes the mean value, and $Var[F_{vcr}]$ is given by

$$Var[F_{vcr}] = [\frac{k\pi^2 E_m}{12(1 - \nu_m^2)(\frac{h}{t})^2}]^2[\Omega_E^2 + \frac{4\nu_m^2}{(1 - \nu_m^2)}\Omega_\nu^2 \nu_m^2] \qquad (5.20)$$

where $\Omega_E$ and $\Omega_\nu$ are the C.O.V.s of the modulus of elasticity and Poisson's ratio, respectively. From the above equations, it is apparent that the C.O.V. of the ultimate shear stress is affected by the web slenderness ratio and the aspect ratio of the web panel. Variations of the C.O.V. of the ultimate shear stress, $\Omega_m$, with respect to the aspect ratio, $\frac{a}{h}$, and the slenderness ratio, $\frac{h}{t}$, are shown in Figure 14, where $E_m$ = 30,000 ksi, $\Omega_E$ = 0.05, $\nu_m$ = 0.3, $\Omega_\nu$ = 0.03 and $F_{yw}$ = 36 ksi have been used (Table 6). Figure 14 shows that the C.O.V. of the shear stress increases with an increase of the web slenderness ratio and the aspect ratio of the web panel. For the selection of $\Omega_M$ associated with the ultimate shear stress, it is assumed that a high slenderness web is not accompanied by a web with a high aspect ratio. Thus, an aspect ratio $\frac{a}{h}$ = 1.5 and $\frac{h}{t}$ = 250 $\sim$ 300 is considered as a typical proportion for plate girders. From this assumption, $\Omega_M$ = 0.25 is selected as the C.O.V. of the ultimate shear stress.

### 5.2.2 Uncertainty of theoretical model

The theoretical formula, which is given by Eq. (5.11) or Eq. (5.14), for predicting the ultimate shear strength inevitably deviates from actual performance due to idealization or simplification in the model. The average error of theoretical models can be measured by comparing the experimental and theoretical ultimate shear strength. Table 10 gives summarized results of comparisons between experimental values and theoretical values of the ultimate shear strength of plate girders. Measured static yield stresses of the web have been used for the theoretical shear strength. From the data in Table 10, $(V_{ex}/V_{th})_m$ = 1.08 and the C.O.V., $\Omega_p$ = 0.12 are obtained. Johnston (33) concluded, from data including only regular girders, that the Basler formula had $(V_{ex}/V_{th})_m$ =
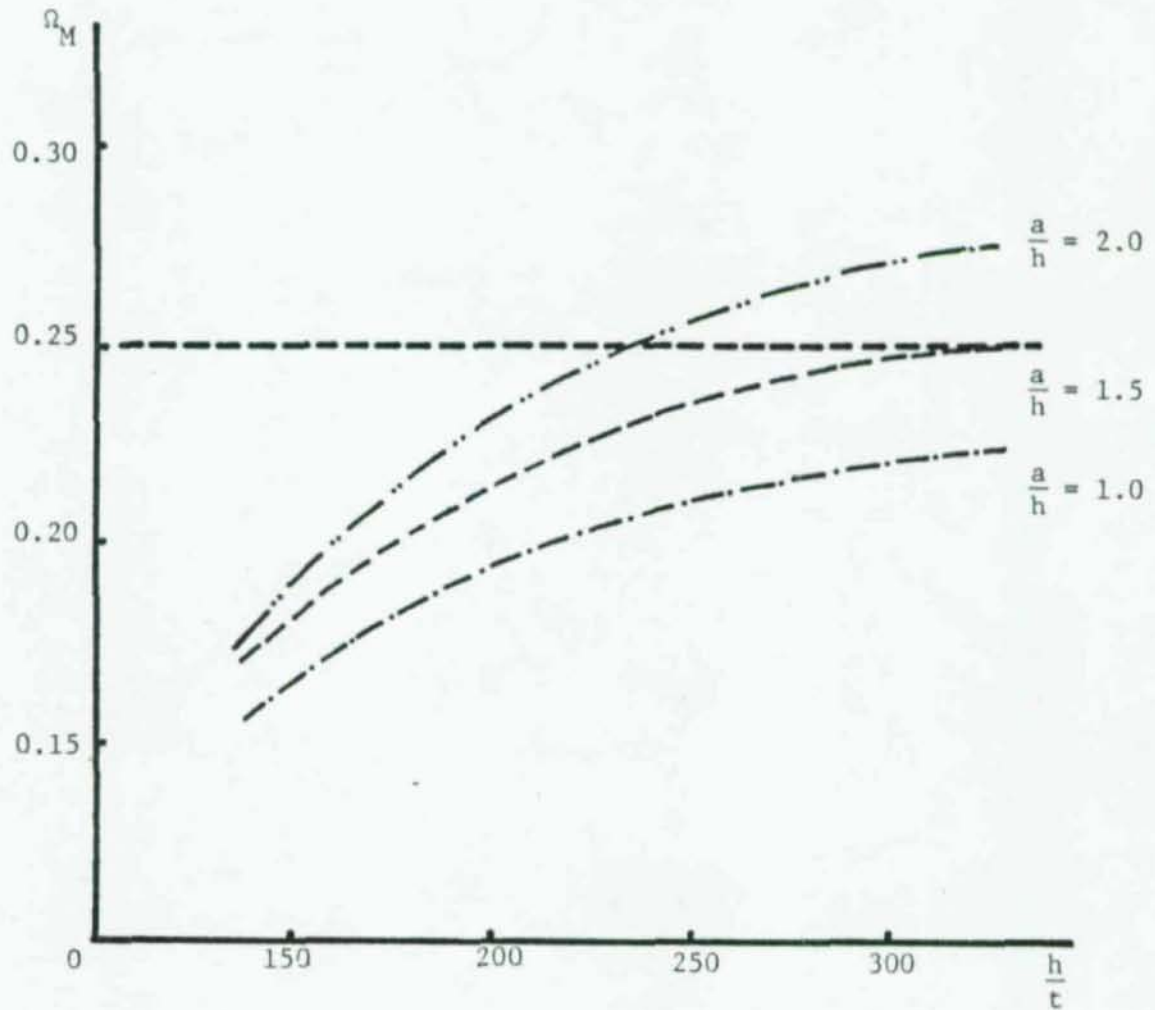
Figure 14.  C.O.V. of ultimate shear stress, $\Omega_M$, vs web slenderness ratio, $\frac{h}{t}$

## Table 10

### Comparison of Experimental and Theoretical
### Ultimate Shear Strength

| Reference Source | Test Number | $\dfrac{a}{h}$ (1) | $\dfrac{h}{t}$ (2) | $F_{ysw}$ (3) (ksi) | $F_{cr}$ (4) (ksi) | $A_w$ (5) (sq.in.) | $\dfrac{V_{ex}}{V_{th}}$ (6) |
|---|---|---|---|---|---|---|---|
| | G6-T1 (a) | 1.50 | 259 | 36.7 | 2.87 | 9.65 | 1.03 |
| | G6-T2 (a) | 0.75 | 259 | 36.7 | 5.45 | 9.65 | 0.95 |
| (11) | G6-T3 (a) | 0.50 | 259 | 36.7 | 10.21 | 9.65 | 0.98 |
| | G7-T1 (a) | 1.00 | 255 | 36.7 | 3.88 | 9.80 | 0.99 |
| | G7-T2 (a) | 1.00 | 255 | 36.7 | 3.88 | 9.80 | 1.02 |
| | UG 1.1 * | 0.80 | 295 | 43.4 | 3.83 | 4.50 | 1.09 |
| (41) | UG 2.1* | 1.20 | 295 | 43.4 | 2.52 | 4.50 | 1.12 |
| | UG 3.1* | 1.60 | 295 | 43.4 | 2.14 | 4.50 | 1.19 |
| (35) | S-1** | 0.83 | 191 | 40.8 | 8.73 | 6.80 | 0.92 |
| | S-2** | 0.83 | 191 | 40.8 | 8.73 | 6.80 | 0.85 |
| (43) | F10-1 | 1.50 | 195 | 38.7 | 5.06 | 12.50 | 1.09 |
| | F10-5 | 1.20 | 195 | 38.7 | 5.77 | 12.50 | 1.02 |
| | G1-1 | 3.00 | 182 | 70.4 | 4.71 | 12.30 | 1.21 |
| (22) | G1-2 | 1.50 | 182 | 70.4 | 5.80 | 12.30 | 1.02 |
| | G2-1 | 3.00 | 144 | 70.4 | 7.53 | 9.70 | 1.34 |
| | G2-2 | 1.50 | 144 | 70.4 | 9.27 | 9.70 | 1.17 |
| (22) | H1-T1 (a) | 3.00 | 127 | 108.1 | 9.68 | 19.65 | 1.33 |
| | H1-T1 (a) | 1.50 | 127 | 108.1 | 11.92 | 19.65 | 1.08 |

Note:  *:  Unsymmetrical girders

       **:  Hybrid girders

       (a):  Data used in Galambos' study.  Some data used for shear analysis in his study cases in this study are categorized as the combined shear and bending.

       (1):  The aspect ratio of the web panel

       (2):  The web slenderness ratio

       (3):  Measured static yield stress of the web

       (4):  Critical stress of the web

       (5):  Area of the web

       (6):  Experimental/theoretical ultimate shear strength

1.05 and the C.O.V. = 0.13. Galambos had lower values, with $(V_{ex}/V_{th})_m =$ 1.03 and the C.O.V. = 0.11 from data taken from two sources. Compared with the data used in those two studies, relatively representative data, have been collected in Table 10. Thus, $(V_{ex}/V_{th})_m = 1.08$ and $\Omega_p = 0.12$ are taken as appropriate values.

## 5.3 Shear Resistance Factor

### 5.3.1 Safety index β

To determine the safety index β given in Eq. (2.13) for the shear strength, values of the ratio of the mean measured ultimate shear strength to the mean applied shear force, $V_{um}/Q_m$, and the C.O.V.s of shear resistance and applied shear force, $\Omega_R$ and $\Omega_Q$ are required.

$\Omega_Q = 0.13$ has been estimated in Section 3.2, and from the values of $\Omega_M = 0.25$, $\Omega_p = 0.12$ and $\Omega_F = 0.25$, the C.O.V. of shear resistance, $\Omega_R$, is found to be 0.28. Thus, by using Eq. (2.17), the linearization factor, $\alpha = 0.75$ is determined.

The ratio of $V_{um}$ to $Q_m$ is obtained through calibration with the AISC Specification, Part 1.

A simply supported plate girder under uniformly distributed dead and live loads is subjected to a maximum shear force given by

$$V_{max} = C_D \cdot D_c + C_L \cdot L_c \cdot R_{LL} \tag{5.21}$$

in which $C_D$ and $C_L$ are influence factors of dead and live loads, respectively, $D_c$ and $L_c$ are the code specified dead and live loads intensities, and $R_{LL}$ is a live load reduction factor which is given by Eq. (4.19).

According to the AISC Specification, the required web area, $A_w$, to resist the applied shear force is

$$A_w = \frac{V_{max}}{F_V} = \frac{C_D \cdot D_c + C_L \cdot L_c \cdot R_{LL}}{F_v} \tag{5.22}$$

where $F_v$ is an allowable shear stress which is approximately equal to

$$F_v = \frac{F_{vu}}{1.65} \qquad (5.23)$$

in which $F_{vu}$ is the ultimate shear stress given in Eq. (5.12).

The mean measured ultimate shear strength, $V_{um}$, can be expressed by

$$V_{um} = F_{vum} \cdot A_w \cdot (V_{ex}/V_{th})_m \quad . \qquad (5.24)$$

Since $F_{vum}/F_{vu}$ is approximately equal to $F_{yswm}/F_{yw}$ which has been pre-viously estimated to be 1.10, substitution of Eqs. (5.22) and (5.23) into Eq. (5.24) gives the mean ultimate shear strength as

$$V_{um} = 1.96(C_D \cdot D_c + C_L \cdot L_c \cdot R_{LL}) \quad . \qquad (5.25)$$

The mean applied shear force can be expressed by

$$Q_m = C_D \cdot D_m + C_L \cdot L_m \qquad (5.26)$$

in which $D_m$ is the mean applied dead load that is assumed to be equal to the code specified dead load, $D_c$, and $L_m$ the mean applied live load that is determined by Eq. (3.3).

By substituting all known values discussed above into Eq. (2.13), the value of the shear safety index $\beta$ can be determined. The variation of $\beta$ with respect to tributary area $A_T$ and code specified dead load $D_c$ are shown in Figure 15. The figure shows that the value of $\beta$ approaches 2.2 with increasing $A_T$. Therefore, $\beta = 2.2$ is taken as the shear safety index.

## 5.3.2  Shear resistance factor $\phi_V$

To determine the shear resistance factor, $\phi_v$, given in Eq. (2.20), the ratio of the mean experimental shear strength to nominal ultimate shear strength, $V_{um}/V_n$, should be known.
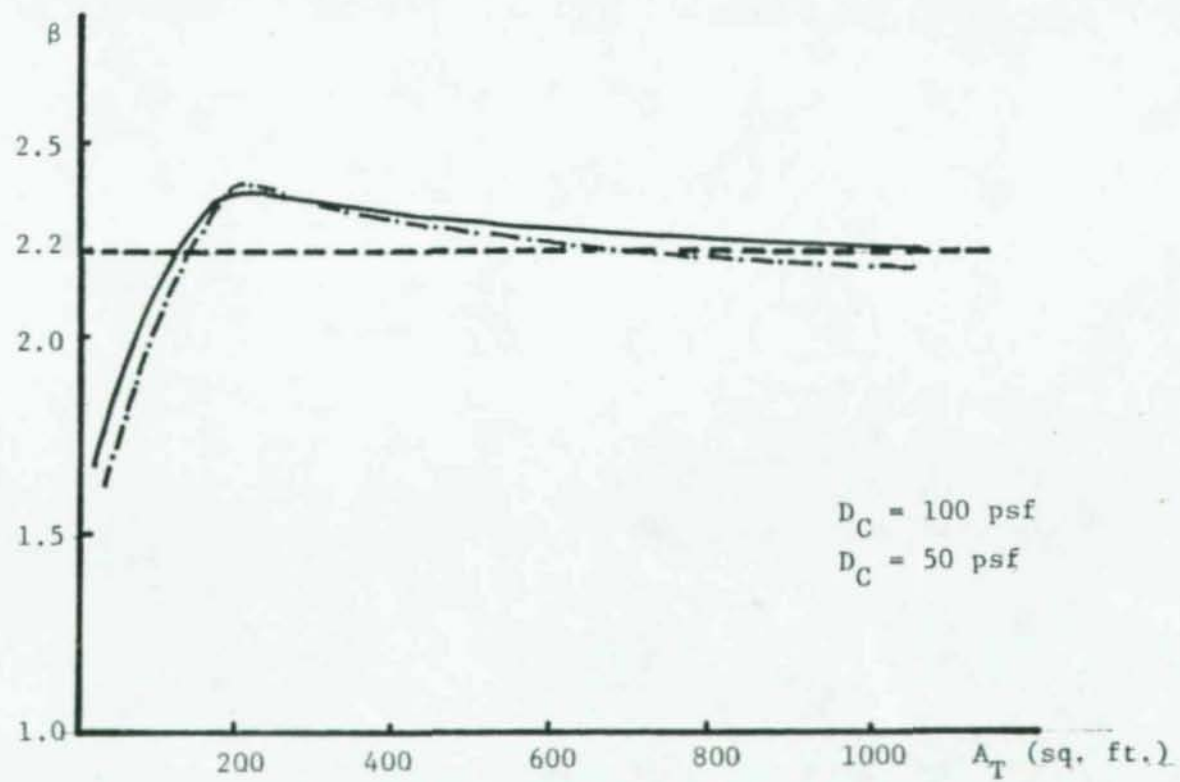
Figure 15. Variation of safety index, $\beta$, for shear with tributary area, $A_T$

The mean experimental ultimate shear strength is expressed by

$$V_{um} = F_{vum} \cdot A_w \cdot (V_{ex}/V_{th})_m \qquad (5.24)$$

and the nominal ultimate shear strength is given by

$$V_n = F_{vu} \cdot A_w \quad . \qquad (5.27)$$

By substituting $F_{vum}/F_{vu} \approx F_{sywm}/F_{yw} \approx 1.1$, $(V_{ex}/V_{th})_m = 1.08$, $\beta = 2.2$ and $\Omega_R = 0.28$ into the corresponding equations, the shear resistance factor, $\phi_v$, is determined to be 0.75.

Compared with $\phi_v = 0.86$ in the work of Galambos (24), $\phi_v = 0.75$ obtained here is quite small, which means it is much more conservative. This is due, as shown in Table 11, to a large difference in the C.O.V. of shear stress between the Galambos work and in this work. Galambos ignored the influence of the web slenderness ratio and the web aspect ratio on the C.O.V. of the shear stress, and took account of stress variation due to only variation of material properties. Galambos' value $\alpha = 0.55$ is, as discussed in Section 4.3, unreasonably small.

Table 11

Summary of Results Related With Shear Resistance Factor

| Parameter | Galambos Value (24) | Selected Value |
|---|---|---|
| $\Omega_R$ | 0.16 | 0.28 |
| $\Omega_M$ | 0.11 | 0.25 |
| $\Omega_F$ | 0.05 | 0.05 |
| $\Omega_P$ | 0.11 | 0.12 |
| $\Omega_Q$ | not shown | 0.13 |
| $\alpha$ | 0.55 | 0.75 |
| $\beta$ | 3.0 | 2.2 |
| $(V_{ex}/V_{th})_m$ | 1.03 | 1.08 |
| $\phi_v$ | 0.86 | 0.75 |

## Chapter 6

### PLATE GIRDERS IN COMBINED SHEAR AND BENDING

#### 6.1 Selection of Interaction Model

Behavior of plate girders subject to high shear and high moment may
be the least known area in analysis of the plate girder. Consequently,
no predominant analytical model explaining the interaction relation
exists.

As shown in Figure 16, there have been several different interaction
models proposed. The primary factors to describe the interaction rela-
tions are the shear strength and the bending strength, which are defined
differently in each model.

If shear and bending strengths of plate girders are plotted in the
ordinate and the abscissa, respectively, in the Cartesian coordinates,
the intersection of a interaction curve with the ordinate represents the
ultimate shear strength of plate girders with no applied bending moment,
and the intersection of an interaction curve with the abscissa defines
the ultimate bending moment of plate girders with no applied shear forces.
For keeping consistency with previous work in this research, these two
ultimate strengths of plate girders should be defined by the same equa-
tions as given in Chapters 4 and 5.

Therefore, it is concluded that the LFD criteria in the American
Association of State Highway and Transportation Officials (AASHTO) Speci-
fication (Figure 16c) in which the ultimate bending strength reflects
instability of the compression flange, is proper as the interaction
model for this research. The AASHTO model, which is a modification of
Basler's interaction model (Figure 16c) was also used in Galambos'
study (24).
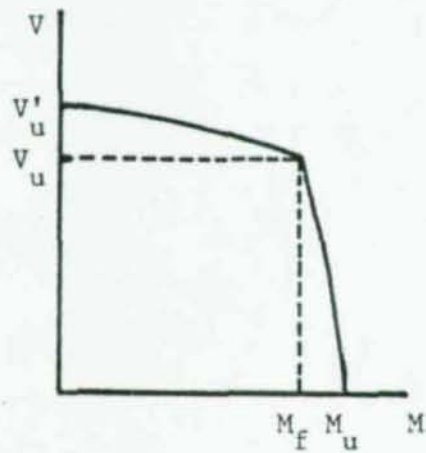
(a)  Höglund (33)
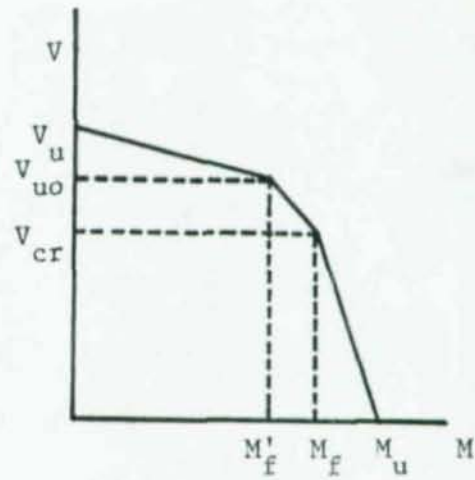
(b)  Fujii (23)
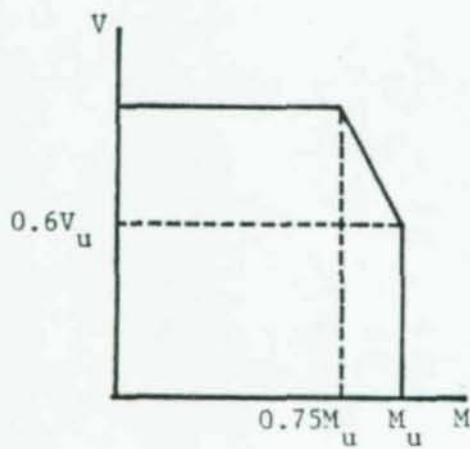
(c)  AASHTO (24)
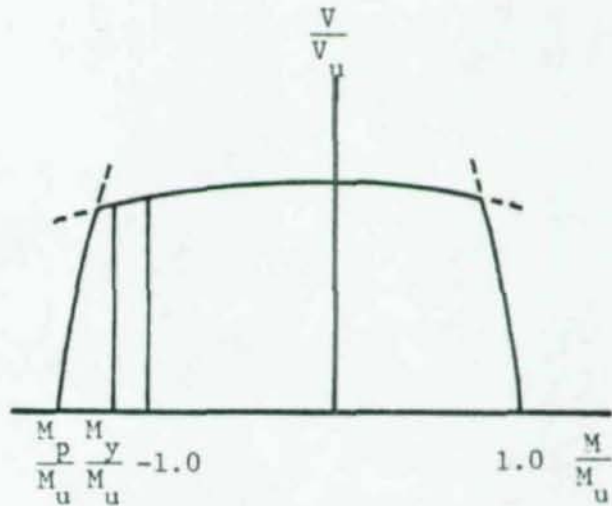
(d)  Chern-Ostapenko (42)
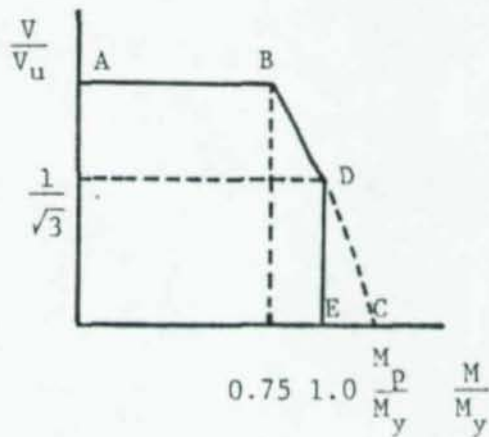
(e)  Basler (8)

Figure 16.  Shear-moment interaction model

## 6.2 Interaction Equations

Assuming the shear in a plate girder to be carried only by the web, shear resistance is maximum when the web has yielded uniformly, or when it has a fully developed tension field, in the case of plate girders with slender webs. This shear resistance is independent of the bending moment in the web panel as long as the moment is less than the flange yield moment, $M_f$. $M_f$ is the moment which can be carried by the flange alone when the stresses over the entire flange reach the yield point. Any large moment than the flange moment must be resisted in part by the web, which reduces the shear resistance of the web, until the shear capacity finally becomes zero. Therefore, the interaction envelope can be described as shown in Figure 16e. In the figure, the yield moment, $M_y$, is defined as the moment initiating yielding at the centroid of the compression flange and the plastic moment, $M_p$, is the moment of a fully yielded cross-section. By approximating the distance between the two flange centroids as the web depth, h, the three referenced moments of a symmetrically proportioned girder can be expressed as

$$M_f = F_{yf} \cdot h \cdot A_f \quad , \tag{6.1}$$

$$M_y = F_{yf} \cdot h \cdot (A_f + \frac{1}{6}A_w) \quad , \tag{6.2}$$

and

$$M_p = F_{yf} \cdot h \cdot (A_f + \frac{1}{4}A_w) \quad . \tag{6.3}$$

The abscissa of points B and C in Figure 16e is a function of $A_w/A_f$ as shown below:

$$\frac{M_f}{M_y} = \frac{F_{yf} \cdot h \cdot A_f}{F_{yf} \cdot h \cdot (A_f + \frac{A_w}{6})} = \frac{1}{1 + A_w/6A_f} \tag{6.4}$$

and

$$\frac{Mp}{My} = \frac{F_{yt} \cdot h \cdot (A_f + \frac{A_w}{4})}{F_{yf} \cdot h \cdot (A_f + \frac{A_w}{8})} = \frac{1 + A_w/4A_f}{1 + A_w/6A_f} \quad . \tag{6.5}$$

The curves resulting from Eqs. (6.4) and (6.5) are given in Figure 17 for various combinations of $A_w/A_f$.

Basler assumed $A_w/A_f = 2.0$ as a representative proportion for plate girders, and selected $M_f/M_y = 0.75$ and $M_p/M_y = 1.125$. However, since development of any moment larger than $M_y$ is doubtful, the portion of the interaction curve to the right of $M/M_y = 1.0$ was disregarded. The curve BDC in Figure 17 intersects the vertical line of $M/M_y = 1.0$ at the $V/V_u = \frac{1}{\sqrt{3}}$ for all values of $A_w/A_f$. Connecting points B and D, and using $M/M_y = 0.75$ and $V/V_u = 0.6$ gives the following equation for the interaction region between points B and D in Figure 17

$$\frac{M}{M_y} = 1.375 - 0.625(\frac{V}{V_u}) \quad . \tag{6.6}$$

However, the Basler interaction model does not take into account the instability of the compression flange. Because of the instability of the compression flange, the flange yield may not be developed. Thus, the maximum moment which can be developed is defined by the ultimate moment, $M_u$, which is expressed by Eq. (4.6) in pure bending cases. By substituting this ultimate bending strength for $M_y$ in Eq. (6.6), the interaction equation becomes

$$\frac{M}{M_u} = 1.375 - 0.625(\frac{V}{V_u}) \tag{6.7}$$

or, in terms of stress,

$$\frac{f_b}{F_{bu}} = 1.375 - 0.625(\frac{f_v}{F_{vu}}) \tag{6.8}$$

74
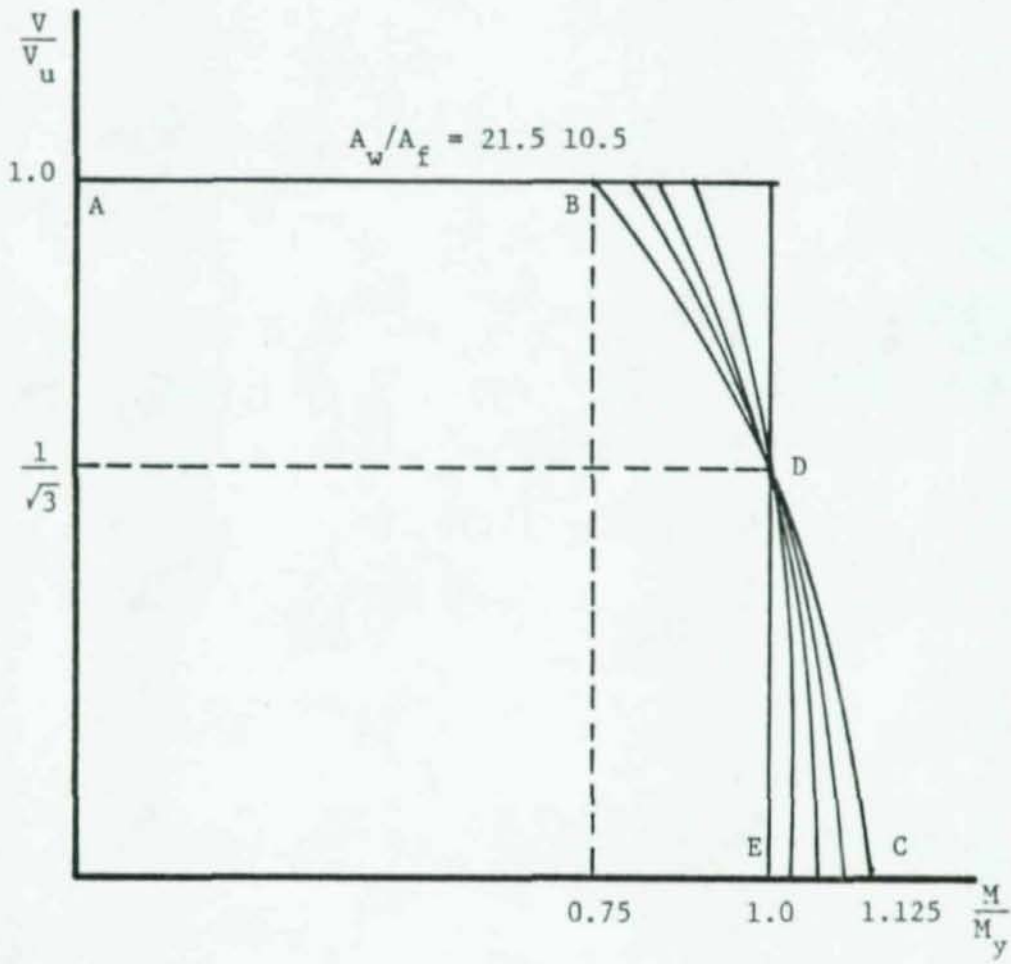


Figure 17. Variation of $\frac{M}{M_y}$ with $\frac{A_w}{A_f}$ (8)

in which $f_b$ and $f_v$ are, respectively, bending stress and shear stress which are defined by

$$f_b = M/S_x \qquad (6.9)$$

and

$$f_b = V/A_w \quad . \qquad (6.10)$$

The ultimate bending stress, $F_{bu}$, is equal to the ultimate bending moment, $M_u$, given in Eq. (4.6) divided by the section modulus, $S_x$.

The above approach has been adopted by the AASHTO Specification.

## 6.3  Uncertainties in Girder Strength

Strength of plate girders in the interaction range would be expressed by two terms; one is bending strength and the other is shear strength, which are given as

$$M_i = f_b \cdot S_x \qquad (6.11)$$

and

$$V_i = f_v \cdot A_w \quad . \qquad (6.12)$$

The stress $f_b$ and $f_v$ are interrelated through Eq. (6.8). To distinguish shear strength and bending strength in the interaction range from the shear strength of plate girders subject to predominant shear force and the bending strength of plate girders in pure bending, hereafter, $M_i$ and $V_i$ are referred to as "interaction bending strength" and "interaction shear strength", respectively.

The interaction shear strength and bending strength vary due to variations of the stresses, $f_b$ and $f_v$, which are a function of ultimate shear stress and yield stress. Error associated with the interaction equation is another factor causing variation of girder strength in the interaction range. Uncertainties in cross-sectional properties, $A_w$, and

$S_x$, also are random variables in predicting girder strength. However, the C.O.V. of cross-sectional properties, $\Omega_F$, has been estimated to be 0.05 for all cross-sectional properties, uncertainties associated with only stresses and the interaction formula are considered as random variables in this section.

### 6.3.1 Variation of stress

The interaction equation given in Eq. (6.8) can be rearranged as either

$$f_b = F_{bu}(1.375 - 0.625\frac{f_v}{F_{vu}}) \qquad (6.13)$$

or

$$f_v = F_{vu}(2.2 - 1.6\frac{f_b}{F_{bu}}) \qquad (6.14)$$

in which $F_{bu}$ and $F_{vu}$ are the ultimate bending stress and shear stress, respectively.

It is assumed, for simplicity, that $f_v$ in Eq. (6.13) is a constant at a given loading condition as far as the interaction bending strength is concerned. Similarly, $f_b$ in Eq. (6.14) is assumed to be a constant. Then, $f_b$ and $f_v$ are each a function of two random variables $F_{bu}$ and $F_{vu}$. As shown in the previous chapters, the C.O.V. of $F_{bu}$ is governed by the C.O.V. of the flange static yield stress. The C.O.V.s of the static yield stress of the flange and of the ultimate shear stress have been estimated in Sections (4.2) and (5.2), to be 0.12 and 0.25, respectively.

By using Eqs. (2.5) and (2.6), the mean values and variances of $f_b$ and $f_v$ are obtained as:

$$f_{bm} = F_{bum}(1.375 - 0.625\frac{f_v}{F_{vum}}) \quad , \qquad (6.15)$$

$$\text{Var}[f_b] = [F_{bum}(1.375 - 0.625\frac{f_v}{F_{vum}})]^2\Omega_1^2 + [0.15625F_{bum}\frac{f_v}{F_{vum}}]^2\Omega_2^2 \quad , \quad (6.16)$$

$$f_{vm} = F_{vum}(2.2 - 1.6\frac{f_b}{F_{bum}}) \quad , \quad (6.17)$$

and

$$\text{Var}[f_v] = [F_{vum}(2.2 - 1.6\frac{f_b}{F_{bum}})]^2\Omega_2^2 + [1.6F_{vum}\frac{f_b}{F_{bum}}]^2\Omega_1^2 \quad . \quad (6.18)$$

In the above equations, $F_{bum}$ is the mean ultimate bending stress of the flange, $F_{vum}$ is the mean ultimate shear stress, $\Omega_1$ is the C.O.V. of $F_{bu}$, and $\Omega_2$ is the C.O.V. of $F_{vu}$.

From Eqs. (6.15) and (6.16), $\Omega_{f_b}$, the C.O.V. of $f_b$, is obtained as

$$\Omega_{f_b} = \sqrt{\Omega_1^2 + \frac{(0.625\frac{f_v}{F_{vum}})^2\Omega_2^2}{(1.375 - 0.625\frac{f_v}{F_{vum}})^2}} \quad (6.19)$$

and from Eqs. (6.17) and (6.18), $\Omega_{f_v}$, the C.O.V. of $f_v$, becomes

$$\Omega_{f_v} = \sqrt{\Omega_2^2 + \frac{(1.6\frac{f_b}{F_{bum}})^2\Omega_1^2}{(2.2 - 1.6\frac{f_b}{F_{bum}})^2}} \quad . \quad (6.20)$$

Since $\Omega_1 = 0.12$ and $\Omega_2 = 0.25$ have previously been established, $\Omega_{f_b}$ and $\Omega_{f_v}$ are, respectively, functions of $f_v/F_{vum}$ and $f_b/F_{bum}$ which are equivalent to $V/V_u$ and $M/M_u$, respectively.

Therefore, $\Omega_{f_b}$ and $\Omega_{f_v}$ have different values for different loading paths. Table 12 gives the values of $\Omega_{f_b}$ and $\Omega_{f_v}$ corresponding to the loading paths shown in Figure 18.
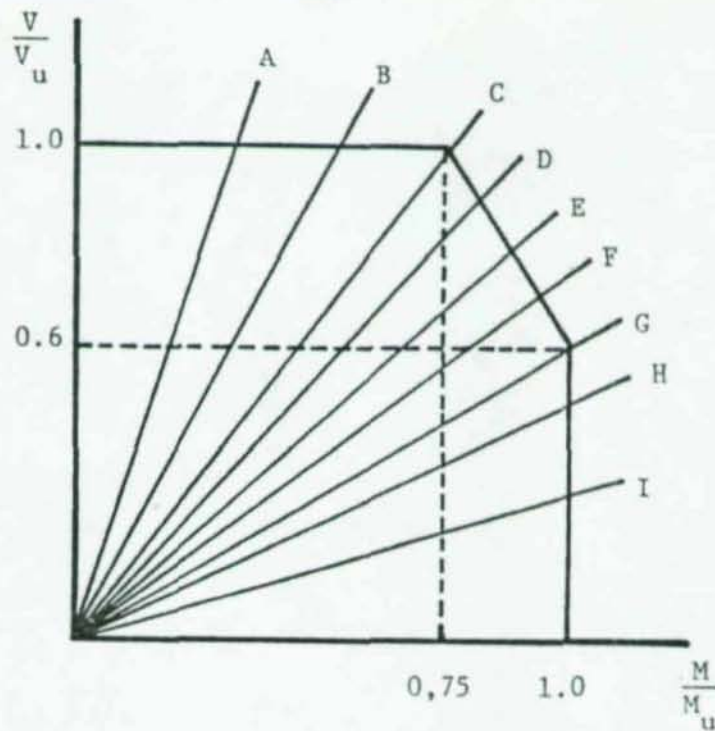
Figure 18. Designation of loading path

Table 12

Values of $\Omega_{fv}$ and $\Omega_{fb}$ Corresponding to Loading Path

| Loading Path | Coordinate $V/V_u$ | $M/M_u$ | $\Omega_{fv}$ | $\Omega_{fb}$ |
|---|---|---|---|---|
| A | 1.0 | 0.3 | 0.252 | 0.240 |
| B | 1.0 | 0.5 | 0.259 | 0.240 |
| C | 1.0 | 0.75 | 0.288 | 0.240 |
| D | 0.9 | 0.8125 | 0.304 | 0.211 |
| E | 0.8 | 0.8750 | 0.326 | 0.187 |
| F | 0.7 | 0.9375 | 0.359 | 0.167 |
| G | 0.6 | 1.0 | 0.406 | 0.152 |
| H | 0.5 | 1.0 | 0.406 | 0.141 |
| I | 0.3 | 1.0 | 0.406 | 0.126 |

### 6.3.2 Uncertainty in interaction formula

Applied shear force and bending moment on a plate girder are induced by applied load P, so they can be expressed in terms of applied load P; for instance, $V = P/2$ and $M = P \cdot x/2$ for any particular cross-section located at distance x from a support of a simply supported girder with a concentrated load at the center of span. Therefore, the ratio of M/V is independent of the applied load P, and characterizes the inclination of the loading path in the interaction diagram if the location of a particular cross-section, in a failed panel, is determined.

The interaction curve ABCD in Figure 19 is defined as the boundary between points on the safe side and those which lead to failure. Because the vector length on the $P/P_u$ axis may be interpreted as a load intensity, the theoretical ultimate load, $P_u$, for any particular cross-section subject to combined bending and shear is, by definition, the intersection (point E) of this particular loading path with the curve ABCD. Thus, once the loading path is determined, in other words once the loading condition and concerned cross-section are determined, the variation between theoretical and experimental girder strength in the interaction range can be measured by comparing $r_{ex}$ and $r_{th}$ in Figure 19.

The choice of the cross-section for which the moment values and the shear values are calculated is important because those values may vary throughout the length of the plate girder. This choice is made by following Basler's method (8); that is, the cross-section is chosen to be in the panel where failure has occurred at a longitudinal distance one half the web depth from the high-moment end, or at the middle of the longitudinal panel when its length is less than its depth.
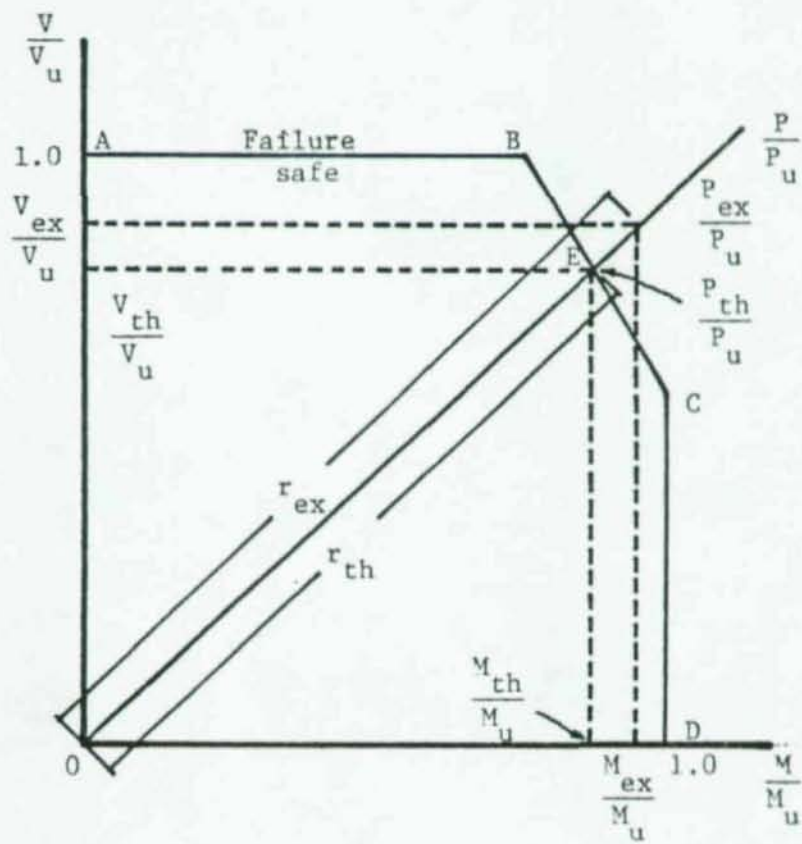
Figure 19. Load-moment and load-shear relationships in interaction diagram

Results of a comparison between the theoretical ultimate load and the experimental ultimate load in the interaction range are summarized in Table 13 and plotted in Figure 20. The data in Table 13 includes only regular girders and unsymmetrical girders. Hybrid girders may have a different trend for the ratio of $P_{ex}/P_{th}$, but they have not been examined due to lack of data in the literature.

The data presented in Figure 20 can be grouped into three regions; these are the shear dominant region, the high shear-high moment region and the moment dominant region. They are termed Region I, Region II and Region III, respectively. However, Region III has not been examined in this study due to lack of data.

The data shows that Region I has $(P_{ex}/P_{th})_m = 0.98$ and the C.O.V. = 0.11 while Region II has $(P_{ex}/P_{th})_m = 1.07$ and the C.O.V. = 0.07. Since the uncertainty in girder strength increases when loading path approaches from A to B or from D to C in Figure 20, it may be expected that Region I and II will have the smaller mean values and the larger C.O.V.s than those of predominant shear or pure bending. However, compared with $(V_{ex}/V_{th})_m = 1.08$ and the C.O.V. = 0.12 for predominant shear, and $(M_{ex}/M_{th})_m = 1.0$ and the C.O.V. = 0.13 for pure bending, the results do not agree with the expectations. This may be due to insufficient data used in the analysis. Since the girder strength in the interaction range is a function of the ultimate shear strength and the ultimate bending strength, it may be safe to select the smaller mean value and the larger C.O.V. of the values of these two parameters. Therefore, $(P_{ex}/P_{th})_m = 1.0$ and the C.O.V. = 0.13 are taken as appropriate values for the interaction range.

## Table 13

Experiment vs Theoretical Strength of Plate Girders in Combined Shear and Bending

| Region | Reference Source | Test No. | $\frac{a}{h}$ | $\frac{h}{t}$ | $A_{w_2}$ $(\text{in}^2)$ | $F_{crf}$ (ksi) | $F_{vu}$ (ksi) | $S_{x_3}$ $(\text{in}^3)$ | $\frac{M_{ex}}{M_u}$ | $\frac{V_{ex}}{V_u}$ | $\frac{P_{ex}}{P_{th}}$ |
|---|---|---|---|---|---|---|---|---|---|---|---|
| Inter-action | 11 | E1-T4 | 1.0 | 131 | 19.10 | 30.3 | 20.43 | 1922 | 0.734 | 0.873 | 0.93 |
| | | E2-T1 | 3.0 | 99 | 25.35 | 31.7 | 16.30 | 1480 | 1.007 | 0.914 | 1.15 |
| | | E2-T2 | 1.5 | 99 | 25.35 | 31.7 | 18.92 | 1480 | 1.010 | 0.789 | 1.09 |
| | | E4-T2 | 0.75 | 128 | 19.60 | 31.3 | 22.27 | 1292 | 1.027 | 0.728 | 1.08 |
| | | E4-T3 | 0.5 | 128 | 19.60 | 31.3 | 27.78 | 1292 | 1.095 | 0.598 | 1.07 |
| | | G8-T3* | 1.5 | 254 | 9.85 | 37.3 | 12.14 | 531 | 0.774 | 0.974 | 1.00 |
| | | G8-T4 | 1.0 | 254 | 9.85 | 37.3 | 15.02 | 531 | 0.861 | 0.875 | 1.02 |
| | 42,48 | UG3.2 | 1.6 | 295 | 4.39 | 32.6 | 12.68 | 224 | 1.003 | 0.767 | 1.08 |
| | | UG3.3 | 1.6 | 295 | 4.39 | 32.6 | 12.68 | 224 | 0.990 | 0.759 | 1.06 |
| | | UG4.3 | 1.46 | 414 | 8.76 | 33.4 | 18.13 | 439 | 1.087 | 0.612 | 1.07 |
| | | UG4.4 | 1.77 | 269 | 8.72 | 33.1 | 9.95 | 464 | 0.925 | 0.806 | 1.04 |
| | 43 | F10.4 | 1.5 | 195 | 12.85 | 23.2 | 5.05 | 756 | 1.080 | 0.990 | 1.23 |
| Shear Dominant | 11 | E1-T1* | 3.0 | 131 | 19.10 | 30.3 | 13.20 | 1922 | 0.596 | 1.101 | 1.10 |
| | | E1-T2* | 1.5 | 131 | 19.10 | 30.3 | 17.39 | 1922 | 0.622 | 0.873 | 0.87 |
| | | E1-T3 | 1.5 | 131 | 19.10 | 30.3 | 17.39 | 1922 | 0.272 | 0.954 | 0.95 |
| | | E4-T1 | 1.5 | 128 | 19.60 | 31.3 | 17.19 | 1292 | 0.367 | 0.883 | 0.88 |
| | | G8-T1* | 3.0 | 254 | 9.85 | 37.3 | 7.80 | 531 | 0.565 | 1.106 | 1.11 |
| | | G9-T1 | 3.0 | 382 | 6.55 | 37.9 | 7.86 | 505 | 0.341 | 0.932 | 0.93 |
| | | G9-T2 | 1.5 | 382 | 6.55 | 37.9 | 13.03 | 505 | 0.231 | 0.879 | 0.88 |
| | | G9-T3* | 1.5 | 382 | 6.55 | 37.9 | 13.03 | 505 | 0.561 | 0.926 | 0.93 |
| | 42,48 | UG2.2 | 1.2 | 295 | 4.39 | 36.2 | 14.96 | 224 | 0.458 | 1.065 | 1.07 |
| | | UG4.1 | 1.77 | 414 | 5.70 | 33.1 | 17.62 | 439 | 0.414 | 0.813 | 0.81 |
| | | UG4.2 | 1.14 | 414 | 5.70 | 33.7 | 21.04 | 876 | 0.543 | 0.994 | 0.99 |
| | | UG4.5 | 0.83 | 269 | 8.72 | 33.9 | 14.18 | 871 | 0.518 | 1.053 | 1.05 |
| | | UG4.6 | 1.77 | 269 | 8.72 | 33.1 | 9.95 | 871 | 0.243 | 1.138 | 1.14 |

Note:  *:  Data used for shear analysis in Galambos' study.  No test data for the interaction case were used in Galambos' study.
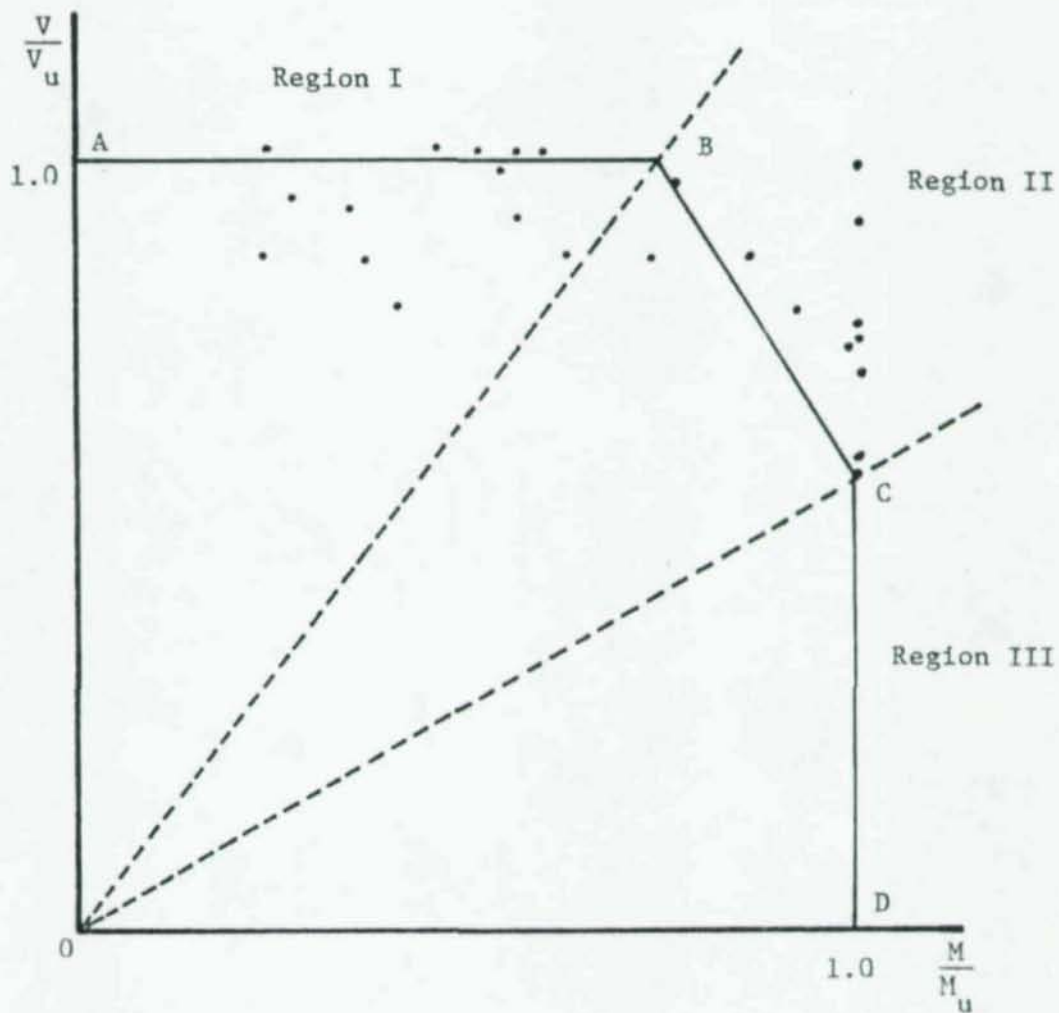
Figure 20. Distribution of experimental girder strength in interaction
region

## 6.4 Resistance Factor $\phi_i$ for Combined Shear and Bending

### 6.4.1 Safety index $\beta$

The safety index $\beta$ given by Eq. (2.13) may be rewritten, by translating the mean measured girder strength into the mean interaction bending strength and the mean interaction shear strength, as

$$\beta_v = \frac{\ln(V_{im}/Q_{vm})}{\sqrt{\Omega_{RV} + \Omega_Q}} \qquad (6.21)$$

and

$$\beta_m = \frac{\ln(M_{im}/Q_{mm})}{\sqrt{\Omega_{RM} + \Omega_Q}} \qquad (6.22)$$

in which $Q_{vm}$ and $Q_{mm}$ are the mean shear force and the mean bending moment, respectively, which are induced from the applied load P, and $\Omega_{RV}$ and $\Omega_{RM}$ are the C.O.V.s of the interaction shear resistance and the interaction bending resistance, respectively. Since $\Omega_{fv}$ and $\Omega_{fb}$ are, as shown in Table 12, different for each loading path, $\Omega_{RV}$ and $\Omega_{RM}$ also have different values for each loading path. The values of $\Omega_{RV}$ and $\Omega_{RM}$ corresponding to the loading paths shown in Figure 18 are given in Table 14, where $\Omega_F = 0.05$ and $\Omega_p = 0.13$ have been used. However, the C.O.V. of the applied load, $\Omega_Q = 0.13$, is unchanged since it is independent of the resistance of plate girders.

The ratio of $(V_{im}/Q_{vm})$ and $(M_{im}/M_{mm})$ is determined through calibration with Part 1 of the AISC Specification. For calibration, a simply supported, adequately braced, two-span girder under uniformly distributed dead and live load is assumed as a standard situation. This type of girder is subjected to high shear and high bending at the intermediate support. Then, applied shear force and bending moment induced by

Table 14

Values of $\Omega_{RV}$ and $\Omega_{RM}$ Corresponding to Loading Path

| Loading Path | Coordinate | | C.O.V. of Stress (a) | | C.O.V. of Resistance (b) | |
|---|---|---|---|---|---|---|
| | $V/V_u$ | $M/M_u$ | $\Omega_{fv}$ | $\Omega_{fb}$ | $\Omega_{KV}$ | $\Omega_{KM}$ |
| A | 1.0 | 0.3 | 0.252 | 0.240 | 0.288 | 0.277 |
| B | 1.0 | 0.5 | 0.259 | 0.240 | 0.294 | 0.277 |
| C | 1.0 | 0.75 | 0.288 | 0.240 | 0.320 | 0.277 |
| D | 0.9 | 0.8125 | 0.304 | 0.211 | 0.334 | 0.253 |
| E | 0.8 | 0.8750 | 0.326 | 0.187 | 0.354 | 0.233 |
| F | 0.7 | 0.9375 | 0.359 | 0.167 | 0.385 | 0.217 |
| G | 0.6 | 1.0 | 0.406 | 0.152 | 0.429 | 0.206 |
| H | 0.5 | 1.0 | 0.406 | 0.142 | 0.429 | 0.199 |
| I | 0.3 | 1.0 | 0.406 | 0.126 | 0.429 | 0.188 |

Note: (a) Values from Table 12

(b) $\Omega_R = \sqrt{\Omega_M^2 + \Omega_F^2 + \Omega_P^2} = \Omega_f^2 + (0.05)^2 + (0.13)^2$

the uniformly distributed loads can be expressed, for the cross-section
at the intermediate support, as

$$V = 0.625(D + L) \cdot s \cdot l \qquad (6.23)$$

and

$$M = 0.125(D + L) \cdot s \cdot l^2 \qquad (6.24)$$

in which D and L denote uniformly distributed dead and live load inten-
sities, and s and l represent girder spacing and length of girder span,
respectively.

According to the AISC Specification, plate girder webs shall be so
proportioned that the maximum bending stress, $f_b'$, due to the moment in
the plane of the girder web, shall not exceed the value determined by

$$f_b' = (0.825 - 0.375\frac{f_v'}{F_v})F_{yf} \leq 0.6F_{yf} \qquad (6.25)$$

in which $f_v'$ is the computed average shear stress and $F_v$ is equal to $F_{vu}$
divided by a safety factor of 1.65 except the limit state where $F_v$ =
$0.4F_y$. It is assumed for calibration that the shear stress and bending
stress defined by the AISC Specification are equal to the stresses
defined by Eqs. (6.13) and (6.14) divided by 1.65.

The mean interaction shear strength, $V_{im}$, and the mean interaction
bending strength, $M_{im}$, can be expressed by

$$V_{im} = f_{vm} \cdot A_w \cdot (P_{ex}/P_{th})_m \qquad (6.26)$$

and

$$M_{im} = f_{bm} \cdot S_w \cdot (P_{ex}/P_{th})_m \qquad (6.27)$$

since $(P_{ex}/P_{th})_m = (V_{ex}/V_{th})_m = (M_{ex}/M_{th})_m$ in the interaction range.

According to Part 1 of the AISC Specification, the required web
area and section modulus to resist the applied shear force and bending
moment are, respectively,

$$A_w = \frac{0.65(D_c + L_c \cdot R_{LL}) \cdot s \cdot 1}{f_v'} \qquad (6.28)$$

and

$$S_x = \frac{0.125(D_c + L_c \cdot R_{LL}) \cdot s \cdot 1^2}{f_b'} \qquad (6.29)$$

in which $R_{LL}$ is a live load reduction factor defined by Eq. (4.19).

Since it is assumed that $f_v = 1.65f_v'$ and $f_b = 1.65f_b'$ and since it has been estimated that $(P_{ex}/P_{th})_m = 1.0$, $f_{vm}/f_v \cong F_{yswm}/F_{yw} \cong 1.1$, and $f_{bm}/f_b \cong F_{ysfm}/F_{yf} \cong 1.0$, substitution of $A_w$ and $S_x$ given in Eq. (6.28) and Eq. (6.29) with these values into the corresponding terms of Eqs. (6.26) and (6.27) yields

$$V_{im} = 1.134(D_c + L_c \cdot R_{LL}) \cdot s \cdot 1 \qquad (6.3)$$

and

$$M_{im} = 0.206(D_c + L_c \cdot R_{LL}) \cdot s \cdot 1^2 \quad . \qquad (6.31)$$

The mean applied shear force, $Q_{vm}$, and the mean applied bending moment, $Q_{mm}$, which are induced by the uniformly distributed dead and live loads can be expressed by

$$Q_{vm} = 0.625(D_m + L_m) \cdot s \cdot 1 \qquad (6.32)$$

and

$$Q_{mm} = 0.125(D_m + L_m) \cdot s \cdot 1^2 \qquad (6.33)$$

in which the mean live load intensity, $L_m$, is defined by Eq. (3.3) and the mean dead load intensity, $D_m$, is assumed equal to the code specified dead load intensity, $D_c$.

Therefore, the denominator in Eqs. (6.21) and (6.22) becomes, respectively,

$$\frac{V_{im}}{Q_{vm}} = 1.815(D_c + L_c \cdot R_{LL})/(D_c + L_m) \tag{6.34}$$

and

$$\frac{M_{im}}{Q_{mm}} = 1.648(D_c + L_c \cdot R_{LL})/(D_c + L_m) \quad . \tag{6.35}$$

For simplicity in calculating $\beta$ in Eqs. (6.21) and (6.22), it is assumed that $(D_c + L_c \cdot R_{LL}) \simeq (D_c + L_m)$ since $L_c \cdot R_{LL}$ defined by ANSI A.58-1980 Draft agrees fairly well with $L_m$ given by the Ellingwood-Culver formula, which has been shown in Figure 3.

Thus, the safety indices for the interaction shear strength and the interaction bending strength are simplified to

$$\beta_v = \frac{0.6}{\sqrt{\Omega_{RV} + \Omega_Q}} = \frac{0.6}{\alpha_v(\Omega_{RV} + 0.13)} \tag{6.36}$$

and

$$\beta_m = \frac{0.5}{\sqrt{\Omega_{RM} + \Omega_Q}} = \frac{0.5}{\alpha_M(\Omega_{RM} + 0.13)} \quad . \tag{6.37}$$

The values of $\beta$ corresponding to the loading paths in Figure 18 are summarized in Table 15.

### 6.4.2 Resistance factor $\phi_i$ in the interaction range

The resistance factor given in Eq. (2.20) for the interaction range can be separated into

$$\phi_{iv} = \frac{V_{im}}{V_{in}} \exp(-\alpha_v \beta_v \Omega_{RV}) \tag{6.38}$$

and

$$\phi_{im} = \frac{M_{im}}{M_{in}} \exp(-\alpha_M \beta_M \Omega_{RM}) \tag{6.39}$$

Table 15

Values of $\beta_V$ and $\beta_M$ in the Interaction Range

| Loading Path | C.O.V. of Resistance (a) | | Linearization Factor (b) | | Safety Index | |
|---|---|---|---|---|---|---|
| | $\Omega_{RV}$ | $\Omega_{RM}$ | $\alpha_V$ | $\alpha_M$ | $\beta_V$ | $\beta_M$ |
| A | 0.288 | 0.277 | 0.756 | 0.752 | 1.899 | 1.634 |
| B | 0.294 | 0.277 | 0.758 | 0.752 | 1.867 | 1.634 |
| C | 0.320 | 0.277 | 0.768 | 0.752 | 1.736 | 1.634 |
| D | 0.334 | 0.253 | 0.772 | 0.743 | 1.675 | 1.757 |
| E | 0.354 | 0.233 | 0.779 | 0.735 | 1.591 | 1.874 |
| F | 0.385 | 0.217 | 0.789 | 0.729 | 1.477 | 1.977 |
| G | 0.429 | 0.206 | 0.802 | 0.725 | 1.338 | 2.053 |
| H | 0.429 | 0.199 | 0.802 | 0.722 | 1.338 | 2.105 |
| I | 0.429 | 0.188 | 0.802 | 0.719 | 1.338 | 2.187 |

Notes: (a) Values from Table 14
       (b) Values defined by Eq. (2.17)

in which $\phi_{iv}$ and $\phi_{im}$ are the resistance factors for interaction shear strength and bending strength, respectively, and

$$V_{im} = f_{vm} \cdot A_w \cdot (\frac{P_{ex}}{P_{th}})_m \quad , \tag{6.26}$$

$$M_{im} = f_{bm} \cdot S_x \cdot (\frac{P_{ex}}{P_{th}})_m \quad , \tag{6.27}$$

$$V_{in} = f_v \cdot A_w \quad , \tag{6.40}$$

and

$$M_{im} = f_b \cdot S_x \quad . \tag{6.41}$$

From the values of $(P_{ex}/P_{th})_m = 1.0$, $f_{vm}/f_v = 1.10$ and $f_{bm}/f_b = 1.0$, Eqs. (6.38) and (6.39) become

$$\phi_{iv} = 1.10 \exp(-\alpha_v \beta_v \Omega_{RV}) \tag{6.42}$$

and

$$\phi_{im} = 1.0 \exp(-\alpha_M \beta_M \Omega_{RM}) \quad . \tag{6.43}$$

The values of $\phi_{iv}$ and $\phi_{im}$ are plotted in Figure 21, which shows that the shear resistance factor decreases as the loading path moves from the shear dominant region to the bending dominant region, and that the bending resistance factor decreases when the loading path moves in the opposite direction. This simply means that uncertainty of girder strength is increased when a plate girder resists two different types of forces, which may be due to a multiplication effect of uncertainty inherent in girder strength associated with each type of force.

From Figure 21, it is concluded that a linear connection of points A, B, C, and D could be a safe interaction envelope reflecting the resistance factor for combined shear and bending. A comparison of this factored interaction envelop with that proposed by Galambos(24) is
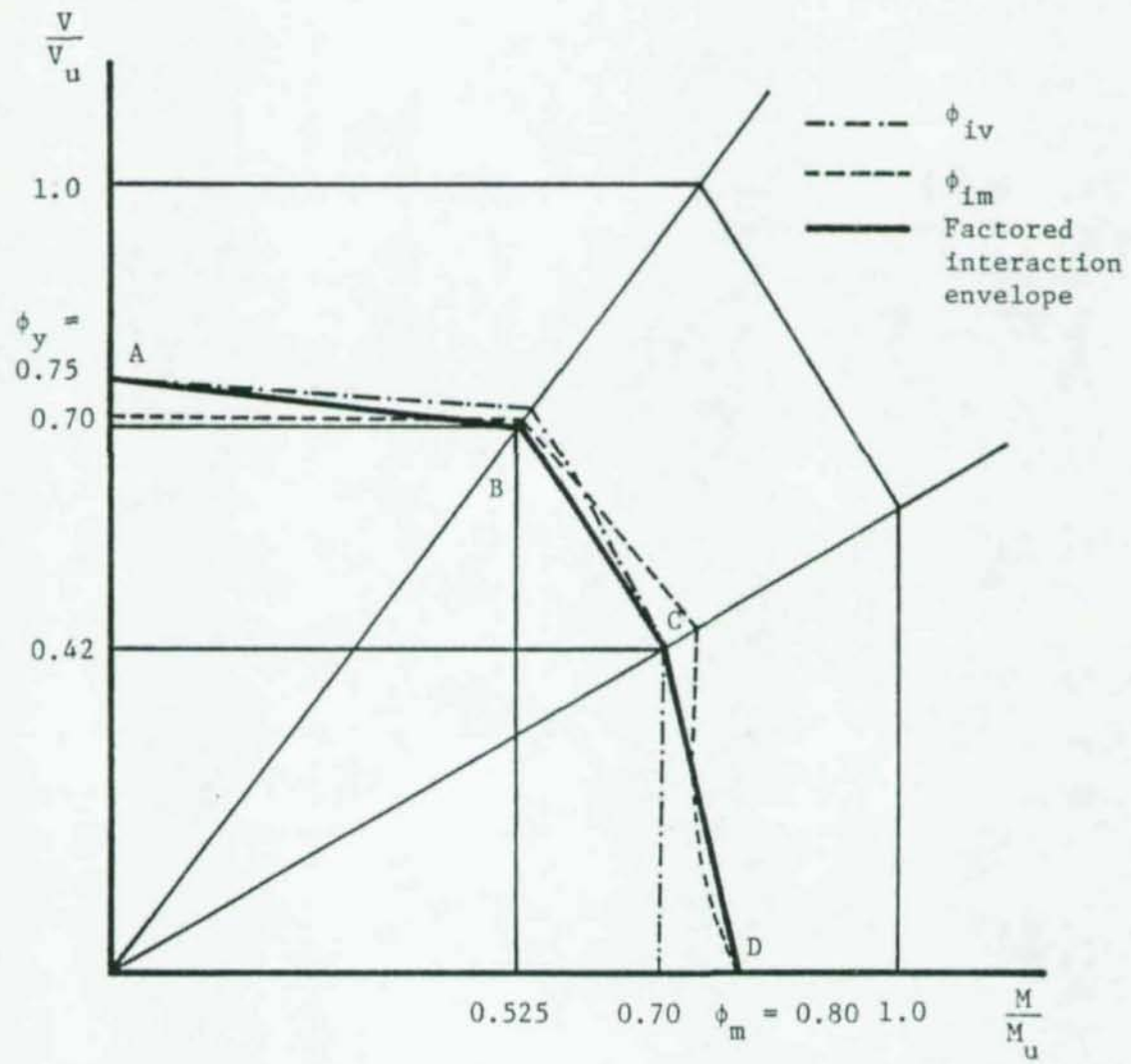
Figure 21. Variation of resistance factor in the interaction range

shown in Figure 22. In developing his factored interaction curve, which is supposed to give safe design values, Galambos ignored variation of the safety index associated with loading path, and assumed that the resistance factor for the interaction range could be determined from the resistance factor for predominant shear, $\phi_v$, and the resistance factor for pure bending, $\phi_m$. But, Figure 22 shows that the resistance factor in the interaction range has different characteristics from what Galambos assumped.

### 6.4.3 LRFD interaction equations

According to the suggested interaction curve shown in Figure 22, the following equations are obtained:

for $0 \leq M \leq 0.75\phi_i M_u$ ,

$$\frac{V}{V_u} + \frac{(\phi_v - \phi_i)M}{0.75\phi_i M_u} \leq \phi_V \quad , \tag{6.44}$$

for $0.6\phi_i V_u \leq V \leq \phi_i V_u$ or $0.75\phi_i M_u \leq M \leq \phi_i M_u$ ,

$$0.625\frac{V}{V_u} + \frac{M}{M_u} \leq 1.375\phi_v \quad , \tag{6.45}$$

and for $\phi_i M_u \leq M \leq \phi_m$ ,

$$\frac{M}{M_u} + \frac{(\phi_m - \phi_i)V}{0.6\phi_i V_u} \leq \phi_m \quad . \tag{6.46}$$

In the above equations, the resistance factor for predominant shear, $\phi_v = 0.75$, the resistance factor for pure bending, $\phi_m = 0.80$ and the resistance factor for combined shear and bending, $\phi_i = 0.70$ are the values estimated in this study.
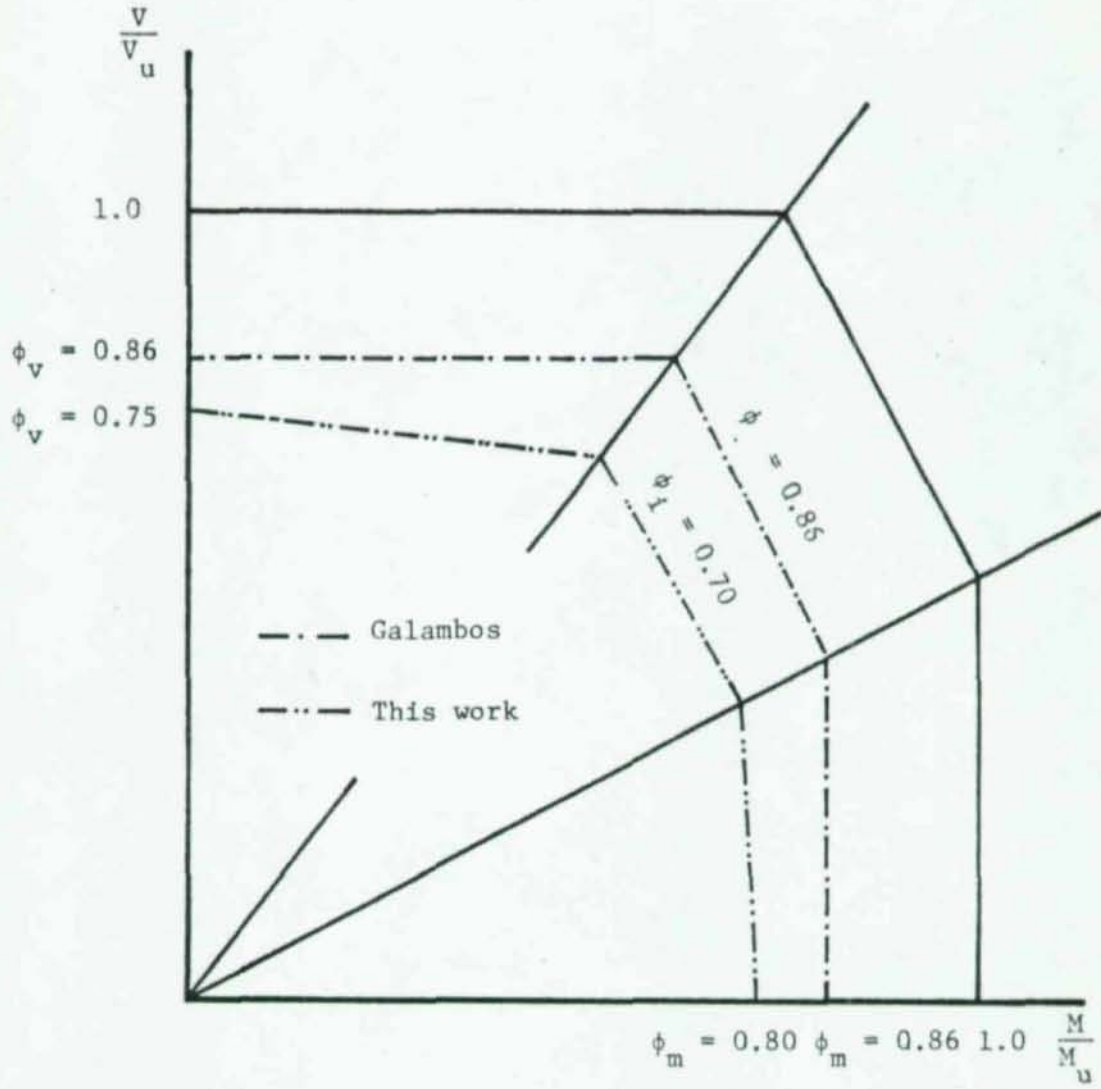
Figure 22. Comparison of interaction envelope

Chapter 7

SUMMARY AND CONCLUSIONS

7.1  Summary

By using Cornell's probabilistic design format, the traditional central factor of safety can be split into the resistance factor and the load factor in an explicit and simple manner.

The study presented here has dealt with only the resistance factors of plate girders in pure bending, shear, and combined shear and bending.

In order to determine the resistance factors, the following studies were carried out.

1.  Cornell's first-order, second-moment formula is selected as a probabilistic design format.  In Galambos' study, the Cornell format was also used.

2.  Part 1 of the AISC Specification is selected as a basis of calibration through which the same degree of safety can be provided in the proposed design criteria as in the current AISC Specification. Galambos performed his calibration with Part 2 of the AISC Specification in which provisions are provided for plastic design.

3.  Predictions of regular and unsymmetrical girder strengths are done by the Basler-Thürlimann models in this research as in the Galambos study.  For hybrid girders, however, prediction is done by the formula which has been recommended by Subcommittee 1 on Hybrid Beams and Girders, Joint ASCE-AASHO Committee on Flextural Members.

4.  Prediction of live load effect on plate girders follows the Ellingwood-Culver formula which is the basis of the ANSI A.58-1980 Draft, while the McGuire-Cornell formula was used in Galambos' study.

5. In order to measure the uncertainty associated with a theoretical structural analysis model, actual measured values in the static yield stress and dimensional properties are used in prediction of girder strengths.

6. Uncertainties in girder strength are assumed to come from three major sources; that is, uncertainties associated with stress, fabrication, and structural analysis models.

7. For estimating variation in stress, the first-order approximation technique is employed, and the mean values and the standard deviation are measured for modulus of elasticity, the static yield stress of the flange and the web, Poisson's ratio and shear modulus of elasticity.

8. The C.O.V. of fabrication error follows the value measured by Galambos though it is much greater than the value reported after this study had been completed (Appendix 2).

9. The C.O.V. associated with the structural analysis model is measured from distribution of the ratio of experimental values of girder strengths reported in the literature to theoretical values predicted by the Basler-Thürlimann models.

The results of this study give the resistance factors of 0.8 for bending, 0.75 for shear, and 0.70 for combined shear and bending, which are smaller than values of 0.86 for all cases as presented by Galambos. Comparisons of the study results with those of Galambos' study are given in the ends of Chapters 3, 4, 5, and 6.

From results of this study, the following design criteria of plate girders are recommended. In the following equations, $V_D$ and $M_D$ are the design shear and the design moment, respectively, computed on the basis of design load intensities at the cross-section under consideration.

For $0 \leq M_D \leq 0.525M_u$

$$\frac{V_D}{V_u} + 0.095\frac{M_D}{M_u} \leq 0.75 \quad . \tag{7.1}$$

For $0.42V_u \leq V_D \leq 0.60V_u$ or $0.525M_u \leq M_D \leq 0.70M_u$

$$0.625\frac{V_D}{V_u} + \frac{M_D}{M_u} \leq 0.96 \quad . \tag{7.2}$$

For $0.70M_u \leq M_D \leq 0.80M_u$

$$\frac{M_D}{M_u} + 0.238\frac{V_D}{V_u} \leq 0.80 \quad . \tag{7.3}$$

The design shear and moment, $V_D$ and $M_D$, may not exceed $0.75V_u$ and $0.80M_u$, respectively.

The ultimate bending strength, $M_u$, for homogeneous, symmetrical and unsymmetrical plate girders is defined by

$$M_u = F_{cr} \cdot S_x [1 - 0.0005\frac{A_w}{A_f}(\frac{h}{t} - \frac{980}{\sqrt{F_{cr}}})] \quad . \tag{7.4}$$

The smaller $F_{cr}$ defined by Eqs. (7.5), (7.6), (7.8), (7.9) or (7.10) should be used in Eq. (7.4):

$$F_{cr} = \frac{296000C_b}{(\frac{K\ell}{r_T})^2} \quad \text{for} \quad \lambda \geq \sqrt{2} \tag{7.5}$$

and

$$F_{cr} = F_y(1 - \frac{\lambda^2}{4}) \quad \text{for} \quad \lambda \leq \sqrt{2} \quad . \tag{7.6}$$

In the above equations, $C_b$ is determined by Eq. (4.11), $r_T$ is given by Eq. (4.9) and $\lambda$ is given by

$$\lambda = \frac{\ell}{r_T}\sqrt{\frac{F_y}{2.96 \times 10^5}} \tag{7.7}$$

in which $\ell$ is the unbraced length of the span.

$$F_{cr} = \frac{11,500}{(\frac{b}{w})^2} \quad \text{for} \quad \frac{b}{w} \geq \frac{151.8}{\sqrt{F_y}} \quad , \tag{7.8}$$

$$F_{cr} = F_y \quad \text{for} \quad \frac{b}{w} \leq \frac{48.3}{\sqrt{F_y}} \quad , \tag{7.9}$$

and

$$F_{cr} = F_y[1 - 0.53(0.0093\frac{b}{w} - 0.45)^{1.36}] \quad \text{for} \quad \frac{48.3}{\sqrt{F_y}} < \frac{b}{w} < \frac{151.8}{\sqrt{F_y}} \tag{7.10}$$

in which b is half the width of compression flange and w is the thickness of the compression flange.

The ultimate bending strength, $M_u$, for hybrid plate girders is determined by either Eq. (7.4) or Eq. (7.11), whichever is smaller.

$$M_u = F_{cr} \cdot S_x \{ \frac{12 + (\frac{A_w}{A_f})[\frac{3F_{yw}}{F_{yf}} - (\frac{F_{yw}}{F_{yf}})^2]}{12 + 2(\frac{A_w}{A_f})} \} \tag{7.11}$$

in which $F_{cr}$ is determined in the same manner as $F_{cr}$ in Eq. (7.4).

The ultimate shear strength, $V_u$, for homogeneous, symmetrical and unsymmetrical plate girders is calculated by

$$V_u + A_w[F_{vcr} + \frac{F_y}{2}(1 - \frac{\sqrt{3}F_{vcr}}{F_y})\frac{1}{\sqrt{1 + (\frac{a}{h})^2}}] \tag{7.12}$$

in which $F_{vcr}$ is determined by

$$F_{vcr} = \frac{27,000k}{(\frac{h}{t})^2} \tag{7.13}$$

where

$$k = 5.34 + \frac{4.0}{(\frac{a}{h})^2} \quad \text{for} \quad (\frac{a}{h}) \geq 1 \tag{7.14}$$

and

$$k = 4.0 + \frac{5.34}{(\frac{a}{h})^2} \quad \text{for} \quad (\frac{a}{h}) \leq 1 \quad . \tag{7.15}$$

If $F_{vcr}$ calculated by Eq. (7.13) is greater than $0.46F_y$, then $V_u$ is determined by

$$V_u = 0.68\sqrt{F_y} \cdot A_w \quad . \tag{7.16}$$

## 7.2 Conclusions

Comparisons of the resistance factors for bending, shear, and combined shear and bending between this study and Galambos' study have been summarized in the ends of Chapters 4, 5, and 6.

The following general conclusions may be drawn from these studies.

1. The dominant parameters in determining the resistance factor are uncertainties associated with the static yield stress and theoretical strength prediction model of plate girders. Uncertainties associated with dimensional properties are negligible.

2. Differences of resistance factors between this study and Galambos' study arise from two main sources; the one is due to different characteristic values of the static yield stress, which results from different sampled data used in two studies, and the other is due to different statistical treatment of the relative parameters. However, the former is the dominant factor causing differences. Calibration with Part 2 (plastic deisgn, employed for calibration in Galambos' study) gives a larger safety index, $\beta$, than that obtained from calibration with Part 1 (elastic design, employed in this research) of the specification. However, Galambos reported that calibration with Part 1 and Part 2 of the AISC Specification had little effect on the resulting resistance factor.

3. The resistance factor varies in the ranges of $0 \leq \dfrac{M}{M_u} \leq 0.75$ and of $0 \leq \dfrac{V}{V_u} \leq 0.6$ for the interaction curve, which was assumed constant in Galambos' research.

4. In general, the design criteria based on the probabilistic design format are very sensitive to the characteristic values of sampled data of parameters which affect the strength of plate girders.

## 7.3 Recommendations for Future Study

The design criteria recommended in this research are based on data available in the literature. During the analysis of the data, it has been found that there are limited data available to develop probability-based design criteria even though numerous tests on plate girders have been performed. Most studies performed in the past fail to report the distribution of test results. In order to develop highly reliable pro-babilistic design criteria, the following additional studies are recom-mended.

1. Tests on the static yield stress of the structural steel — The static yield stress has not been widely used in structural design. Consequently, most tests of plate girders or structural steel has been performed on the basis of the upper or lower yield stress. Limited data is available in the literature, especially for the static yield stress of high strength steel. Since the static yield stress is affected by the thickness of steel plate and the direction or location of the speci-men in the plate, attention must be given on these aspects.

2. Tests on the strength of plate girders in combined shear and bending -- There have been very limited reports on the strength of plate girders, especially hybrid girders in combined shear and bending, which limits reliable analysis of the interaction relationships between shear

and bending.  The number of tests is important for obtaining statistic-
ally significant results.

Study of the load factors which is excluded in this research is an-
other subject which needs additional attention prior to complete accept-
ance of the LRFD criteria.

REFERENCES

1.  Alpsten, G. A., "Variations in Mechanical and Cross-Sectional Properties of Steel," Planning and Design of Tall Buildings, Vol. 1b, Proceedings, International Conference on Planning and Design of Tall Buildings, Lehigh University, Behtlehem, PA., 1972, pp. 755-805.

2.  Ang, A. H-S., "A Comprehensive Basis for Reliability Analysis and Design," Reliability Approach in Structural Engineering, ed. by Freudental, M., Konish, I., Shinozuka, M. and Kanazawa, T., Maruzen Co., Ltd., Tokyo, 1975, pp. 25-47.

3.  Ang, A. H-S. and Cornell, C. A., "Reliability Bases of Structural Safety and Design," Journal of the Structural Division, ASCE, Vol. 100, Sept., 1974, pp. 1755-1769.

4.  Ang, A. H-S. and Tang, W. H., Probability Concepts in Engineering Planning and Design, John Wiley & Sons, Inc., New York, N.Y., 1975.

5.  "ANSI A58.1-1972; American National Standard Building Code Requirement for Minimum Design Loads in Building and Other Structures," Manual of Steel Construction, AISC, New York, N.Y., 1973, pp. 5-221~ 5-224.

6.  "ANSI A58.1-1980 Draft; Building Code Requirements for Minimum Design Loads in Buildings and Other Structures," National Bureau of Standards, United States Department of Commerce, Nov., 1979.

7.  Baker, M. J., "Variations in the Mechanical Properties of Structural Steels," Final Report of Symposium on Concepts of Safety of Structures and Methods of Design, International Association for Bridge and Structural Engineering, London, Sept., 1969.

8.  Basler, K., "Strength of Plate Girders under Combined Bending and Shear," Journal of the Structural Division, ASCE, Vol. 87, Oct., 1961, pp. 181-195.

9.  Basler, K., "Strength of Plate Girders in Shear," Journal of the Structural Division, ASCE, Vol. 87, Oct., 1961, pp. 151-180.

10. Basler, K. and Thürlimann, B., "Strength of Plate Girders in Bending," Journal of the Structural Division, ASCE, Vol. 87, Aug., 1961, pp. 153-181.

11. Basler, K., Yen, B. T., Mueller, J. A. and Thürlimann, B., "Web Buckling Tests on Welded Plate Girders," Bulletin No. 64, Welding Research Council, New York, N.Y., 1960, pp. 1-63.

12. Benjamin, J. R. and Cornell, C. A., Probability, Statistics and Decision for Civil Engineers, McGraw-Hill Book Co., Inc., New York, N.Y., 1970.

13. Bleich, F., Buckling Strength of Metal Structures, McGraw-Hill Book Co., Inc., New York, N.Y., 1952.

14. Cooper, P. B., "The Ultimate Bending Moment for Plate Girders," Proceedings of International Association for Bridge and Structural Engineering Colloquium, London, 1971, pp. 291-298.

15. Cornell, C. A., "A Probability-Based Structural Code," Journal of American Concrete Institute, Vol. 66, Dec., 1969, pp. 974-985.

16. "Design of Hybrid Steel Beams," Report of the Subcommittee 1 on Hybrid Beams and Girders, Joint ASCE-AASHO Committee on Flexural Members, Journal of Structural Division, ASCE, Vol. 94, June, 1968, pp. 1397-1426.

17. Ditlevsen, O., "On the Second Moment Structural Reliability Theory," Safety of Structures under Dynamic Loading, Vol. 1, ed. by Holand, I., Kavlie, D., Moe, G. and Sigbjörnsson, R., TAPIR, Norwegian Institute of Technology, Trondheim, Norway, 1978, pp. 176-206.

18. Ellingwood, B. E. and Culver, C., "Analysis of Live Loads in Office Buildings," Journal of the Structural Division, ASCE, Vol. 103, Aug., 1977, pp. 1551-1560.

19. Ellingwood, B. R. and Ang, A. H-S., "Risk-Based Evaluation of Design Criteria," Journal of the Structural Division, ASCE, Vol. 100, Sept., 1974, pp. 1771-1788.

20. Fiorato, A. E. and Sahlin, S., "Dimensional Tolerance in Concrete," Planning and Design of Tall Buildings, Vol. 1b, Proceedings of International Conference on Planning and Design of Tall Buildings, Lehigh University, Bethlehem, PA., 1972, pp. 893-895.

21. Freudental, A. M., "Safety and the Probability of Structural Failure," Proceedings of ASCE, Vol. 80, Separate No. 488, Aug. 1954, pp. 468-1-468-46.

22. Fujii, T., "A Comparison between the Theoretical Values and the Experimental Results for the Ultimate Shear Strength of Plate Girders," Proceedings of International Association for Bridge and Structural Engineering Colloquium, London, 1971, pp. 161-171.

23. Fujii, T., Fukumoto, Y., Nishino, F. and Okumura, T., "Research Works on Ultimate Strength of Plate Girders and Japanese Provisions on Plate Girder Design," Proceedings of International Association for Bridge and Structural Engineering Colloquium, London, 1971, pp. 21-47.

24. Galambos, T. V., Cooper, P. B. and Ravindra, M. K., "LRFD Criteria for Plate Girders," Journal of the Structural Division, ASCE, Vol. 104, Sept., 1978, pp. 1389-1407.

25. Galambos, T. V. and Ravindra, M.K., "Load and Resistance Factor
    Design for Steel," Journal of the Structural Division, ASCE, Vol.
    104, Sept., 1978, pp. 1337-1353.

26. Galambos, T. V. and Ravindra, M. K., "Properties of Steel for Use
    in LRFD," Journal of the Structural Division, ASCE, Vol. 104, Sept.,
    1978, pp. 1459-1468.

27. Gaylord, E. H., Jr. and Gaylor, C. N., Design of Steel Structures,
    McGraw-Hill Book Co., Inc., New York, N.Y., 1972.

28. "General Requirements for Rolled Steel Plate, Shapes, Sheetpiling,
    and Bars for Structural Use," 1980 Annual Book of ASTM Standard,
    A6-79b, Part 3, 1980.

29. Herzog, M. A. M., "Ultimate Static Strength of Plate Girders from
    Tests," Journal of the Structural Division, ASCE, Vol. 100, May,
    1974, pp. 849-864.

30. Horne, M. R. and Narayanan, R., "Ultimate Capacity of Longtudinally
    Stiffened Plate Girders used in Box Girders," Proceedings of
    Institute of Civil Engineers, Part 2, London, 1976, pp. 253-280.

31. Horne, M. R., Narayanan, R. and Montague, P., "Influence on Strength
    of Compression Panels of Stiffner Section, Spacing and Welded Con-
    nections," Proceedings of Institute Civil Engineers, Part 2, London,
    1977, pp. 1-20.

32. Huber, A. W. and Beedle, L. S., "Residual Stresses and the Compres-
    sive Strength of Steel," Welding Journal, Vol. 33, No. 12, Dec.,
    1954, pp. 589s-614s.

33. Johnston, B. G., Guide to Stability Design Criteria for Metal Struc-
    tures, 3rd edition, John Wiley & Sons, Inc., New York, N.Y., 1976.

34. Kiureghian, A. D., "Reliability Analysis under Stochastic Loads,"
    Journal of the Structural Division, ASCE, Vol. 106, Feb., 1980,
    pp. 411-429.

35. Lew, H. S., Natarajan, M. and Toprac. A. A., "Static Tests on Hybrid
    Plate Girders," Welding Research Supplement, Feb., 1969, pp. 86s-96s.

36. Lind, N. C., "Consistent Partial Safety Factors," Journal of the
    Structural Division, ASCE, Vol. 97, June, 1971, pp. 1651-1669.

37. McGuire, R. K. and Cornell, C. A., "Live Load Effects in Office
    Buildings," Journal of the Structural Division, ASCE, Vol. 100,
    July, 1974, pp. 1351-1366.

38. McGuire, W., Steel Structures, Prentice-Hall, Inc., Englewood Cliffs,
    N.J., 1968.

39. Mirza, S. A. and MacGregor, J. G., "Variability of Mechanical Properties of Reinforced Bars," Journal of the Structural Division, ASCE, Vol. 105, May, 1979, pp. 921-937.

40. Nagaraja Rao, N. R., Lohrmann, M. and Tall, L., "Effect of Strain Rate on the Yield Stress of Structural Steels," Journal of Materials, Vol. 1, March, 1966, pp. 241-262.

41. Ostapenko, A. and Dimitri, J. R., "Pilot Tests on the Static Strength of Unsymmetrical Plate Girders," Bulletin No. 156, Welding Research Council, Nov., 1970, pp. 1-22.

42. Ostapenko, A., Chern, C. and Parsanejad, C., "Ultimate Strength Design of Plate Girders," Report 328.12, Lehigh University, Fritz Engineering Laboratory, January, 1971.

43. Patterson, P. J., Corrado, J. A., Juang, J. S. and Yen, B. T., "Fatigue and Static Tests of Two Plate Girders," Bulletin No. 155, Welding Research Council, New York, N.Y., Oct., 1970, pp. 1-18.

44. Ravindra, M. K., Lind, N. C. and Siu, W., "Illustrations of Reliability-Based Design," Journal of the Structural Division, ASCE, Vol. 100, Sept., 1974, pp. 1789-1811.

45. Rockey, K. C., Evans, H. R. and Porter, D. M., "A Design Method for Predicting the Collapse Behavior of Plate Girders," Proceedings of Institute of Civil Engineers, Part 2, 1968, pp. 85-112.

46. Rockey, K. C. and Skaloud, M., "The Ultimate Load Behavior of Plate Girders Loaded in Shear," Proceedings of International Association for Bridge and Structural Engineering Colloquium, London, 1971, pp. 1-19.

47. Rosenblueth, E., "Code Specification of Safety and Serviceability," Planning and Design of Tall Buildings, Vol. 1b, Proceedings of International Conference on Planning and Design of Tall Buildings, Lehigh University, Bethleham, PA., 1972, pp. 931-959.

48. Schuller, W. and Ostapenko, A., "Tests on A Transversely Stiffened and on A Longitudinally Stiffened Unsymmetrical Plate Girders," Bulletin No. 156, Welding Research Council, Nov., 1970, pp. 23-47.

49. Siu, W. W. C. and Lind, N. C., "Some Aspects of Office Design Live Loads," Journal of the Structural Division, ASCE, Vol. 99, Nov., 1973, pp. 2245-2258.

50. "Specification for the Design, Fabrication and Erection of Structural Steel for Buildings," American Institute of Steel Construction, New York, N.Y., 1969.

51. "Standard Methods and Definition for Mechanical Testing of Steel Products," 1980 Annual Book of ASTM Standard, A370-773, Part 4, 1980.

52. Timoshenko, S. P. and Gere, J. M., _Theory of Elastic Stability_, 2nd edition, McGraw-Hill Book Co., Inc., New York, N.Y., 1961.

53. Tomonaga, K., "Measured Error on Fabrication of Kosumigaseki Building," _Planning and Design of Tall Buildings_, Vol. 1b, Proceedings of International Conference on Planning and Design of Tall Buildings, Lehigh University, Bethlehem, PA., 1972, pp. 833-844.

54. Wen, Y. K., "Statistics of Extreme of Live Load on Buildings," _Journal of the Structural Division_, ASCE, Vol. 105, Oct., 1979, pp. 1893-1900.

## Appendix 1

### ESTIMATION OF THE CHARACTERISTIC VALUES FROM MULTI-SETS
### OF DATA AND HYPOTHESIS TESTING

A1.1 Estimation of the Characteristic Values From Multi-Sets of Data

It is assumed that only the mean, $\overline{X}_2$, variance, $S_1^2$, and sample size,

$n_i$, of k sample sets taken from a population as shown in Figure A.1 are

known. Then, by definition, the mean value of the $i^{th}$ sample set, $\overline{X}_i$,

is written as (4)

$$\overline{X}_1 = \frac{\sum_{m=1}^{n_i} X_{mi} f_{mi}}{n_i} \quad \text{or} \quad \sum_{m=1}^{n_i} x_{mi} \cdot f_{mi} = n_i \cdot \overline{X}_i \qquad (A1.1)$$

where $x_{mi}$ denotes the $m^{th}$ variate in the $i^{th}$ sample set, and $f_{mi}$ repre-

sents the frequency corresponding to $x_{mi}$. The variance of the $i^{th}$ sample

set, $S_i^2$, can be expressed, by definition, as (4)

$$S_i^2 = \frac{\sum_{m=1}^{n_i} f_{mi} \cdot (x_{mi} - \overline{X}_i)^2}{n_i - 1} = \frac{\sum_{m=1}^{n_i} f_{mi} \cdot x_{mi}^2 - n_i \overline{X}_i^2}{n_i - 1} \qquad (A1.2)$$

or

$$\sum_{m=1}^{n_i} f_{mi} \cdot x_{mi}^2 = (n_i - 1)S_i^2 + n_i \overline{X}_i^2 \quad . \qquad (A1.3)$$

The unbiased mean, $\overline{X}$, and variance, $S^2$, of the pooled sample of k

sample sets are given by

$$\overline{X} = \frac{\sum_{i=1}^{k} \sum_{m=1}^{n_i} f_{mi} \cdot x_{mi}}{\sum_{i=1}^{k} n_i} \qquad (A1.4)$$

and

$$S^2 = \frac{\sum_{i=1}^{k} \sum_{m=1}^{n_i} f_{mi} \cdot x_{mi}^2 - \sum_{i=1}^{k} n_i \overline{X}^2}{\sum_{i=1}^{k} n_i - 1} \quad . \qquad (A1.5)$$
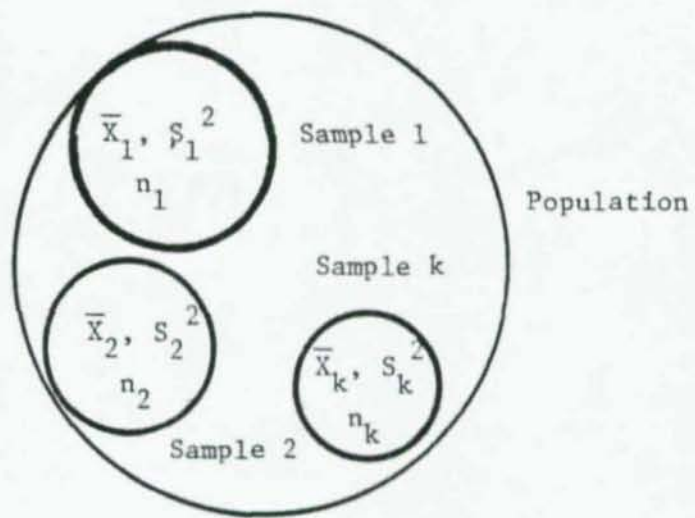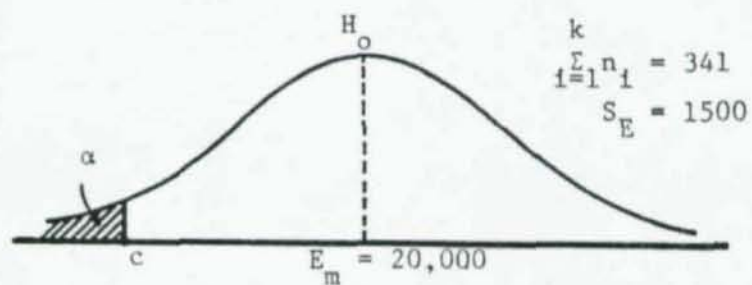
Figure A.1.  Sampled data from population



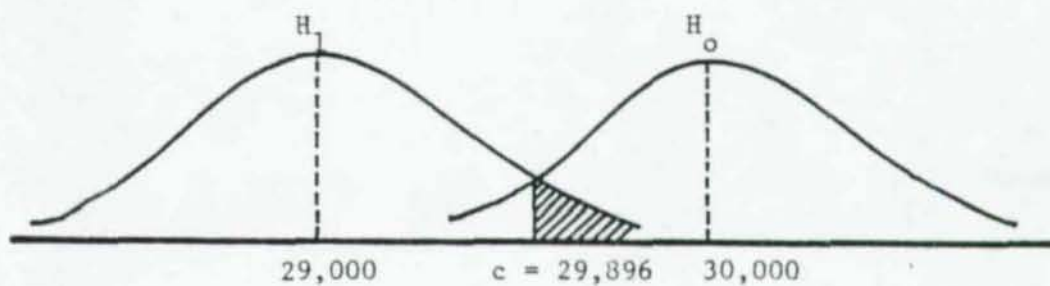Figure A.2.  Probability of a Type I error



Figure A.3.  Probability of a Type II error

Substitution of Eq. (A1.3) into Eq. (A1.5) yields

$$S^2 = \frac{\sum\limits_{i=1}^{k}(n_i - 1)\cdot S_i^2 + \sum\limits_{i=1}^{k}n_i \bar{X}_i^2 - \bar{X}^2 \sum\limits_{i=1}^{k}n_i}{\sum\limits_{n=1}^{k}n_i - 1} \quad . \tag{A1.6}$$

With the known mean and variance of a random variable x, the C.O.V. of the variable x is determined by

$$\Omega_x = \frac{S}{X} \tag{A1.7}$$

where S is the standard deviation of random variable x.

## A1.2 Hypothesis Testing on Modulus of Elasticity (12)

By using Eqs. (A1.4) and (A1.6), the mean of the modulus of elasticiyt, $E_m$ = 30,013 ksi and the standard deviation of E, S = 1324 ksi are obtained from the data given in Table 3. By substituting these two values into Eq. (A1.7), the C.O.V. of E, $\Omega_E$, is found to be 0.044.

Now, assume that the true population-mean of the distribution of E is 30,000 ksi and the standard deviation of 1500 ksi. Then by applying the hypothesis testing method, it can be determined whether this assumption, the so-called null hypothesis $H_o$, could be accepted or not. This kind of decision procedure could lead us to either of two wrong conclusions; the so-called Type I error or the Type II error. A Type I error is committed if we reject the null hypothesis when it is true, and a Type II error is committed if we accept the null hypothesis when it is false.

The probability of committing a Type I error is called the level of significance of the test and is denoted by α. Figure A.2 and Figure A.3 show the concept of the probability of a Type I error and of a Type II error, respectively. In Figure A.2, the probabiliy of a Type I error is

represented by the shaded area, and a Type II error is measured by the probability that values of a random variable fall in the shaded area of Figure A.3 when the true mean is $H_1$. In both figures, c is determined by selecting the significance level of the test.

Testing about a Type I error is performed with the significance level of $\alpha = 1\%$ and an alternative hypothesis $H_1$ which is set by the mean of E, $E_m$ = 30,000 ksi. Thus, we reject the null hypothesis if the observed mean value lies in the shaded area, or we accept the null hypothesis if the observed sample mean is greater than c in Figure A.2. The value of c is determined in the following manner:

Null hypothesis $H_o$: $E_m$ = 30,000 ksi,

Alternative hypothesis: $E_m$ < 30,000 ksi,

Probability of committing a Type I error: $\alpha$ = 0.01, and

$\alpha$ = P[Type I error] = P[E < c|$H_o$ is true] .

The standardized normal variable z corresponding to c is expressed by

$$ z = \frac{c - E_m}{S_E/\sqrt{n-1}} = \frac{c - 30,000}{1500/\sqrt{340}} = \frac{c - 30,000}{81.35} . \qquad (A1.8) $$

Thus,

$$ \alpha = P[z < \frac{c - 30,000}{81.35}] = 0.01 . \qquad (A1.9) $$

The area under the normal curve is given in most statistic books. The corresponding value of z to $\alpha$ = 0.01 is -1.28. Hence

$$ \frac{c - 30,000}{81.35} = -1.28 \quad \text{or} \quad c = 29,896 . \qquad (A1.10) $$

The value of c means that we can not reject the null hypothesis if the observed mean value is greater than c. Therefore, we can accept the hypothesis of $E_m$ = 30,000 ksi because our observed mean value was 30,013 which is greater than E = 29,896.

But, the test about a Type I error does not guarantee that $E_m$ = 30,000 ksi is the true mean. Thus, it is necessary to perform the second test about a Type II error.

Assume that the true mean lies in the left side of the shaded area in Figure A.3, for instance, $E_m$ = 29,000 ksi. Then, the probability of a Type II error, β, with a significance level α = 0.01 is

$$\beta = P[\text{Type II error}] = P[E > c | H_1 \text{ is true}] = P[E > 29,896 | E_m = 29,000] . \quad \text{(A1.11)}$$

The standardized normal variable z is given by

$$z = \frac{29,896 - 29,000}{81.35} = 11.01 \quad . \quad \text{(A1.12)}$$

From most standard statistics references, β corresponding to z = 11.01 can be said to equal zero. Consequently, there would be little chance of accepting the null hypothesis, $H_o$, when it is false.

In conclusion, it is reasonable to use the mean modulus of elasticity, $E_m$ = 30,000 ksi and the C.O.V., $\Omega_E$ = 0.05.

## Appendix 2

### FUKUMOTO REFERENCE

Upon completion of this study, the author became aware of a new reference. Fukumoto and Itoh reported the mean equal to 0.998, the standard deviation equal to 0.78 and the C.O.V. equal to 0.0254 of the cross-sectional area of welded beams based on test results. Though the C.O.V. equal to 0.0254 is quite small compared to the C.O.V. equal to 0.05 used in this study, the effect of the new value on the resistance factors would be negligible because the other C.O.V.'s affecting the resistance factor are considerably larger than the C.O.V. of cross-sectional properties.

Listed below is the Fukumoto reference:

Fukumoto, Y. and Itoh, U., "Statistical Study of Experiments on Welded Beams," Journal of the Structural Division, ASCE, Vol. 107, Jan., 1981, pp. 89-103.